FORSCHUNGSZENTRUM
ROSSENDORF e.V.

FZR

FZR 93 - 12
April 1993

INSTITUTE OF BIOINORGANIC AND RADIOPHARMACEUTICAL CHEMISTRY

Annual Report 1992

Editor: B. Johannsen

CONTENTS

I.
INTRODUCTION

The ***Institute of Bioinorganic and Radiopharmaceutical Chemistry of the Research Center Rossendorf Inc. (FZR)*** herewith presents its 1992 Annual Report to document research activities in the first year of its existence.

The FZR, located 10 km to the east of the Saxon capital Dresden, took up work on 1 January 1992. So did its five institutes. The Institute of Bioinorganic and Radiopharmaceutical Chemistry is thus in its initial stages. Providing suitable working conditions, facilities and methods required substantial effort. Due to the new situation in eastern Germany, licensing procedures for handling radioactive material have become uncommonly difficult. However, thanks to manifold help and support, some ambitious aims have meanwhile been achieved. As part of the FZR, which is principally supported by the Free State of Saxony and the Federal Republic of Germany on a parity basis, the Institute has experienced most helpful support in the form of additional grants and a temporary increase in staff under a job-creation programme. The generous willingness of colleagues from various parts of the world to cooperate with us is highly appreciated.

The Institute's research programme and profile are derived from an awareness of the very important advances taking place in modern nuclear medicine. Based on sophisticated radiotracers and focused on the molecular level, nuclear medicine offers unique opportunities for studying tissue functions and translating the findings into ways of caring for sick people. To fully exploit this discipline of *in vivo* chemistry requires great commitment to interdisciplinary research into radiotracers and a thorough appreciation of the complexity involved. Contributions from radiochemistry, organic and inorganic chemistry, radiopharmacy, radiopharmacology, physics, biology and medicine have all to be combined and merge in tracer design. The Institute's profile is such that it is prepared for the challenge of sophisticated interdisciplinary work in order to gain a deeper insight into the fundamentals of the chemistry and biobehaviour of biochemical tracers.

With the emphasis on biochemical processes, positron emission tomography (PET) is the essential modality for assessing the global and regional functional status of the brain, heart or other organs of interest. In line with the recommendations of the Scientific Council for the Federal Republic of Germany, chemical and biological research into radiotracers will be combined with PET at Rossendorf. Medical research, together with a limited clinical application of PET, will be conducted in cooperation with the Dresden Medical Academy, and will initially focus on diseases of the brain. The task of establishing a PET centre - which

calls for substantial scientific, financial and administrative commitment - dominated the activities of the Institute in 1992 and will continue to do so in the years to come.

Since single photon emission computed tomography (SPECT) continues to be the principal way of translating PET advances into broad clinical practice, specific SPECT tracers are one of the main subjects of research. An analogue concept of rational tracer design makes it possible to go from ^{11}C or ^{18}F PET tracers to ^{123}I SPECT tracers. Such a straightforward concept of development of biochemical tracers does virtually not exist for ^{99m}Tc, the workhorse of nuclear medicine. Technetium has an intricate coordination chemistry that does not go well with the organic nature of biochemical substrates. Overcoming this problem as far as possible by gaining a better insight into technetium chemistry and exploiting its versatility is a crucial task.

With this aim in mind our Institute's SPECT tracer group has been concentrating on the chemistry of new radiopharmaceutically relevant technetium compounds. Research has focused in particular on the reaction of technetium with sulphur-donor ligands and the corresponding products. They are considered to be of special value for a new generation of specific ^{99m}Tc tracers. Analogous rhenium compounds have also been studied in view of their therapeutic potential.

The two working directions - PET and SPECT tracer research - will be closely combined in the hope that they mutually stimulate each other and that biochemical tracer concepts of PET can be transferred to technetium compounds, going from PET to SPECT.

The aims and tasks as outlined above have given rise to the current structure and staffing of the Institute of Bioinorganic and Radiopharmaceutical Chemistry as shown in Scheme 1.

B. Johannsen
Acting Director of the
Institute of Bioinorganic and Radiopharmaceutical Chemistry

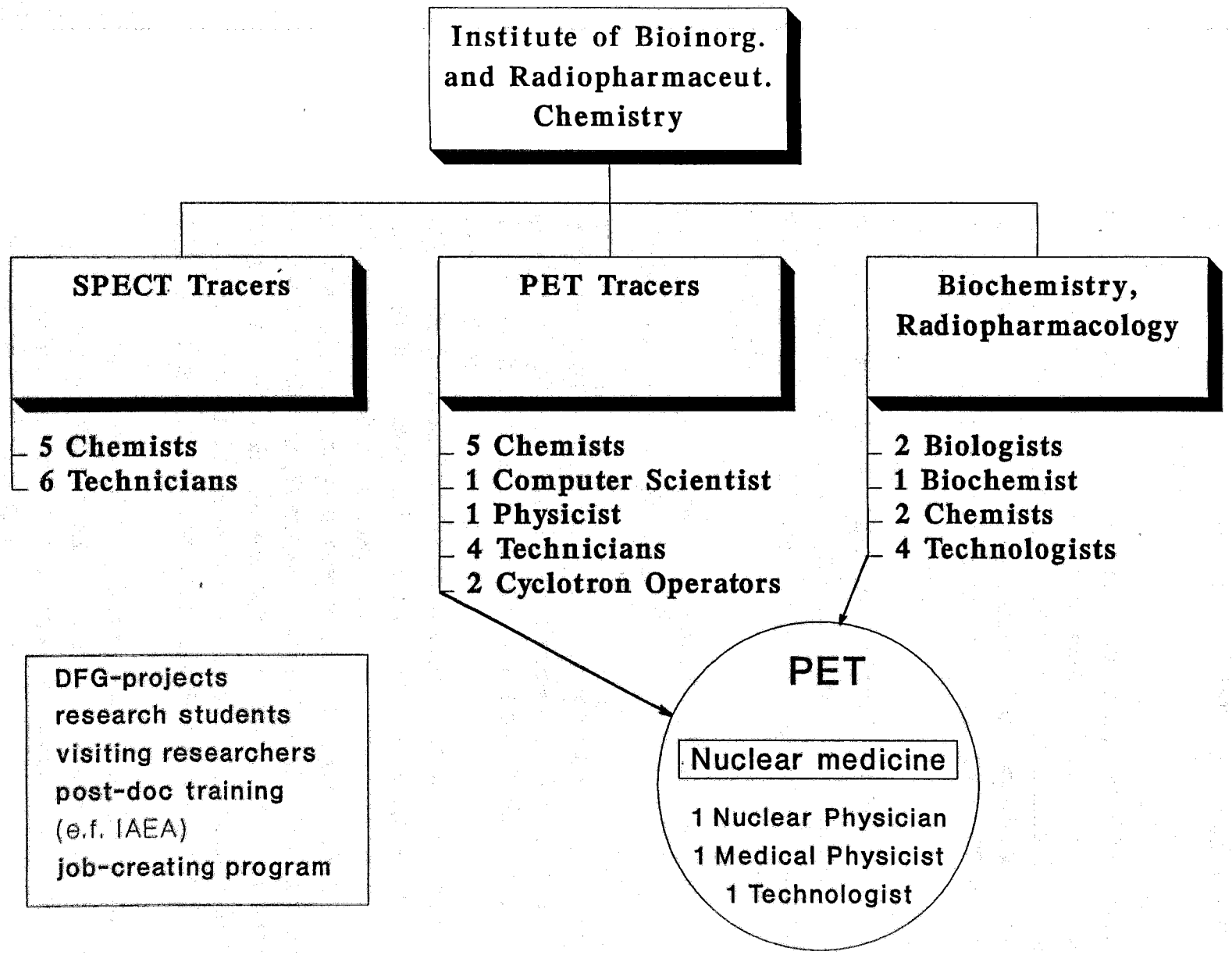
Institute of Bioinorg. and Radiopharmaceut. Chemistry
SPECT Tracers
PET Tracers
Biochemistry, Radiopharmacology
5 Chemists
6 Technicians
5 Chemists
1 Computer Scientist
1 Physicist
4 Technicians
2 Cyclotron Operators
2 Biologists
1 Biochemist
2 Chemists
4 Technologists
DFG-projects
research students
visiting researchers
post-doc training
(e.f. IAEA)
job-creating program
PET
Nuclear medicine
1 Nuclear Physician
1 Medical Physicist
1 Technologist

II.
SUMMARY OF ACTIVITIES AND RESULTS

The subjects of our work are described in this volume in 27 individual reports devoted to various aspects of radiotracers for nuclear medicine.

The first part contains a description of the setup of a PET facility, for which extensive efforts have already been undertaken. Its main components will be a new cyclotron (Cyclone 18/9) as a replacement for the present U120 machine, an automated transport system to cover the distance of 500m to the radiopharmceutical labarotory with its three hot cells, radiochemical laboratories, and the medical section with a POSITOME IIIp PET camera.

In addition to technological installations, the establishment of Good Manufacturing Practice (GMP) and analytic and synthetic work preparatory to routine preparation of radiopharmaceuticals, emphasis has been given to studying ^{11}C ring labelling of aromatics to obtain metabolically stable tracers.

Miscellaneous topics include the quality of labelling agents, such as ^{123}I iodide and ^{99m}Tc pertechnetate, and software for pharmacological studies.

The papers on technetium chemistry are closely related to each other. Major activities were devoted to the synthesis and characterization of novel technetium complexes as well as to reaction routes and products in intricate technetium/ligand systems. Studies focused primarily on complexes with sulphur donor ligands:
Earlier work on defined Tc(V)oxo complexes of dimercaptosuccinic acids was extended and produced new insights into the existence and behaviour of isomers and enzymatic cleavage of ester bonds in the dimercaptosuccinic ester complexes.
Significant progress was made in obtaining new complexes with thioether ligands. With bidentate thioethers, neutral oxotechnetium(V) complexes were synthesized and characterized. X-ray structure analysis reveals either single-bonded or bridging oxygen in trans position to the Tc=O core as a characteristic feature of the new class of compounds. Cationic nitridotechnetium(V) complexes with thiacrown ethers provide a new approach in radiotracer design.
Fundamental studies with mercapto-containing peptides were continued. The results are significant for the current discussion of new radiopharmaceuticals. They are most helpful for a better understanding of the very sensitive interplay between the various donor atoms in the bioligands during complexation of technetium.

Work on precursors and mixed-ligand complexes was continued and intensified in order to improve the assortment of candidates for the bifunctional concept of designing new radiopharmaceuticals. Preliminary investigations were carried out into metabolizable technetium complexes and redox-active markers as tentative studies in the search for more specific tracers.

III.
RESEARCH REPORTS

1. THE ESTABLISHMENT OF THE ROSSENDORF PET CENTER

B. Johannsen, J. Steinbach

Introduction

Positron Emission Tomography (PET) is unique in its ability to image and quantify physiological and chemical processes in human beings. More and more diseases are now being defined biochemically. Until now a research tool for studying the physiology and biochemistry of mainly the brain and heart, PET is also evolving into an applied clinical technique. The potentials of PET to characterize diseases in regional biochemical terms essentially depend on radiotracers. Development of new radiotracers has become more complicated and challenging. Extensive background research by radiochemists, radiopharmacologists and physicians is required before a new PET tracer can be used in diagnostics. As stated recently [1], PET is also a highly complicated imaging technology and requires someone who understands the problems and is still willing to do it, plus enough money to get the thing going.

The new Research Center Rossendorf, which is located 10 km to the east of Dresden (Fig.1), provides excellent prerequisites and conditions for housing a PET centre for the Dresden region. With an adequate multidisciplinary profile of its own and strong ties with the nearby universities and medical institutions, in particular the Dresden Technical University and the Medical Academy, it has started setting up a PET facility, the first in the new federal states of Germany.

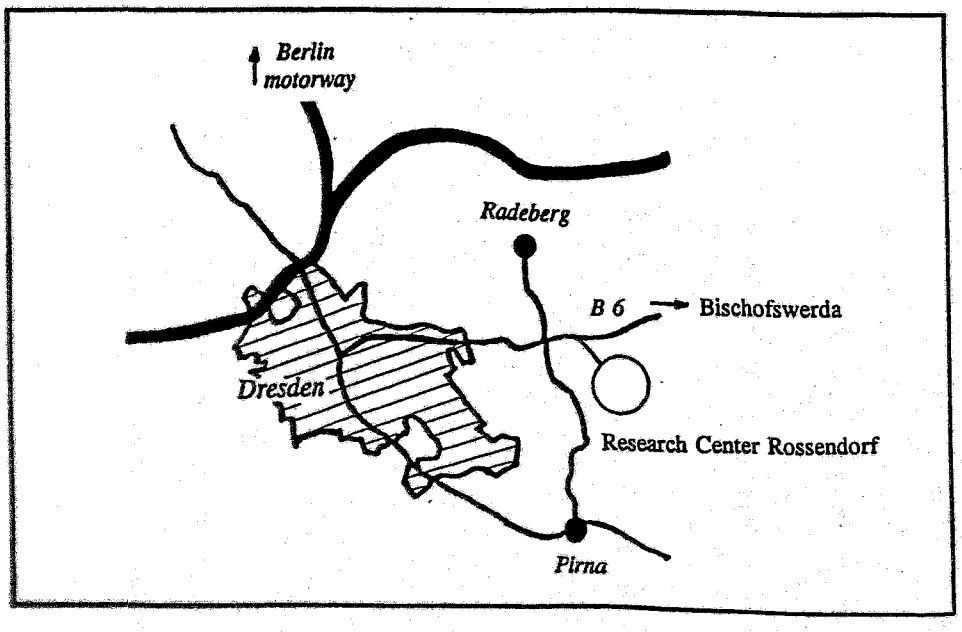

Fig.1: Rossendorf within the Dresden region

The installation and operation of the PET centre at Rossendorf greatly benefits from previous achievements in targetry, nuclide production with the U-120 cyclotron, applied research on positron-emitting nuclides and their compounds, preparation of radiopharmaceuticals, and experimental radiopharmacology, as well as the design and construction of PET detectors and a special PET camera. As part of the Institute of Bioinorganic and Radiopharmaceutical Chemistry with its second focus on the chemistry and radiopharmacology of ^{99m}Tc compounds, the PET centre makes it possible to combine PET and SPECT tracer research, aiming for a broader application through the use of ^{123}I and especially ^{99m}Tc, the workhorse of nuclear medicine.

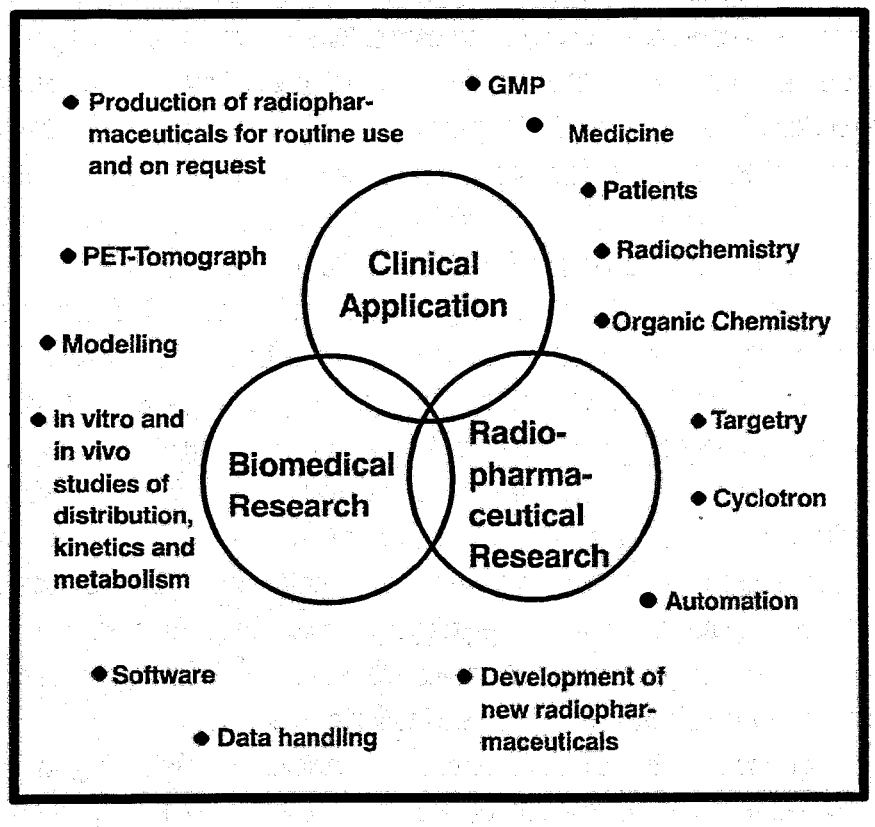

Fig.2: Multidisciplinarity of the PET centre at Rossendorf

Objectives of the PET Center

1. Medical Research

One of the PET centre`s goals is the application of ***PET for medical research***. It is focused on the type of medical research wich was not possible before and has now become possible by applying PET with its potential for non-invasive investigation of the biochemical states of the human body.

An important field of research is the application of tracers in neurology and psychiatry for studying brain dysfunctions. Various basic and specifically prepared radiopharmaceuticals will be used for this purpose.

Medical research will be performed in close cooperation with the Dresden Medical Academy. There are two projects:

The ***function of the serotonergic system in psychiatric diseases*** will be one subject of our joint work. The neurotransmitter serotonin is involved in the regulation of various physiological functions. Changes in serotonin metabolism play an important role in a number of psychiatric diseases such as depressions. PET opens up the possibilities for investigating such changes and for assessing the effects of pharmacological intervention.

The second project is concerned with a ***characterization of myotonic dystrophies***, which has been very difficult until now. This problem is of great importance, because patients suffering from this disease require lifelong care. There are some indications that changes in the brain glucose metabolism are involved.

2. Development of tracers and radiochemical developments

One goal of our research work is the development of radiopharmaceuticals labelled in positions which are practically not metabolized within central fragments of the molecules. These are no carrier added ^{11}C- labelled compounds, e.g. compounds containing cyclic fragments, especially aromatic rings. The details are described by Mäding et al. [this report, p. 18].

The special importance of ^{18}F labelled tracers is based on its suitable half-life (110 minutes). Other clinical PET centres within a radius of 3...4 hours` transport time can be regularly supplied with ^{18}F-based radiopharmaceuticals (conception of satellites). With regard to labelling procedures with electrophilic ^{18}F, there is a strong demand for specialist knowledge for generation of no-carrier-added ^{18}F in high yields and in new techniques for the synthesis of appropriate radiopharmaceuticals.

The PET technique is associated with certain characterizations originating in the short half-life of the radioisotopes used and resulting in a very high activity level and the necessity of handling small amounts of molecules. This specific feature demands fundamental radiochemical research, including hot synthesis, micro analysis and special equipment.

3. Biochemistry

With PET only the radioactivity within a field of view is measured. The visualized tracer distribution does not provide information about tracer binding or metabolism in the region of interest. Quantitative information has to be obtained indirectly by kinetic modelling. The development of models which can be applied to human PET studies includes animal experiments and computer-assisted simulation. An example of the modelling of methionine metabolism is shown by Bergmann et al. (this report, p. 28).

4. Future prospects of PET in Rossendorf

The *future prospects of PET* at Rossendorf are bound up with the future of other parts of the Research Center. One of the future subjects of research - also in connection with the Dresden Medical Academy - is the treatment of cancer. The light ion tumour therapy in particular requires a pre-therapeutic diagnosis (hypoxic state, pH-value), a therapy prognosis depending on the state of the tumour, and an evaluation of the therapeutical effects by PET. Similar requirements will have to be met for neutron and neutron capture therapy. The neutron capture therapy affords an opportunity of assessing the distribution of boron-labelled pharmaceuticals before neutron treatment.

The doses absorbed with these methods can be calculated in advance with the aid of PET.

Layout

Given the structure of operating facilities and existing components, such as a cyclotron building with the U-120 cyclotron and radiochemical and biochemical laboratories 500 m away from the cyclotron, the setup concept is designed to both complete the PET centre and to improve its potentials, operability, cost-effectivness and licensability.

The completion includes as a key item the extension to tomography in biochemical and clinical research, which will be jointly done in colloboration with the nuclear medicine of the university hospital. Fig.3 shows the layout of the PET centre.

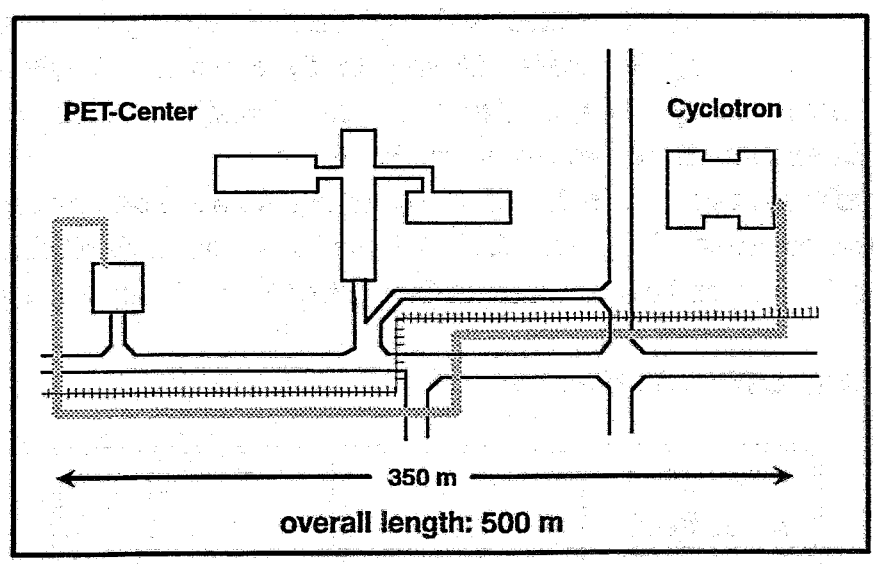

Fig. 3: Components of the Rossendorf PET Center

Cyclotron and targetry

The U-120 cyclotron at Rossendorf is a fixed energy machine which has been in operation for 36 years now. It was built for the requirements of nuclear physics. Its main parameters are as follows:

Particle	Energy (MeV)	External beam current (μA)	Max. beam current on PET-target (μA)
H^+ (p)	**13**	**30**	**7**
$^2H^+$ (d)	**13.5**	**50**	**10**
He^{2+}( )	27	20	-
$H_2^+/2$	6.75	30	-
$^3He^{2+}$	27	2	-

These are maximum parameters with respect to the beam current. This machine is expensive to run in terms of maintenance and energy consumption, its reliability and flexibility are poor and the operational parameters instable.

To overcome these problems, a specially designed Siemens system for large-scale generation of PET radionuclides, based on the "CYCLONE 18/9" cyclotron produced by IBA, Belgium (Fig. 4), will be installed this summer. For cost reasons it will be sited near the old cyclotron. The cyclotron building project and shielding requirements have been planned by the responsibility of the Rossendorf PET group.

The new machine is a compact cyclotron employing negative ion technology. Negative ions (H^-, D^-) allow extraction of more than 99.9 % of the beam. Such high efficiency results in greater safety for personnel and environment (low activation) and lower running costs.

Parameters of the CYCLONE 18/9:

Particle acceler/extract	Energy MeV	External beam current μA
H^-/H^+	18	100
D^-/D^+	9	35

This beam current is available on all targets.

The cyclotron and targets are completely automated with a highly reliable industrial programmable logic controller. The system is capable of producing the desired compounds

$[^{18}F]F_2$, $[^{18}F]F^-$, $[^{11}C]CO_2$, $[^{13}N]NH_3$, $[^{15}O]O_2$ and $[^{15}O]CO_2$. $[^{11}C]HCN$ and $[^{15}O]H_2O$ can be generated too.

Generation of various other radionuclides is in preparation. A beam line system to be added to the CYCLONE 18/9, including control system, has been developed and will be delivered by IBA. The vertically movable target changing device, our own development, will be attached to this beam line. It is designed for eight target positions with a set of targets for gaseous, liquid and solid target materials. This is an important prerequisite for educational purposes.

Capability for radionuclide production of the Cyclone 18/9:

Radio-nuclide	Half-life (min)	max. Activity (GBq)
^{11}C	20	74
^{18}F	110	92
^{15}O	2	9
^{13}N	10	15

Fig. 4: The Cyclone 18/9 cyclotron

Transport system

As a special feature of the Rossendorf PET centre, the PET cyclotron and the PET centre are separated by a distance of 350m. A transport system for radioactive gases and liquids over 500m is therefore being installed on the basis of gas-capillaries and rabbit post lines (Fig. 5). This system, which works fully automatically, has been designed and constructed at the Research Center Rossendorf. The transport system and the synthesis units automatically driven by a SIMATIC system.

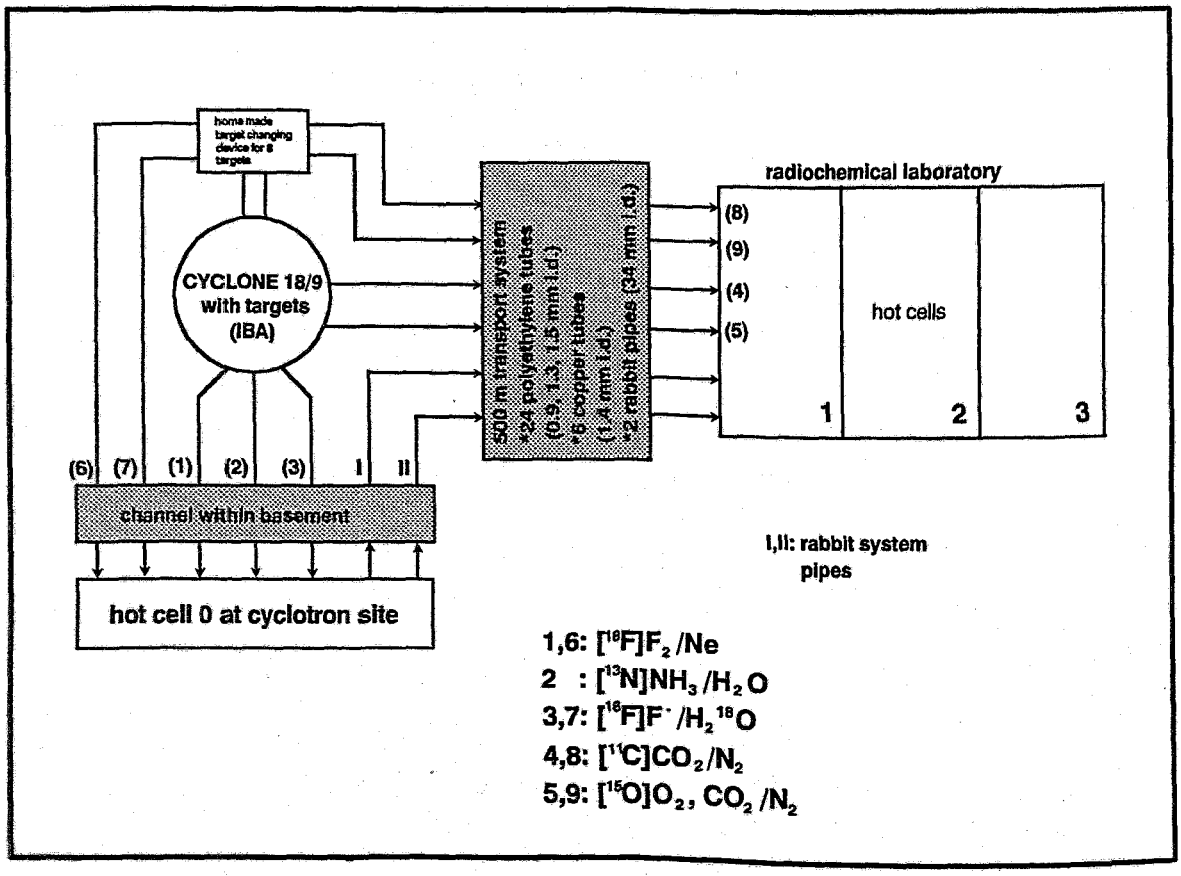

Fig. 5: Scheme of the transport system

Radiopharmaceutical laboratories

The radiopharmaceutical laboratories are situated on the ground floor (Fig. 6). The automated transport system terminates here in a hot cell laboratory especially designed for GMP preparation of PET radiopharmaceuticals. This laboratory will house a system of remote controlled units for preparation of these substances. The first unit is a remote controlled system for routine preparation of [^{18}F]FDG, others will follow. An analytical laboratory serves for tests of identity, apyrogenity, osmometric pressure and pH. It includes are equipment for analytical purposes like HPLC, GC, CE, TLC and others.

Radiochemical research is based in a laboratory equipped with a double hot cell for tracer development. Precursor preparation and development of synthetic routes for hot synthesis are carried out in a laboratory for organic synthesis.

All special equipment for radiochemical, radiopharmaceutical and biomedical purposes has to be of a high technical standard. Maintenance and further development are therefore important. A high degree of automation is also required for many procedures. In addition, the devices have to meet the requirements of safe operation, in particular with respect to radiation protection.

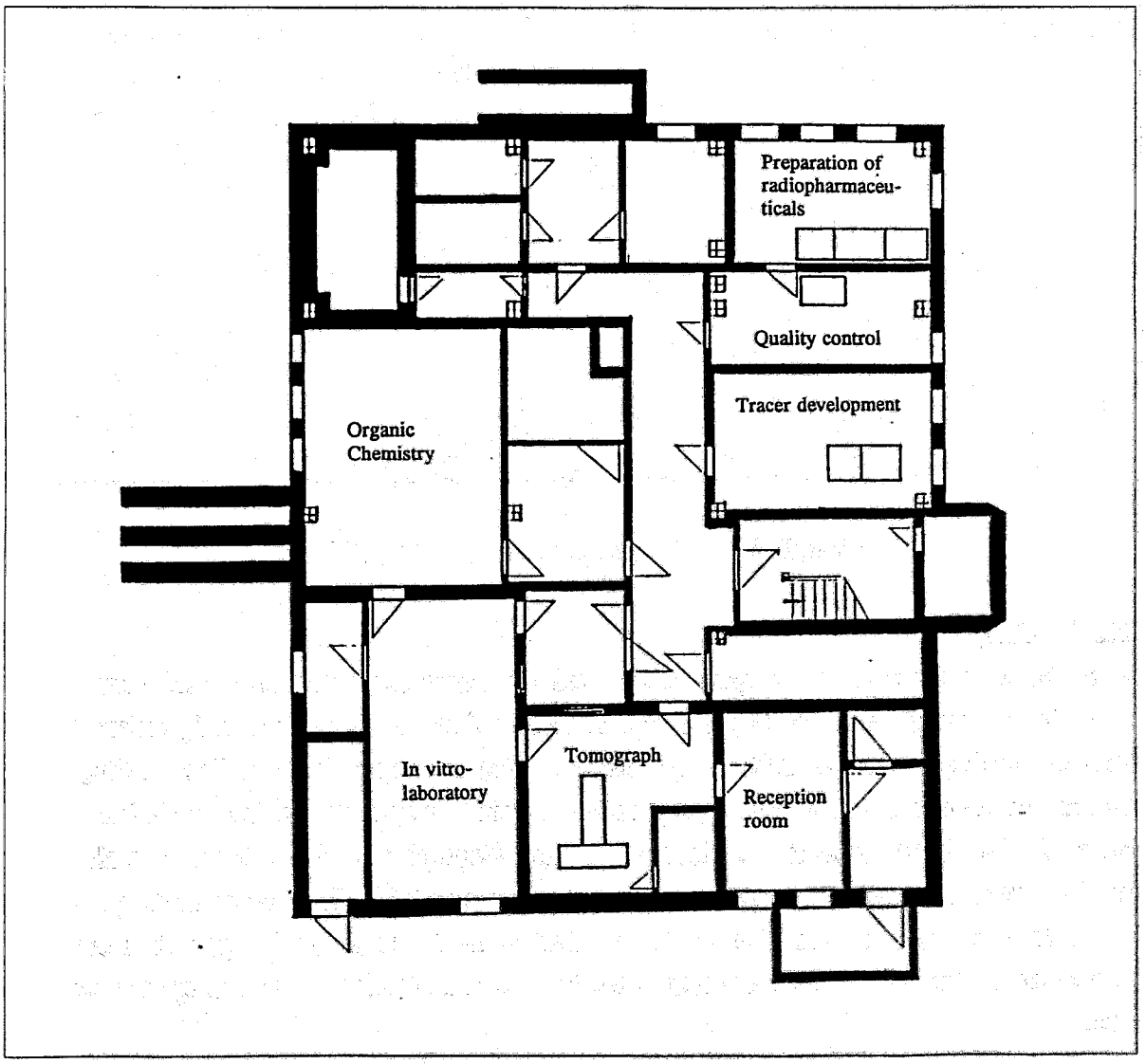

Fig. 6: Layout of the Rossendorf PET centre

Tomograph

A PET tomograph POSITOME IIIp* (Fig. 6) developed at the Montreal Neurological Institute was installed in June 1992. For further details see Will et al. (this report, p. 16).

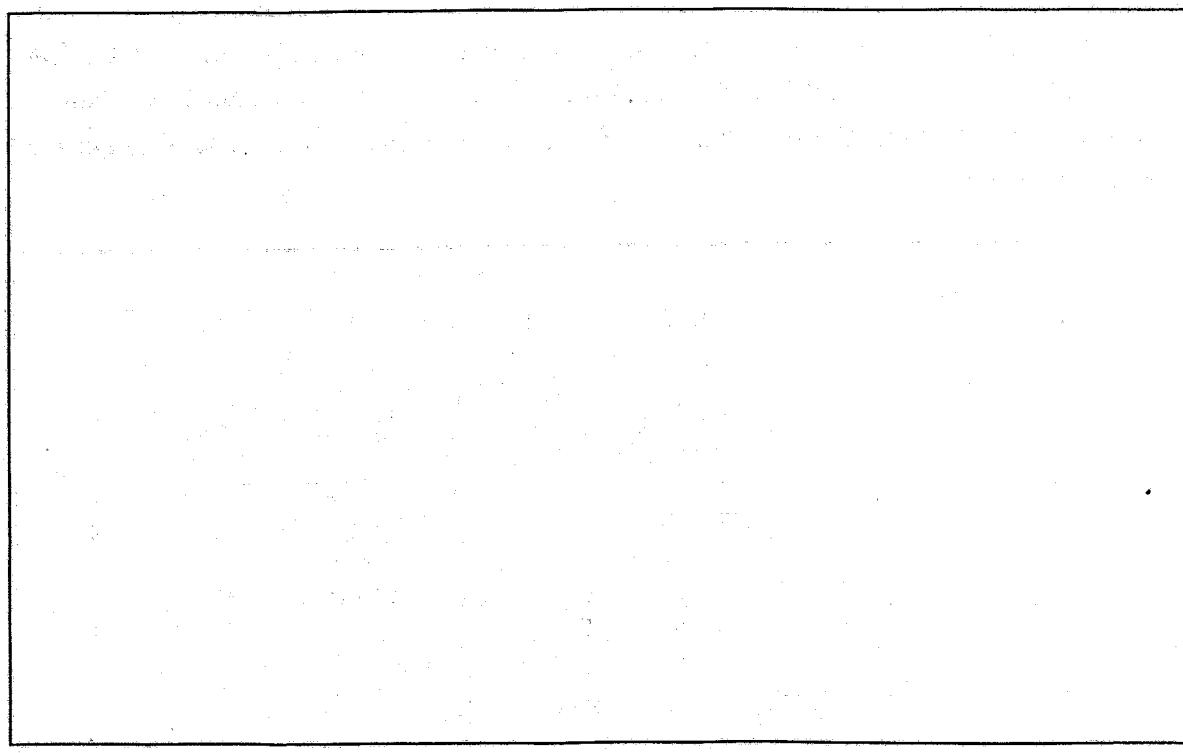

Fig.7: The PET tomograph POSITOME IIIp

Biochemistry

In addition to the usual techniques as required for tracer characterization and metabolite analysis, a comprehensive facility for experimental radiopharmacology already exists. This includes binding assays for different (serotinergic, dopaminergic) ligands. The binding studies are performed either on tissue preparations (brain homogenate, brain endothelial cells, cultured fibroblasts) or on tissue slices using autoradiographic methods. There are also several biochemical methods for measurement of enzyme activities in various tissue preparations. In vivo methods are also used. In addition to the traditional organ distribution, tracerkinetic models are being developed for in vivo characterization of radiopharmaceuticals.

Schedule

Phase 1 of the project is the replacement of the old U-120 cyclotron by the CYCLONE 18/9 for PET purposes and establishment of a temporary unit of nuclear medicine.

Phase 2 envisages an expansion of the medical section by housing it in a separate building, and rearrangement of the laboratories in the radiopharmaceutical and biochemical sections.

1993: Completion of the installarion of the Cyclone 18/9 PET-cyclotron. Reconstruction of a building as the permanent home of the Rossendorf PET centre`s medical section in conformity with the relevant pharmaceutical and medical regulations.

1994: Completion of the automatic transport system for radioactive substances between cyclotron and hot laboratory. Some first items of equipment for automatic synthesis of important radioactive tracers will be developed and put into operation.

1995: Installation of a whole-body PET-camera.

Reference:

[1] Wagner, H.N., Jr. J.Nucl. Med. **32**(1991) 11N

*Acknowledgement: We are deeply thankful for the outstanding support by the "Kulturstiftung Dresden der Dresdner Bank" and the Montreal Neurological Institute

2. INSTALLATION OF THE PET-CAMERA POSITOME IIIp IN ROSSENDORF

W. Enghardt, H. Linemann, M. Mazza[1], C. Thompson[1], E. Will
[1]Montreal Neurological Institute

The PET camera POSITOME IIIp from the Montreal Neurological Institute (MNI) arrived at Rossendorf at the end of 1991. This head tomograph, sponsored by the Kultur-Stiftung Dresden der Dresdner Bank, was developed and built by the group of C. Thompson in 1978 and continuously modernized till 1986 [1,2].

The POSITOME IIIp has a high efficiency in comparison with other PET tomographs. Its high usable frame rate makes it especially suitable for dynamic brain studies.

The tomograph was installed in the new medical section of the Rossendorf PET centre. One of the problems was the installation of a 110V power supply for the electronic equipment of the POSITOME scanner. The first test of the detector system showed, that there was no transport damage. Some adaptions were necessary on the bed in order to comply with German safety standards. The final installation and testing of the POSITOME IIIp at Rossendorf took place in June 1992 in cooperation with C. Thompson and M. Mazza from the MNI. We carried out fine corrections for the gain, the threshold and the coincidence window for all detectors.

The programs for data acquisition and reconstruction were written by C. Thompson [3]. The reconstruction program runs on PDP11 and VAX computers. Image display and analysis will be performed on a VAX with a Lexidata display after solving some technical problems. Time measurement in the acquisition and evaluation programs is based on the power frequency, the time calibration coefficients must therefore be changed from 60Hz to 50Hz.

For putting all parts of the tomograph and the aquisition programs into operation, calibration measurements and simulations of studies were performed using ^{18}F and ^{22}Na sources. Usually ^{68}Ge-sources are used for POSITOME IIIp calibration, we used ^{18}F phantoms.

The axial resolution was measured with a ^{22}Na source in air

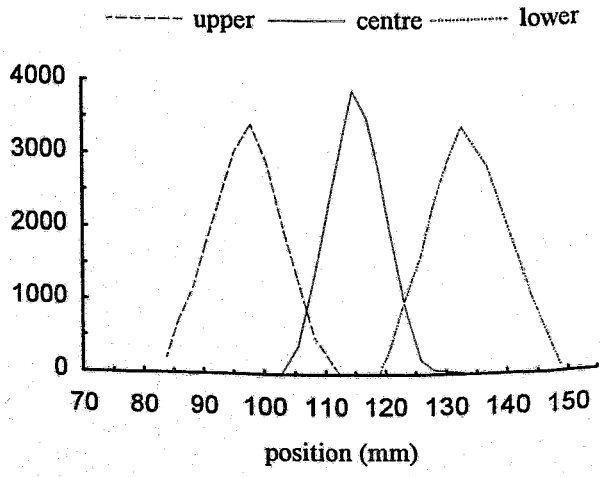

Fig. 1: Axial resolution measured for the lower-, centre- and upper-slice with a ^{22}Na source on the axis of POSITOME IIIp (in air).

(Fig. 1). We obtained a resolution of 15mm FWHM for the lower and upper slice and 13mm FWHM for the centre slice. The distance between the lower and upper slice is about 35.5mm. These values are in a good agreement with the values measured by C. Thompson at the MNI [2].

The technical layout for the POSITOME IIIp is as follows:

Number of rings:	2
Number of slices:	3 (2 direct, 1 cross)
Number of detectors:	64/ring, BGO 30x30x(22 to 18)
Resolving time:	18ns
Image resolution:	10.9mm (FWHM)
Axial resolution:	15.9mm (FWHM)
Maximum activity conc.:	40KBq/cm^3 in 20cm dia. flood phantom
True count efficiency:	75kcounts/sec/($\mu C \cdot cm^3$) in 20cm dia. source
Scatter fraction:	27% in 20cm diameter flood phantom
Max. frame rate:	1 frame/3s
Patient port:	26cm diameter

References:

[1] Thompson, C. J, et al., IEEE Trans. Nucl. Sci., NS-26 (1979) 583

[2] Thompson, C. J, IEEE Trans. Med. Imag., MI-5 No. 4 (1986) 183

[3] Dagher, A, et al., IEEE Trans. Nucl. Sci., NS-32 (1985) 811

3. SUBSTANCES LABELLED IN METABOLICALLY STABLE POSITIONS:

INACTIVE EXPERIMENTS FOR THE SYNTHESIS OF ^{11}C-RING-LABELLED AROMATICS

P. Mäding, J. Steinbach, F. Füchtner, H. Kasper, K. Neubert

During the last two decades a flood of ^{11}C-labelled compounds were synthesized. Only a few are of significance with regard to their practical use. One of the reasons may be underestimation of the importance of the labelled atom's fate within the living body. Investigations of radiopharmaceuticals of the same origin but labelled at different positions produce new biochemical information. An alternative way might be the synthesis of compounds labelled in metabolically stable fragments of the molecule. The metabolic pathways of these compounds should be known or must be explored for their application. Aromatic fragments of molecules in particular were found to be metabolically stable components of compounds. Experiments with biologically active aromatic substances in biological systems may be expected to produce long-living metabolites, including unchanged aromatic rings.

There are many important biologically active aromatic compounds, e.g. phenylalanine, tyrosine, DOPA, dopamine, adrenaline, ephedrine, amphetamine etc.

To our knowledge only one experiment has been carried out to synthesize ^{11}C-ring-labelled aromatics [1]. In this study the classic synthesis of benzene/toluene was modified via trimerization of carrier-added [^{11}C]alkines. The result was a mixture of products with very low specific activities (60μmol acetylene for the synthesis of benzene) and low yields (about 25% benzene), which is unacceptable for our application. An early publication [2] deals with the reaction of cyclopentadiene and ^{11}C-atoms in hot and thermal systems. respectively. As described, mixtures of many different products were formed. The main portion consisted of polymers, but also [^{11}C]benzene was produced in yields of 8-11%. This kind of conversion is also unsuitable for a specific synthesis.

The following criteria must be considered for the synthesis of ^{11}C-ring-labelled aromatics:

- the limited availability of ^{11}C-synthones
- as few synthetic steps as possible
- short reaction times
- sufficient radiochemical yields.

In principle, the various possibilities of synthesis are:

- Conversion of synthesized ^{11}C-alkyl-substituted 5-rings (substituted cyclopentanes, cyclopentadienes) or ^{11}C-ring-labelled 6-rings (cyclohexanes, cyclohexenes, cyclohexadienes) by means of catalytic, thermal or chemical processes (reactions of isomerization, dehydrogenation, dehydratization) into ^{11}C-ring-labelled 6-ring aromatics

- Synchronous six-electron cyclization of hexatriene systems into aromatics.

The last mentioned synthetic method represents a promising basis for the synthesis of manifold ^{11}C-ring-labelled aromatic compounds because of the possible variation of substituents at the inactive precursor.

The synchronous six-electron cyclization of hexatriene systems into aromatics takes place in two steps [3]:

1. thermal cyclization of hexatrienes into cyclohexadienes as a reversible process
2. irreversible conversion of cyclohexadiene into a 6-ring aromatic by means of an elimination step if the starting hexatriene has got a suitable leaving group, e.g. a dimethylamino group, preferably trans at C-1, and additionally a cis-proton at C-6:

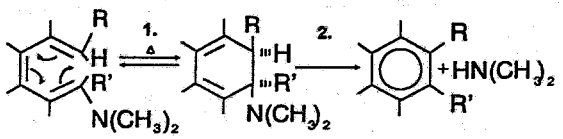

Our first aim is to synthesize ^{11}C-ring-labelled phenylalanine. We therefore developed a suitable way for synthesis of phenylalanine. Prerequisite for this synthesis is the availability of [^{11}C]nitromethane, which can be prepared according to [4,5] by reaction of [^{11}C]MeI with $AgNO_2$. In inactive experiments, the following route of synthesis was tested and optimized as a one-pot process on the 2mmol scale:

1. In the presence of a base (NEt_3) nitromethane as a C-H-acid compound reacts with the pentamethinium salt 5-dimethylaminopenta-2,4-dienylidene-dimethylammoniumperchlorate into 6-nitro-1-dimethylamino-hexatriene and dimethylamine. The cyclization/ aromatization into nitrobenzene occurs by elimination of the second dimethylamino group at increased temperature [3]. The synthesis was carried out in DMF at 100°C.

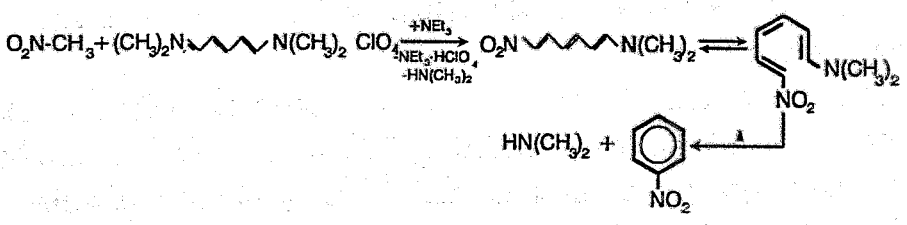

2. The nitrobenzene formed was reduced with $Na_2S_2O_4$ in boiling DMF/H_2O to aniline [6]:

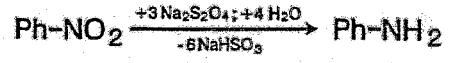

3. At 0°C the aniline was converted into the appropriate diazonium bromide with HNO_2 in hydrobromic organic-aqueous solution [7]:

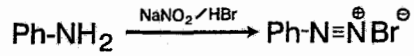

4. This was followed by the so-called "Meerwein arylation" of acrylic acid with the diazonium salt, with formation of α-bromo-ß-phenyl-propionic acid. This reaction occurs with CuBr as a catalyzer at room temperature [7]:

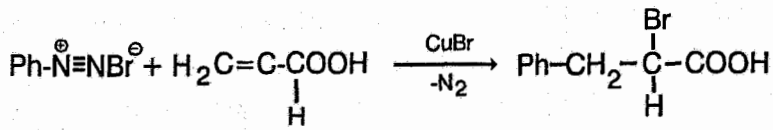

5. The desired phenylalanine was formed by ammonolysis of α-bromo-ß-phenyl-propionic acid while refluxing [7]:

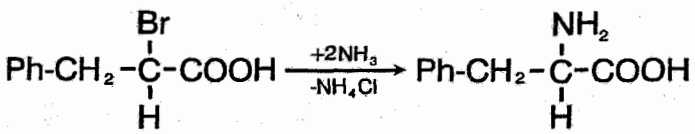

The course of the reactions was followed by HPLC.

The processing of the reaction mixture occurs as follows: The reaction solution containing an excess of ammonia is evaporated. The acidified mixture is introduced onto a column of cation exchange resign (Wofatit KPS, 8% DVB, 160-320μm, H^+-form, neutral). In this way all inorganic salts and organic products without amino groups can be separated by washing with water. The synthesized phenylalanine can be eluated with diluted NH_3 (2.5%). Further column-chromatographic purification can be performed after evaporation of the NH_3 solution (conditions: silicagel 60 (0.2-0.5mm, Merck)/water followed by LiChroprep RP-18 (40-63μm, Merck)/water). In this way colourless crystalline phenylalanine can be obtained.

Analyzing thin layer chromatography (TLC) was performed on silufol (Kavalier, CSFR). The plate was developed in acetone/ MEK/NH_3/H_2O = 60 : 30 : 20 : 10. Phenylalanine can be visualized as red spots on spraying the chromatogram with ninhydrin solution and heating. The system of TLC plates RP-18 F_{254S} (Merck)/water is also suitable for this problem.

This overall procedure will be adapted to the use of [^{11}C]CH_3NO_2 in the near future.

The necessary inactive precursor for the synthesis of phenylalanine, the 5-dimethylaminopenta-2,4-dienylidene-dimethylammonium-perchlorate, can be prepared as follows:

1. Pyridine is reacted with 1-chloro-2,4-dinitrobenzene to form N-(2,4-dinitrophenyl)-pyridinium chloride [8]:

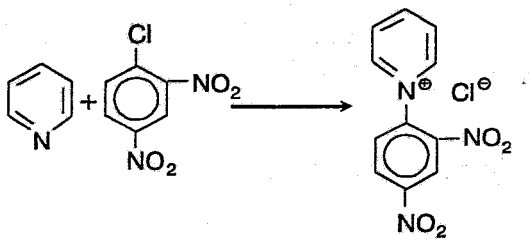

2. The pyridinium salt formed is very unstable in the presence of bases, which open the pyridine ring by removing the pyridine nitrogen. Reaction of this pyridinium salt with dimethyl-amine produces the 5-dimethylaminopenta-2,4-dienal, a so-called merocyanine and 2,4-dinitroaniline [9]:

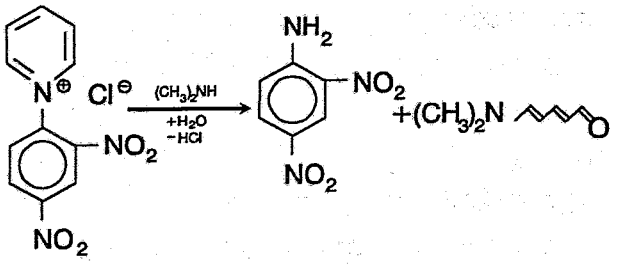

3. The merocyanine reacts with dimethylamine perchlorate to form the desired penta-methinium-salt, a so-called azacyanine, by elimination of water [9]:

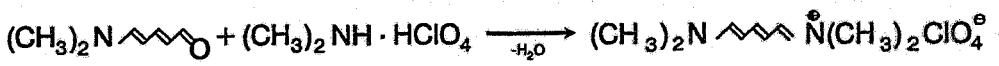

The structures of the merocyanine and the azacyanine were confimed by ^{13}C NMR-data.

References:

[1] Speranza, M., et al., J. Lab. Comp. Radiopharm. **19** (1982) 61

[2] Rose, T., et al., J. Am. Chem. Soc. **88** (1966) 1064

[3] Jutz, Ch., et al., Angew. Chem. **84** (1972) 299

[4] Schoeps, K.-O., et al., Appl. Radiat. Isot. **40** (1989) 261

[5] Schoeps, K.-O., et al., J. Lab. Comp. Radiopharm. **25** (1988) 749

[6] Bredereck, H., et al., Chem. Ber. **88** (1955) 1306

[7] Cleland, G. H., J. Org. Chem. **34** (1969) 744

[8] Zincke, Th., Lieb. Ann. **333** (1904) 296

[9] Malhotra, S.S., et al., J. Chem. Soc. (1960) 3812

4. IONCHROMATOGRAPHIC DETERMINATION OF THE RADIOCHEMICAL PURITY OF [^{123}I]NaI SOLUTIONS

F. Füchtner, C. Kretzschmar, R. Scholz, J. Steinbach

Introduction

Radioiodine has been produced for decades for a wide range of uses. One of its main applications is the labelling of radiopharmaceuticals. Since the late seventees ^{123}I has become more and more important. Its characteristics are a low radiation dose (only 1% of that of ^{131}I), a suitable γ-energy (159keV) and a favourable half life (13.3h). ^{123}I should be produced by the ^{124}Xe (p,2n) ^{123}Cs → ^{123}I process. This is the only way that allows generation of a product of very high radionuclide purity.

For labelling purposes the iodine has to be of special quality in terms of radiochemical as well as chemical purity.

We studied the radiochemical purity of the [^{123}I]NaI solution produced at the Nuclear Research Centre Karlsruhe for commercial purposes. Owing to oxidation by radiolysis and oxygen all [^{123}I]NaI solutions without stabilizers contain iodate [IO_3^-] and, after a prolonged storage, periodate [IO_4^-]. Another quality marker is the specific activity of the solution, i.e. the relation of radioactive and stable forms of iodine.

The aim of this work was to find an analytical method for determination of the concentration of the various stable and radioactive iodine species. This method has to meet the following demands:

- short analysis time,
- simple handling of radioactive samples,
- small sample volume,
- low detection limit (1% of the starting concentration is equivalent to approximately 40nM or 5ppb IO_3^- or IO_4^-),
- the results have to be reproducible.

An ion-exchange method performed with the help of an automatic liquid-chromatographic system is expected to meet these demands.

The problem associated with the simultaneous determination of the various iodine species is the separation of anions of very different selectivities in a short analysis time and in low concentrations:

The iodate ion has a short retention time and is eluated near the dead volume of the column. Iodide reacts in a different way. It is very hydrophobic and strongly interacts with the ion exchanger [1]. On most commercial columns, mainly developed for environmental analysis, the iodide ions have a high retention time and are usually not eluated as a detectable peak.

The retention increases more than proportionally to the capacity of the column [2]. Periodate ions may exist in the solution in the meta, meso and orthoform and we can therefore expect a higher charge of the anion and accompanied this by a strong retention.
A column of a low capacity should therefore be used. The ion exchange columns used were made by modifying a hydrophobic support with strong lipoidic ionic substances. For anion chromatography it is possible to coat silica-based RP(reversed phase) materials with alkyle quarternary ammonium salts.
Determination of radioactive impurities is carried out with a simple scintillation NaI(Tl) crystal. This detection system works with reproducible results up to 740MBq/20μl [^{123}I]iodine radioactivity level.
As there was no possibility at the time to work with real radioactive solutions inactive investigations to optimize separation conditions were carried out.

Experimental

For the investigations an HPLC system (Merck-Hitachi) was used, including a pump, a manual injection valve with 20μl sample loop, a column thermostat with column and a UV/vis detector.
As RP-18 support material we applied LiChrospher (5μm), Superspher (4μm), EnVisil (4μm) and Separon (7μm). The glass columns (150 x 3.3mm; LP-Prague) were filled with the supports by a slurry technique. In order to achieve ion exchange properties, a solution of the quarternary ammonium salts was pumped through the column up to equilibrium. During the process of coating a definite capacity was produced by using different kinds of salts (cetyl-trimethylammonium bromide (CTMA-Br), tetra-n-octylammonium bromide (TOA-Br) or tetra-kisammonium bromide (TKA-Br)) and different concentrations of the organic modifier
(50 - 80% acetonitrile/water). The capacity of the ion exchangers was determined by the UV break-through curve while modifying or equilibrating the column with a UV absorbing ionic solution.
For elution we used different solutions of citric acid and $H_2PO_4^-/HPO_4^{2-}$ buffer (pH 4...7, equilibrated with NaOH) and Na_2SO_4 (pH 3...7, equilibrated with H_2SO_4) in the concentration range of 1 to 10mmol/l.
Detection was accomplished by measuring the UV-absorption of iodate, bromide and nitrate at 205nm, while 225nm is more suitable for detection of iodide and periodate.
To determine separation factors and to estimate interferences with other possible anionic impurities, we also used chloride, bromide and nitrate in the standard solutions in a concentration range of 0.1 to 1mmol/l.

Results

The most effective chromatographic separation was obtained with the supports LiChrospher and Superspher. In the chromatograms with EnVisil all peaks have a tailing. Using columns filled with Separon, the backpressure was too high after modification so that the analytical times increased too much.

For an optimal separation we used a column with a capacity of about 10... 40μmol/g.

Applying Na_2SO_4 solutions as eluent the iodide peak shows a strong tailing, which cannot be reduced either by application of the varioas support materials or by modification with quarternary ammonium salts of various alkyl chain lengths (hydrophobia of the functional groups of the ion exchanger). The tailing was only reduced by application of an eluent with pH <5.0. At a pH value ≤6 a reduction of periodate is observed during analysis. When examining periodate in the chromatogram, an additional iodate peak is detected. At a pH value of 4.0 only iodate is found.

The optimum pH value is 5.5. No significant reduction of periodate occurs at this values, and iodide and periodate are eluted with only a small tailing. A 1mM solution of citric acid proved to be a suitable eluent of sufficient elution strength. The chromatographic conditions are shown in Fig. 1. The analysis is carried out within 10 minutes.

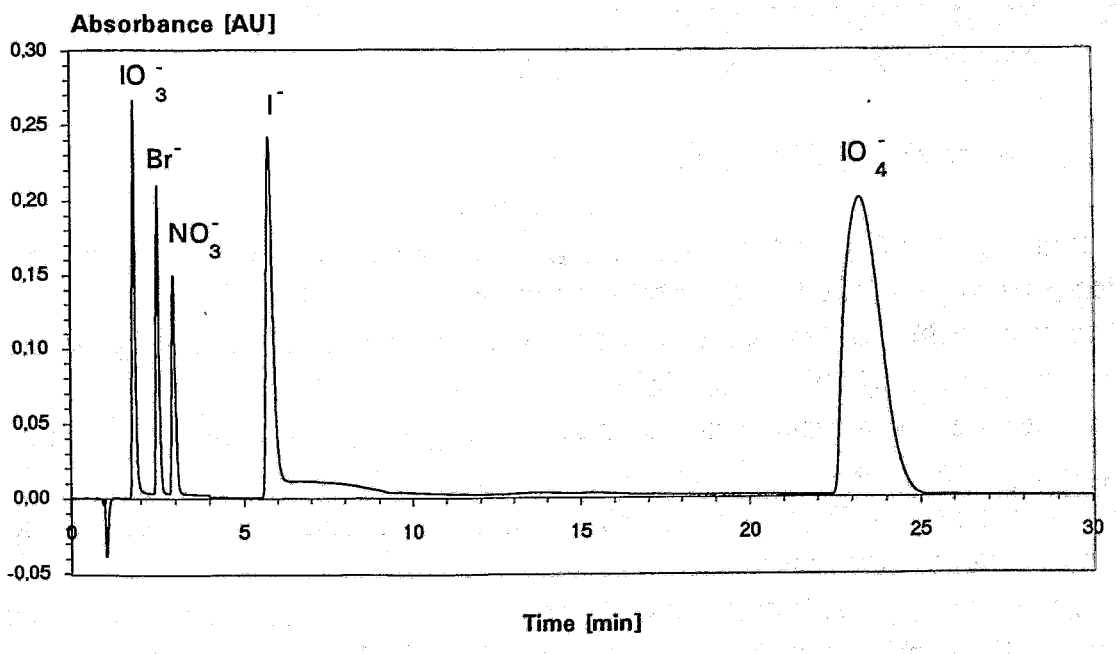

Fig. 1

analytical column:	d_I = 3.3mm; L = 150mm; T = 25°C;
ion exchanger:	LiChrospher RP-18; 5μm;
	coated with 5 mM TKA-Br in 80vol% acetonitrile;
	capacity: 21μM/column;
eluent:	1mM citric acid; pH 5.5;
	flow-rate:: 0.8ml/min; p = 9.8MPa;
detection:	1 - IO_3^-, 2 - Br^-, 3 - NO_3^-, 4 - I^-, 5 - IO_4^-;
	Peak 1 - 3: 205nm; Peak 4 - 5: 225nm;
sample:	injection volume: 20μl
	1, 2, 3, - 0.1mM; 4, 5 - 0.2mM

References:

[1] Weiss, H., "Handbuch der Ionenchromatographie", VCH Verlagsgesellschaft mbH, Weinheim, 1985

[2] Füchtner, F., "Aufbau und Erprobung eines HPLC-Meßplatzes zur Ionenchromatographie für den KKW-Betrieb", interner Bericht, 1988

5. CONCENTRATION AND PURIFICATION OF PERTECHNETATE SOLUTIONS BY CHEMICAL METHODS

S. Seifert, F. Schneider; G. Wagner

There are a lot of attempts to produce $(n,\gamma)^{99}Mo/^{99m}Tc$-generators with sufficient radioactive concentration of pertechnetate eluate for nuclear medical use.
Because of the high content of inactive molybdenum in the irradiated MoO_3 large generator columns containing alumina are needed.
That results in large elution volumes containing relative high Mo contents and low radioactive concentration on ^{99m}Tc.
For these reasons a simple and convenient method for concentration and purification of pertechnetate solutions may be desirable.
The methods used in the laboratory are either expensive (sublimation) or have the disadvantage that the resulting pertechnetate solution contains impurities of the extracting medium (extraction with methylethylketone) which decrease the labelling yield.

To overcome these drawback, two different methods have been tested:.

Complex formation with following adsorption and reoxidation

Reduction to "Tc-hydroxide" with following adsorption and reoxidation.

Complex formation

Tc forms a reactive complex with ethyleneglycol (eg) in alkaline solution. The Tc(V)-complex $[TcO(eg)_2]^-$ is commonly used as a precursor for the syntheses of other Tc-complexes [1]. Its preparation is also possible in a large volume at n.c.a. level and pH 12 by reduction of pertechnetate with 0.05ml stannous chloride (1mg/ml ethanolic solution) in the solution of 0.5ml eg in 50ml pertechnetate generator eluate.
The Tc-eg complex is stable in ligand excess over some hours and can be adsorbed on Sephadex G 100. By washing with water the ligand excess is removed and the Tc-eg complex decomposes on the adsorbent. After 1-2h the Tc is oxidized to pertechnetate and can be eluted from the Sephadex column.
The method described is a possible way of concentrating pertechnetate solutions but the procedure takes a long time and the yield is only about 50-60%.

Reduction to "Tc-hydroxide"

The reduction of $[^{99m}Tc]$-pertechnetate solutions with a suitable reducing agent in connection with the adsorption of the "reduced hydrolyzed technetium" represents a better method for concentration.

The most suitable reducing agent is stannous chloride. 50μg allows a quantitative reduction of pertechnetate at n.c.a. level also from big volumes of 50-100ml in a short time of 1-2min.

For adsorbing the "Tc-hydroxide" different materials were tested (alumina, glass spheres, glass filters G4 and G5, cellulose acetate filters).

The most promising results were obtained by using alumina. The reduced hydrolyzed technetium is adsorbed quantitatively on 1-2g alumina (98.4% adsorbed Tc-hydroxide evaluated by 20 experiments).

For reoxidation of Tc(IV) to Tc(VII) we studied treatment both with H_2O_2 in ammonia and oxidation by nitrate ions at higher temperatures.

For oxidizing the reduced technetium on alumina 2-3 drops of a 25% H_2O_2/ammonia solution are sufficient. After evaporation of H_2O_2 the pertechnetate can be eluted by 2-3ml isotonic saline.

It is known that alkali nitrates lose oxygen during heating. Sodium nitrate adsorbed on alumina gives up NO_2 which decomposes to NO and O at temperatures $>140^oC$ [2]. The native oxygen should be able to oxidize the Tc(IV) to Tc(VII), which can be eluted from alumina.

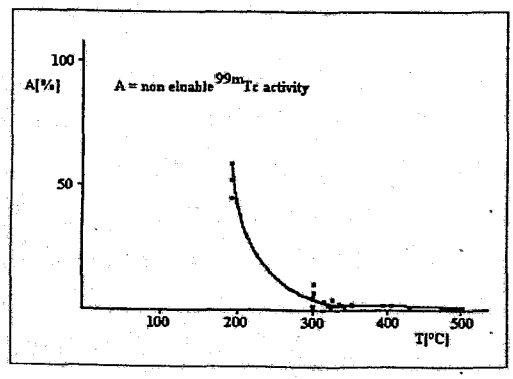

Fig. 1: Dependence of the non-eluable Tc-activity on the reoxidation temperature (alumina/$NaNO_3$)

We tested $NaNO_3$ and NH_4NO_3 and found that both compounds oxidize more than 95% of the Tc(IV) to Tc(VII) at temperatures $>300^oC$ (Fig.1). The elution of pertechnetate is quantitative only by using alumina. 10-20% of the Tc activity remain on the column if other adsorbing materials are used.

Whithout nitrate only less than 2% of Tc-hydroxide is oxidized at 300^oC. A sufficient amount of nitrate is adsorbed if the alumina is washed with a 0.9% $NaNO_3$ solution before adsorption of Tc-hydroxide. If pertechnetate is reduced in 0.9% $NaNO_3$ solution with stannous chloride, the low Cl^--concentration does not interfere with reoxidation.

The oxidation of Tc(IV), adsorbed on alumina, by nitrate ions represents a suitable method for concentration and purification of pertechnetate solutions. In connection with a simple equipment, similar to a commercial generator, it should be applied if fission molybdenum generators are not available.

References:

[1] Thomas, R.W. et al., Inorg. Chem. **19** (1980) 2840

[2] Gmelins Handbuch der Anorg. Chemie, Band **21** (1966) 1007

6. COMPARTMENTAL ANALYSIS OF BLOOD-BRAIN TRANSFER AND PROTEIN INCORPORATION OF L-[^{75}Se]SELENO-METHIONINE IN RAT BRAIN

R. Bergmann, P. Brust, G. Kampf, M. Kretzschmar, H.H. Coenen[1], K. Hamacher[1], G. Stöcklin[1]

[1]Institut für Chemie 1, Forschungszentrum Jülich

Different attempts have been made to measure the rate of protein synthesis in the brain with positron emission tomography (PET). Usually [^{11}C]-labelled amino acids with a half-life of 20.48min, e.g. L-[^{11}C]leucine or [^{11}C]methionine, are used for this purpose. Also [^{18}F] labelled amino acids are recommended for the evaluation of protein synthesis by PET. However the synthesis yields are relatively small. In methionine the sulphur atom may be replaced by the positron-emitting [^{73}Se] or the γ-emitting [^{75}Se] with half-lives of 7.15h and 119.78d, respectively. In principle, selenium-labelled methionine should be appropriate particularly for studying long-time metabolic processes like protein synthesis with PET. In order to check this possibility we have studied in rats the blood-brain transfer, protein incorporation and metabolism of L-[^{75}Se]selenomethione (SeMet) with high specific activity.

Methods

The experiments were performed on 42 male Wistar rats. The animals were slightly anaesthetised with ether. SeMet (500KBq, > 10Ci mmol^{-1}) (1) was injected i.v. and the rats were decapitated at 14 different times (3 animals/time) up to 360min p.i. The brain was removed and immediately stored in liquid nitrogen. Blood and plasma samples were put on ice. All plasma sample and brain samples at 1.5, 5.1, 20, 120, 240, and 360min were analysed for labelled fractions of free SeMet, metabolites, and SeMet bound to t-RNA and proteins. A three-compartment model was applied to the data to calculate the blood-brain transfer constant, K_1, as well as the rate constant of SeMet incorporation into proteins (k_3) using the following equations:

$$\frac{dM_p(t)}{dt} = k_3 M_e(t) - k_4 M_p(t) \quad (1)$$

$$\frac{dM_e(t)}{dt} = K_1 C_a(t) - k_2 M_e(t) - k_3 M_e(t) + k_4 M_m(t) \quad (2)$$

where M_e and M_p are the amounts of free SeMet and SeMet incorporated into proteins, respectively. M_m represents the amount of [^{75}Se] bound in proteins and different metabolites. The rate constants k_3 and k_4 were calculated directly from equation 1 using the measured amounts of free and protein-bound SeMet in the rat brain. These constants were used in equation 2 to calculate K_1 and k_2.

Results

The means of the measured values are listed in Tab. 1. The rate constants k_3 and k_4 estimated from equation 1 are 0.020 ± 0.003min^{-1} and 0.003 ± 0.001min^{-1}, respectively. From equation 2 the blood-brain transfer constant K_1 was calculated (0.151 ± 0.031ml g^{-1} min^{-1}). The rate constant of brain-blood transfer was 0.124 ± 0.006min^{-1}.

Tab. 1: Amounts of L-[^{75}Se]selenomethione (nmol/g) in plasma and brain at different times after injection

Time (min)	Plasma	Brain (total)	Brain (protein)	Brain (t-RNA)	Brain (free Met)
1.5	0.0712	0.0505	0.0058	0.0012	0.0420
5.1	0.0347	0.0371	0.0063	0.0008	0.0299
20	0.0239	0.0509	0.0118	0.0011	0.0230
120	0.0125	0.0398	0.0270	0.0007	0.0066
240	0.0129	0.0320	0.0268	0.0006	0.0044
360	0.0105	0.0395	0.0340	0.0007	0.0041

Comments

The kinetic constants obtained in this study are on the one hand higher (K_1) and on the other hand lower (k_3 and k_4) than those measured recently in anaesthetised dogs with L-[^{11}C]methionine (2). Different affinities to binding sites (transporter, enzymes) or species differences may be the reason for this. The apparent incorporation rate of methionine is expected to be about 0.6nmol/min/g in our studies, assuming a content of free endogenous methionine in the brain of 28nmol/g (3). This is very close to values obtained with L-[^{35}S]methionine (0.68 nmol/min/g) in rats (4). It is concluded from the studies that L-[^{73}Se]-selenomethione may be an appropriate tracer for measuring brain protein synthesis with PET.

Supported by grant No. 41143309 (27/09/90); NBL 031a / Forschungszentrum Jülich GmbH.

References:

[1] Römer J. et al., Appl. Radiat. Isot. 43 (1992) 495

[2] Brust P. et al. J. Neurochem. 59 (1992) 1421

[3] Planas AM et al., J Cereb Blood Flow Metab 12 (1992) 603

[4] Grange E et al., J Cereb Blood Flow Metab 11 (1991) (Suppl. 2) S356.

7. APPLICATION OF AN IMAGE PROCESSING SOFTWARE FOR QUANTITATIVE AUTORADIOGRAPHY

E. Sobeslavsky, R. Bergmann, M. Kretzschmar, U. Wenzel

The present communication deals with the utilization of an image processing device for quantitative whole-body autoradiography, cell counting and also for interpretation of chromatograms.

It will be shown that the system parameters allow an adequate and precise determination of optical density values. Also shown are the main error sources limiting the applicability of the system.

Extensive biological research requires high speed image processing techniques to promptly manipulate and analyse images. Such systems are realized both on the hardware and on the software sector. They improve accuracy and reduce the time required for analysis. Examples of application in biochemical research are cell counting, visualisation both of organizing and functioning of the brain etc. A broad field of utilization is autoradiography in receptor-ligand studies, see e.g. [2], in chromatography or in investigations of tissue sec-tions.

The images being investigated are captured by an optical acquisition system (converting a source image to a digital one) and in a following step manipulated by the image processing software VISILOG^{TM} [1]. This software is able to produce e.g. a number of statistical measures of the incoming image data including ensemble averages, variances, minima/ maxima etc.

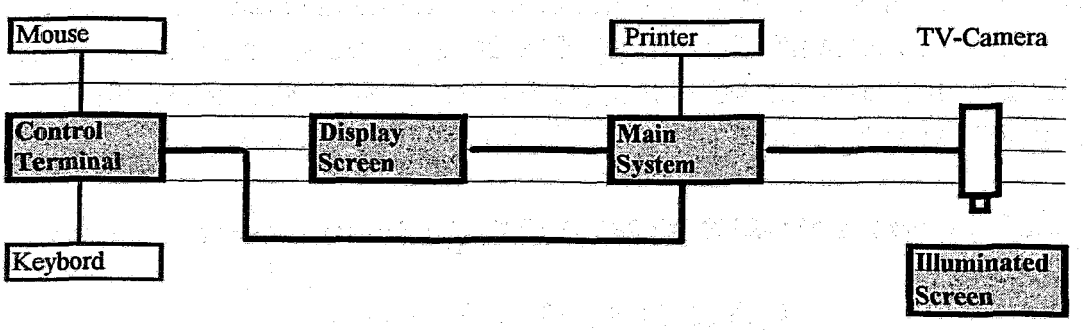

Fig.1. System configuration

The actual system configuration to run VISILOG^{TM} is composed of a standard IBM compatible PC (486DX/33 MHz+246KB Cache), a display device, a control terminal, from which one issues commands to the system, an acquisition device offering camera input by a video camera (SONY, CCD Video Camera Module, H/V Version, model XC-57CE) and image digitalization.

The actual design should be preferably applied to quantitative autoradiography, it should be used to characterize cell agglomerations also. Autoradiography appears to be suitable to test the given image processing device because of its precision.

As a first step one has to find out how the system responds to a well defined sequence of gray values related to the optical density of the autoradiogram. With this standard curve in hand, the optical density of autoradiograms produced from radioactively labelled thin tissue sections can be quantitatively converted to radioactive concentration.

The sequence used for testing the system was available as Amersham autoradiographic [^{3}H] micro-scales [5] calibrated for a range of tissue equivalent values approximately of 1.4 - 32.0 nCi/mg. A log-log linear relationship exists between tissue equivalent tritium content and the corresponding optical density.

The film was placed on a illuminated screen, cf. Fig. 1, digitalized and for further use stored in the image memory ("incore processing storage"). It can be visualized on the display screen if necessary. Once the image is captured, processing does not depend on the actual conditions of the image acqusition (e.g. time of recording, adjustment of the camera lens, illumination of the screen etc.).

Care has been taken to exclude a feed back of the TV camera. One has also to take into account that the response of the camera is related in a non-linear manner to the illuminant intensity of light which strikes the phototube of the camera, e.g. [3].

As a next step regions of interest (ROI) were specified for every gray level available on the film. The image processing system now computes the histogram and the intensity centered moments of order one to four over the region selected before. Such regional intensity measurements provide increased statistical confidence as compared to individual spot or point measurements and compensate for random noise variations.

Fig. 2 represents the system response on a gray level stage, see above. The curves show that one has to interpolate between non-linear regions if one wishes to determine the relationship between the amount of radioactivity and the computer generated digitized optical densities.

The reproducibility of the calibration curve is fairly satisfactory. The main error sources are listed in Tab. 1.

Tab. 1. Error sources characterizing the actual image processing device

errors within an given gray level of the calibrating micro-scale film	5% - 10%
errors outside a gray level, e.g. scratches, shadows on the film	3% - 7%
errors resulting from the optical system, TV camera etc. (i.e. errors from the bare illuminated screen without the film)	3% - 5%
errors originating from outer conditions, e.g. time of recording, power fluctuations etc.	1%
errors from individual choice of ROI (regions of interest) by the operator	1%

On the present status of work no attempt was made to exclude inhomogeneities in the screen illumination nor to exclude undesired high frequency (e.g.scratches) and low frequency (e.g. shadowing) perturbations on the film itself. Note that VISILOG^{TM} is able to provide such corrections.

The problem of counting cell agglomerations was attacked by help of a very simplified model.. Here the precision of intensity determination seems not so crucially affect the measurement as in a smooth density change typically for autoradiography.

For higher comfort a VISILOG^{TM} playback routine could be used to combine successive operations on the investigated images. Most of current problems, however, need to interactively operate on VISILOG^{TM} functions. So the applicability of such routine is rather limited.
Image analysis usually provides large quantities of analysable data. So VISILOG^{TM} allows to include the image functions in a C-language (version 4.0 and above) or in a FORTRAN program to use the results of analysis for subsequent mathematical interpretation, storage on external files etc. At the present, however, early stage of investigation no use was done of that possibility.

As an example for the use of quanitative autoradiography (QAR) served the biodistribution of the antiarrhytmic compound Bonnecor labelled with ^{14}C. A Wistar rat weighing 170g was orally given 1.1MBq of ^{14}C- Bonnecor (3-carbethoxyamino-5-dimethylamino-[1-^{14}C]- acetyl-10,11-dihydro-dibenz [b,f] azepine hydrochloride). 24 hours after application the rat was sacrified and a whole body autoradiography was performed as described by Ullberg [4]. The

optimum exposure time for the 50µm thick freeze dried cryosections on the ORWO RF64 X-ray film was eleven weeks.

A stock solution of benzylic acid-1,1 [^{14}C] dimethylpiperidinylesteriodide containing 296 kBq/ml served for the preparation of radioactive standard scale. From this a series of dilution were made in a geometric order in the range from 296kBq/ml to 259Bq/ml. Strips of FND thin layer chromatography foils with 50µm cellulose coating were immersed singly into the radioactive dilutions. The dried impregnated strips were mounted parallel on plastic foils in the correct order of dilutions and exposed along with the 50µm thick dried whole body cryosection for varying lengths of exposure on ORWO RF64 X-ray films.

Using the VISILOG^{TM} image processing system to analyze the autoradiograms we measured the average optical density values over the entire standard area. From these measurements, we constructed exposure curves relating optical density to Bq/g tissue equivalent.

Tab. 3 presents radioactivity data derived from autoradiograms of whole body section and radioactive scale, respectively, exposed along on X-ray RF 64 ORWO film for eleven weeks.

Results obtained by the actual VISILOG^{TM} configuration agree fairly well with liquid scintillation spectrometry data and with visual observation.

Tab. 2: Calibration of autoradiographic [^{3}H] micro-scales (Amersham), cf. [5].
The table demonstrates that the calibration of the given system remains fairly reproducible for altered recording conditions (e.g.time of recording, power fluctuations, adjustment of the optical system), see column (a), (b), and enlargment, case (c).

level	tissue equivalent, [nCi/mg]	optical density of the gray level staircase in a scale of 255 density units		
		(a) 1 pixel=1.013 x 10^{-2} cm *optical density of the illuminated screen without film:* I = (224 ± 8) units (of 255)	(b) 1 pixel = 1.013 x 10^{-2} cm I = (224 ± 8) units (of 255)	(c) 1 pixel = 1.244 x 10^{-2} cm I = (182 ± 9) units (of 255)
1	32.0	53± 4	49 ± 5	55± 4
2	22.4	69 ± 5	68± 5	72± 6
3	13.2	90 ± 6	88 ± 6	88± 5
4	9.1	116 ± 7	115 ± 8	114 ± 5
5	5.5	136 ± 9	135 ± 9	131± 5
6	3.2	150 ± 10	151± 10	145± 7
7	2.2	164± 10	162± 11	162± 9
8	1.4	172 ± 9	173± 10	172 ± 7

Tab. 3.1.: Biodistribution of Bonnecor marked by ^{14}C.
Calibration of the gray level staircase.

Level	Tissue equivalent, [µCi/g]	optical density as measured by VISILOG^{TM} in a 255-degree-scale
1	0.005	210 ± 8
2	0.01	162 ±8
3	0.03	88 ± 11
4	0.06	30 ± 5
5	≥0.12	≤9 ± 3

Tab. 3.2: Biodistribution of Bonnecor marked by ^{14}C.

Organ	optical density as measured by VISILOG^{TM} in a 255-degree-scale	tissue equivalent, [µCi/g]
Content of intestines	≤30	≥0.056
Liver	74± 8	0.037 ± 0.004
Kidney:		
total	138±22	0.012 ± 0.002
inner renal cortex	118 ± 11	0.022 ± 0.002
external renal cortex	128±8	0.019 ± 0.001
calix of the kidney	135± 4	0.017 ± 0.001
renal medula	155± 8	0.012 ± 0.001
Testicle	146 ± 14	0.014 ± 0.001

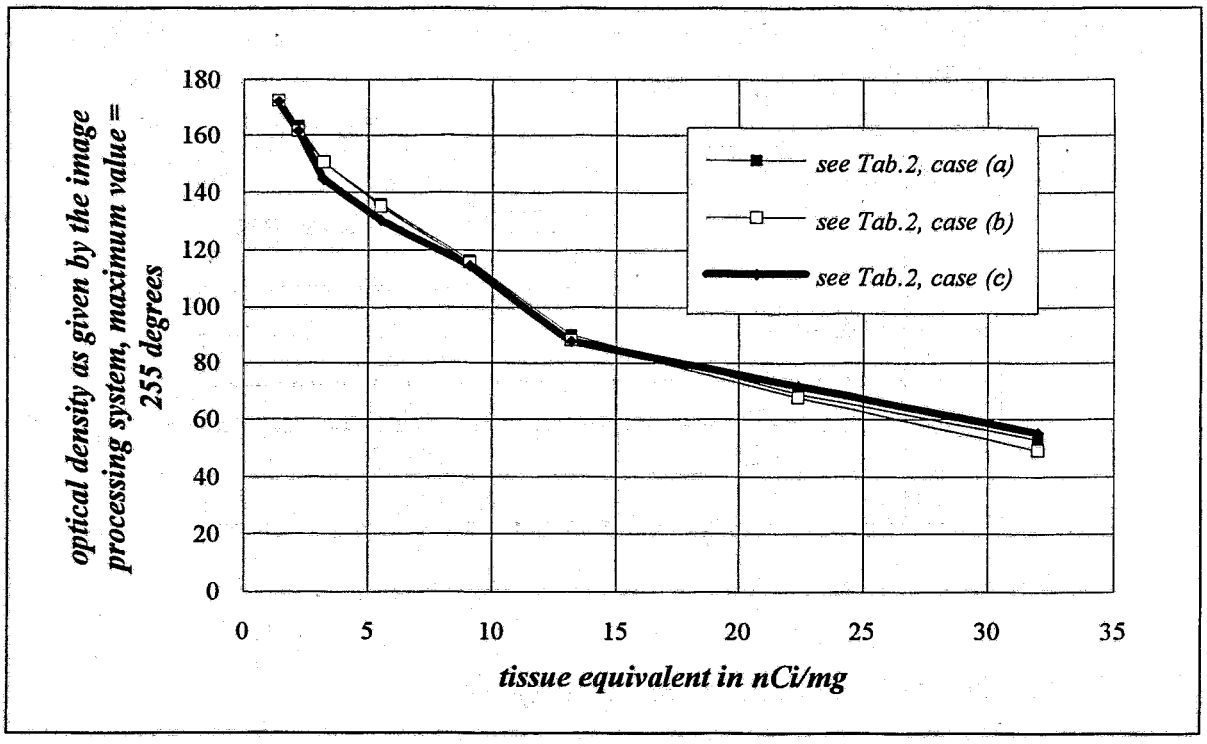

Fig. 2. Standard curve for 4 weeks exposure time. Abscissa represents tissue equivalent ^{3}H-concentration, and ordinate - the corresponding optical density values (in a 255-degree scale) for each of the eight activity levels in a [^{3}H] micro-scale, cf. [5].

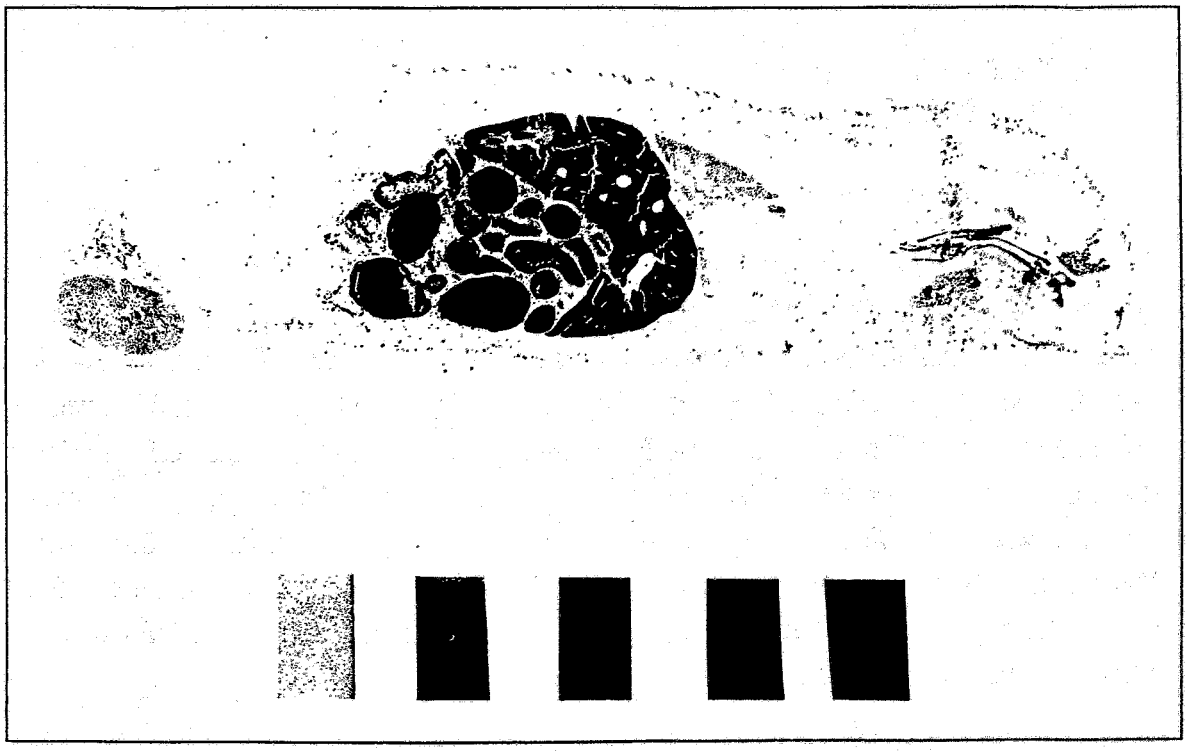

Fig. 3. Whole body autoradiogram of a rat 24 h after oral application of 1.1 MBq ^{14}C - Bonnecor, exposure time 11 weeks, see text

References:

[1] VISILOG^{TM}, Image Processing Software, NOESIS S.A., Centre d'Affaires de Jouy, 5 bis, Rue de Petit Robinson, 78350 Jouy-de-Josas, France, Version 3.6.1, June 1991

[2] Kuhar, M.J., et al., J.Chemical Neuroanatomy **4** (1991) 319

[3] Miller, J.A., et al., J. Neurosc. Meth. **22** (1988) 233

[4] Ullberg, S., Acta Radiol. Suppl. **118** (1954) 1

[5] Autoradiographic [^{3}H] micro-scales, Certificate, Amersham, 1991.

8. DEVELOPMENT OF A LABORATORY INFORMATION MANAGEMENT SYSTEM (LIMS) FOR RADIOPHARMACOLOGICAL RESEARCH PROJECTS

E. Zugehör, R. Syhre

The characterization of radioactive preparations in vitro and in vivo requires a wide spectrum of radiochemical and analytical, biological, biochemical and animal experimental methods. Such methods produce heaps of highly diversified data and information, including those required to meet legal obligations. This information hase to be managed, processed and documented efficiently and reliably. Commercial programs do not exist for that particular range of functions. The extent of functions cannot be realized with simple database programs like DBASE (Ashton Tate Corp.). A Laboratory Information Management System (LIMS) was therefore developed. This System is based on OBJECT VIEW (Matesys Corp.) as a database development system and EXCEL (Microsoft Corp.) as a table calculation component.

Tasks and Requirements

LIMS includes the following functions: registration, calculation, documentation, book-keeping and management of various laboratory data and information in large numbers. Flexible association of data as well as guaranteed permanent and central access to data and results are essential requirements for research projects and have to be met by an LIMS. Attention to security and authorization are necessary. Up-do-date book-keeping and archiving of data are required to comply with legal stipulations.

Concept

LIMS is based on window applications, specified by the experimental method used. It uses a common database as well as common program routines to manage and process the data. A relational model was chosen to describe data, data relationships and consistency . The result is a specific set of tables for each method, connected logically through references. The windows front end database development system OBJECT VIEW (Matesys Corp.) was used for application of the model . The main advantages of this system are:

- Interface to QuadBase SQL with Security and Authorization, Transaction Processing, Referential Integrity (SQL=Structured Query Language, the standard relational database language)
- Optimized access to Microsoft/Sybase SQL Server
- Visual Interface to create objects on the screen
- High Level Functional Interface for associating a method with an object
- Low Level Functional Interface, optionally in Object View BASIC or C

- Interface for EXCEL, WORD (Microsoft Corp.) and other window applications which support the DDE protocol (DDE=Dynamic Data Exchange)

The structure of an application developed with OBJECT VIEW may be illustrated by a staircase model (Fig.1)

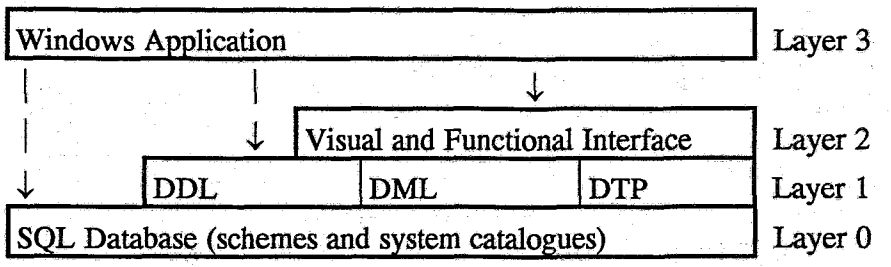

Fig. 1: Staircase model of an LIMS Application

Layer 0:SQL Database (SQL=Structure Querry Language)
Layer 1:SQL Components (DDL=Data Definition Language, DML= Data Manipulation Language, DTP=Data Transaction Processsing)
Layer 2:Visual and Functional Interface
Layer 3:Application Layer

Application

As a first application a SQL Tool was developed . The user can work with the database without any knowledges of the database language. Convenient inserting and updating of tables and views is provided. For data input, output and processing the standard calculation program EXCEL (Microsoft Corp.) was fully included into the SQL Tool . The SQL Tool is not only an important part of the LIMS, but has also been used for programs like financial calculations and registers of chemicals and literature.

For animal experiments, i.e. investigation of the biodistribution and biokinetics of radioactive preparations, a relational data model was developed and integrated into a database. Fig 2. shows the components of the database application, that can be varied by the user according to the individual scope of functions.

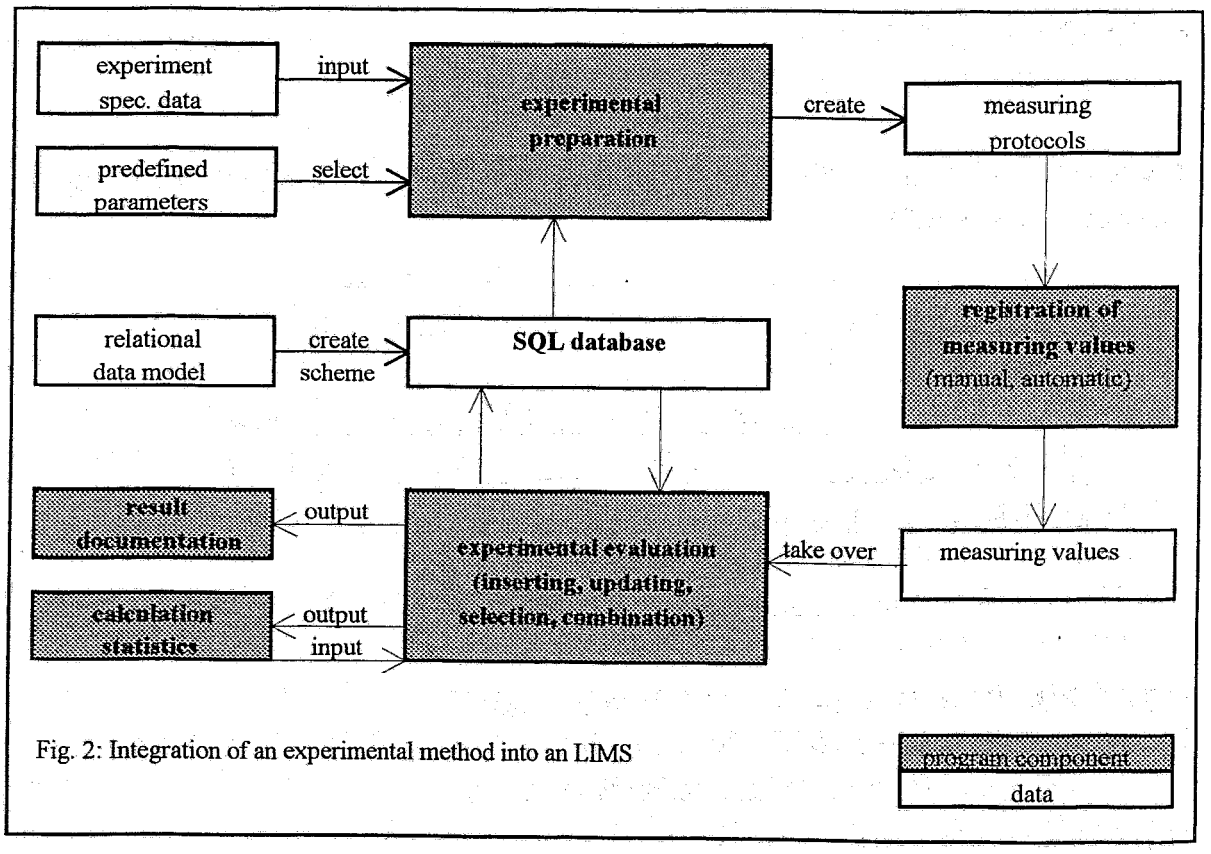

Fig. 2: Integration of an experimental method into an LIMS

References:

[1] Korth, H. F., Database System Concepts (1991) ISBN 0-07-044754-3

[2] Trautloft, R., Datenbanken: Entwurf und Anwendung (1990) ISBN 3-341-00861-6

[3] MATESYS CORPORATION; N.A. Object View, The grafical Front End Relational Databases: User Guide, Reference Guide, SQL Primer, An Introduction to QuadBase SQL

9. HPLC SEPARATION OF PENTAVALENT ISOMERIC TECHNETIUM-99m-COMPLEXES OF DIMERCAPTOSUCCINIC ACID AND THEIR BEHAVIOUR UNDER VARIOUS CONDITIONS

L. Lindemann[1] , C. Schüttler[1] , C. Neumann[2] , R. Michael[2], S. Seifert, B. Johannsen
[1]Bundesgesundheitsamt, Institut für Sozialmedizin und Epidemiologie, Berlin
[2]Medizinische Fakultät (Charité) der Humboldt-Universität zu Berlin, Klinik für Nuklearmedizin

Pentavalent technetium-99m-dimercaptosuccinic acid (^{99m}Tc(V)-DMSA) has become established as a new sensitive and specific radiopharmaceutical for imaging a number of tumours. It is used in particular for localization of metastases of medullary thyroid carcinomas [1-3].
The mechanism of the Tc(V)-DMSA uptake in tumours has not yet been identified. The radiopharmaceutical has been discussed as a metabolic mimic of phosphate [4] without knowledge of the structure of the complex. Any rational explanation however requires a known molecular structure as a prerequisite.
Now it is known that the radiopharmaceutical contains technetium in the pentavalent state coordinated by 1,2-dithiolate ligands. The complex is identical with chemically characterized $[^{99}TcO(DMSA)_2]^-$ showing a square pyramidal configuration [5,6].
Carrier-added and also no-carrier-added preparations consist of mixtures of three stereoisomers [7]. All three isomers are also significant components of the radiopharmaceutical, which raises the question which of them are tumour-specific [4].
The isomers result from different orientations of the carboxylate groups in the DMSA ligands as illustrated in Fig. 1.

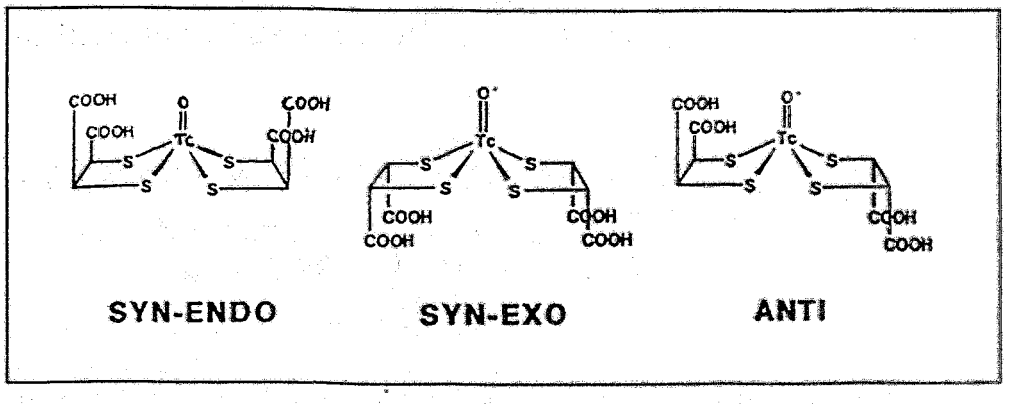

Fig. 1: Geometrical isomers of $[TcO(DMSA)_2]^-$

The radiopharmaceutical preparation described in [8] contains two major and one minor isomer. In the present work we have investigated the occurence of the three isomers in dependence on the method of preparation.

Preparation methods:

(1) Reduction with $SnCl_2$ (Radiopharmaceutical preparation)

2ml of ^{99m}Tc pertechnetate saline and 0.1ml of a solution of 7% $NaHCO_3$ were added to a vial of ROTOP-DMSA-kit for renal imaging containing 1.0mg of dimercaptosuccinic acid, 0.42mg of stannous chloride dihydrate and 0.1mg of ascorbic acid.

The alkaline solution (pH 9) was shaken and allowed to stand for 10 minutes.

In analogous carrier added experiments an amount of 0.5µmol ^{99}Tc was also added.

(2) Ligand exchange reaction with Na gluconate

Up to 80µl of a solution of $SnCl_2$ (2mg/ml in 0.1N HCl) was gradually added to a solution containing 2ml ^{99m}Tc pertechnetate, 25 mg sodium salt of gluconic acid and, in case of carrier-added tests, 0.5µmol ^{99}Tc.

The quality of the Tc gluconate preparation was checked by thin layer chromatography (chromatographic method A). When Na gluconate was formed a solution of 50mg DMSA in 1ml physiological saline was added.

(3) Ligand exchange reaction with $[TcOCl_4]^-$

A small amount (1-2mg) of $Bu_4N[TcOCl_4]$ dissolved in 0.5ml acetone was added to 0.5 ml of a solution of 50mg DMSA in acetone. Tc-complex formation was completed within a few minutes.

The quality of preparations (1) and (2) was checked by thin-layer chromatography (chromatographic method B). A typical TLC-chromatogram is shown in Fig. 2.

Samples of Tc(V)DMSA prepared in the three ways described were analyzed by HPLC. The gradient system used in this study [4] (chromatographic method C) separated all three isomers by baseline separation and made it possible for us to estimate their relative concentrations.

Chromatographic methods:

(A) Thin layer chromatography (TLC) on SILUFOL eluting with acetone for quality control of ^{99m}Tc gluconate preparations.

R_f-values	0.0	Tc(V) gluconate
	0.95 - 1.0	TcO_4^-

(B) Thin layer chromatography (TLC) on Silicagel 60 (MERCK) for preparation control of DMSA complex, eluting with n-butanol/acetic acid/water (3/2/3)

R_f values	0.00 - 0.35	Tc(IV)DMSA
	0.40 - 0.50	Tc(V)DMSA
	0.65 - 0.70	TcO_4^-

The thin layer strips were scanned under a gamma well probe detector (Berthold).

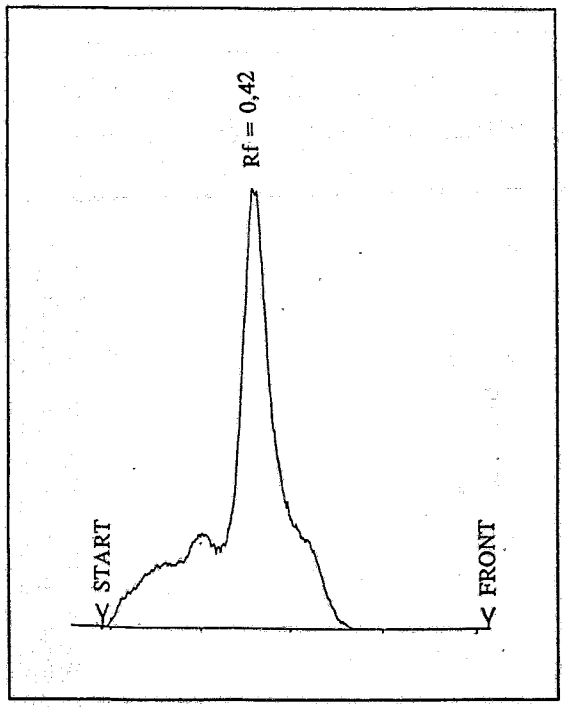

Fig. 2: TLC chromatogram of a Tc(V)DMSA complex solution according to procedure (1)

(C) High performance liquid chromatography (HPLC)

Precolumn:	3cm C_{18} on Nucleosil (Machery & Nagel)
Column:	15cm PRP-1 (Hamilton)
Eluent:	A= 0.1% trifluoroacetic acid in water
	B= 0.1% trifluoroacetic acid in acetonitrile
Rate of total flow:	2ml/min
Gradient:	0min B = 0%
	10min B = 50%
	16min B = 50%
	20min B = 0% (stop)
	created by SHIMADZU-pumps (LC-6A)

Detection: For no carrier added experiments by gamma-radiation monitoring with a gamma well probe detector (Berthold); for carrier added tests by UV detection at 420 nm (SHIMADZU SPD-6AV)

R_T values [min]:		
	0.9 - 1.0	TcO_4^-
	4.8 - 5.2	isomer I
	6.1 - 6.2	isomer II
	7.1 - 7.2	isomer III

Fig. 3 shows typical chromatograms of preparations according to method (1).

The portion of each isomer in the mixture depends on both the methods used and the conditions of storage. We studied the influence of pH-value and temperature on the ratio of the isomers. Tab. 1 shows the relative isomer distribution for the different preparation methods.

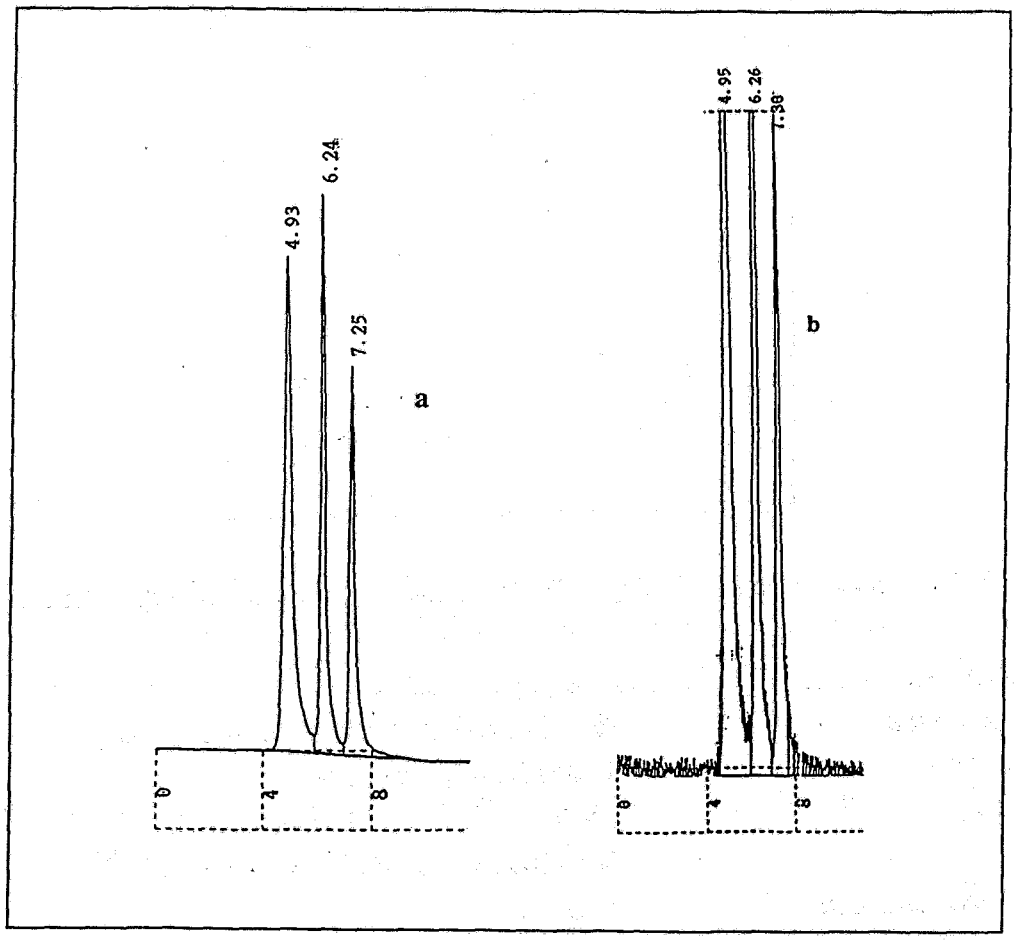

Fig. 3: HPLC chromatograms of the $^{99/99m}$Tc(V)-meso-DMSA complex (pH=9)
a=UV detection ; b=gamma radiation monitoring

Tab. 1: Relative isomer distribution for the three different preparation methods used

Preparation method	isomer I	isomer II	isomer III
(1) $SnCl_2$ reduction	45 %	31 %	24 %
(2) Tc gluconate	45 %	30 %	25 %
(3) $TcOCl_4^-$	37 %	28 %	35 %

In further experiments the influence of pH-value and temperature on the isomer ratio was studied.

To a usual radiopharmaceutical preparation at pH=9, 0.1N HCl was added up to pH~1. This acidic solution was analysed by HPLC immediately after preparation and then at hourly

intervals. The pattern changes with time. After 5h isomer II represents the major peak, as seen in Fig. 4 (I / II / III = 40 / 50 / 10%). There is no further change after a period of 72 hours.

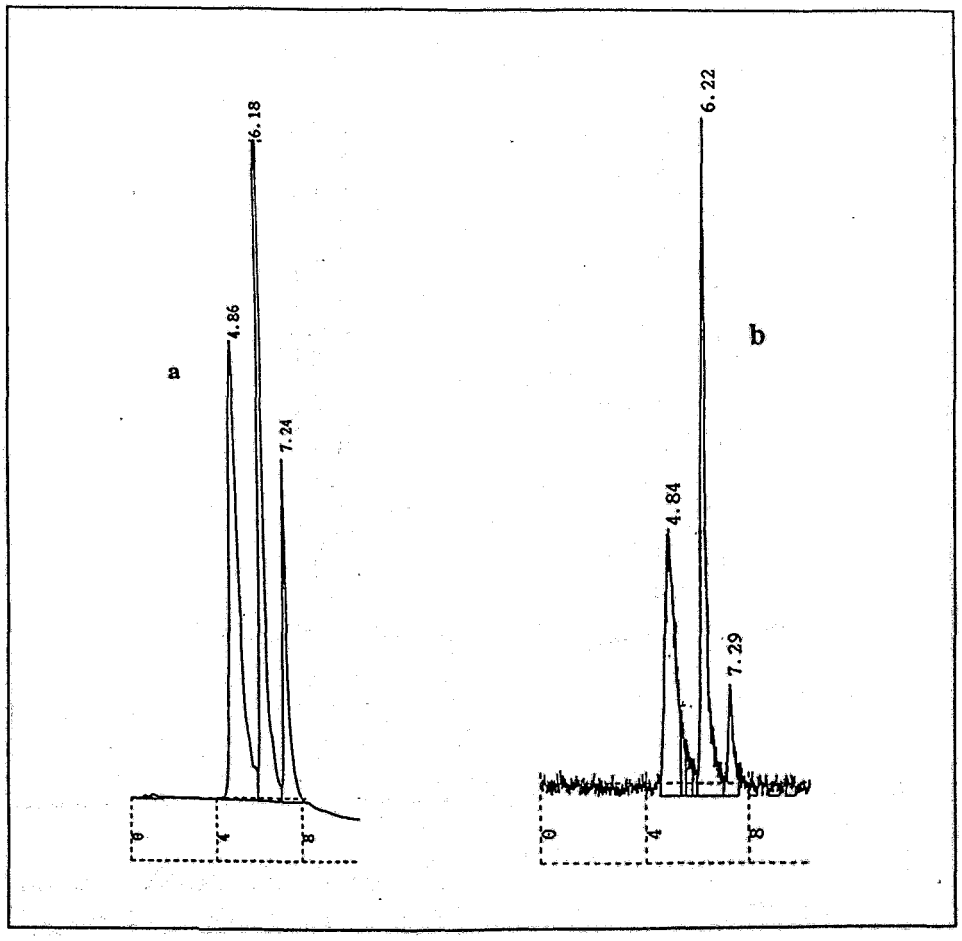

Fig. 4: HPLC chromatograms of the $^{99/99m}$Tc(V)-meso-DMSA complex solution 5 hours after pH decrease at pH=1; a=UV detection; b=gamma radiation monitoring

Temperature is another factor that could affect distribution. After heating the preparation at 85°C in a water bath for 45 minutes isomer III was found to have increased (I / II / III = 43 / 22 / 35%) (Fig. 5). However, after 1 to 2 hours at room temperature, the original ratio (Tab. 1) was detected.

Another point of interest was the peak allocation for the Tc(V)DMSA complex prepared with racemic DMSA as the ligand. For this experiment a ligand exchange reaction (preparation method 2) was carried out with 50mg rac. DMSA. The result was checked by HPLC. Fig. 6 shows a chromatogram of the complex solution. In addition to the known isomers of Tc(V) meso DMSA (peak 1: R_T=4.99; peak 3: R_T=6.21 and peak 5: R_T=7.27min) we also found other components, as expected, viz. at R_T=5.64, 6.68 and 8.00min. The relative isomer concentrations are also given in Fig. 6.

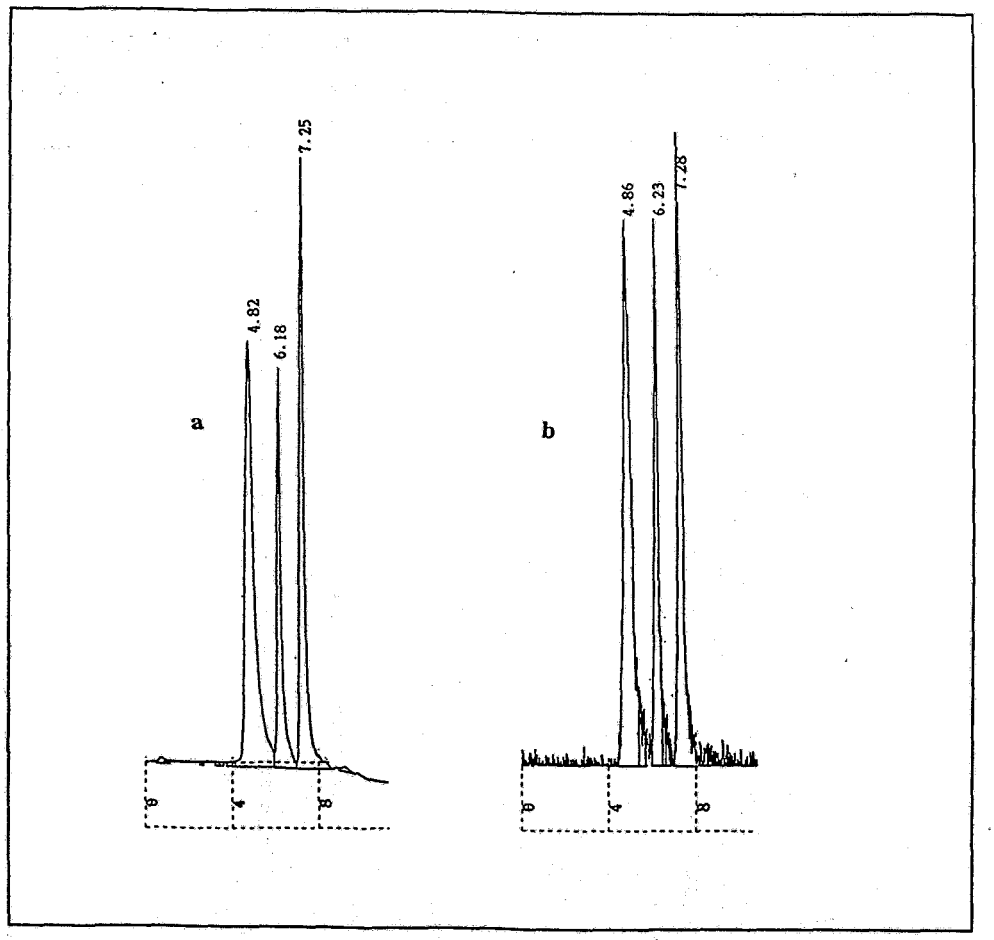

Fig. 5: HPLC chromatograms of the $^{99/99m}$Tc(V)-meso-DMSA complex solution after heating at 85°C for 45min; a=UV detection; b=gamma radiation monitoring

The same chromatogram was obtained for a usual alkaline kit preparation with meso DMSA after standing for 48 hours at room temperature.

The behaviour of separated isomers was studied in the following way:
Typical alkaline complex solution was separated by HPLC (UV and gamma detection) and 1ml of each of the fractionated column eluates containing the separated isomers I, II or III was used for the following stability tests.

(a) 100µl of individual isomer solution was reinjected into the HPLC system about 20 minutes after separation.
(b) Part of the eluate was placed in a water bath (85°C) for 30 minutes, and then 100µl of the treated solution was analyzed by HPLC.
(c) 500µl isomer solution was evaporated to dryness in a water bath (85°C) under nitrogen for 10 minutes. The residue was dissolved in 150µl acetonitrile and 100µl was injected into the chromatographic system.

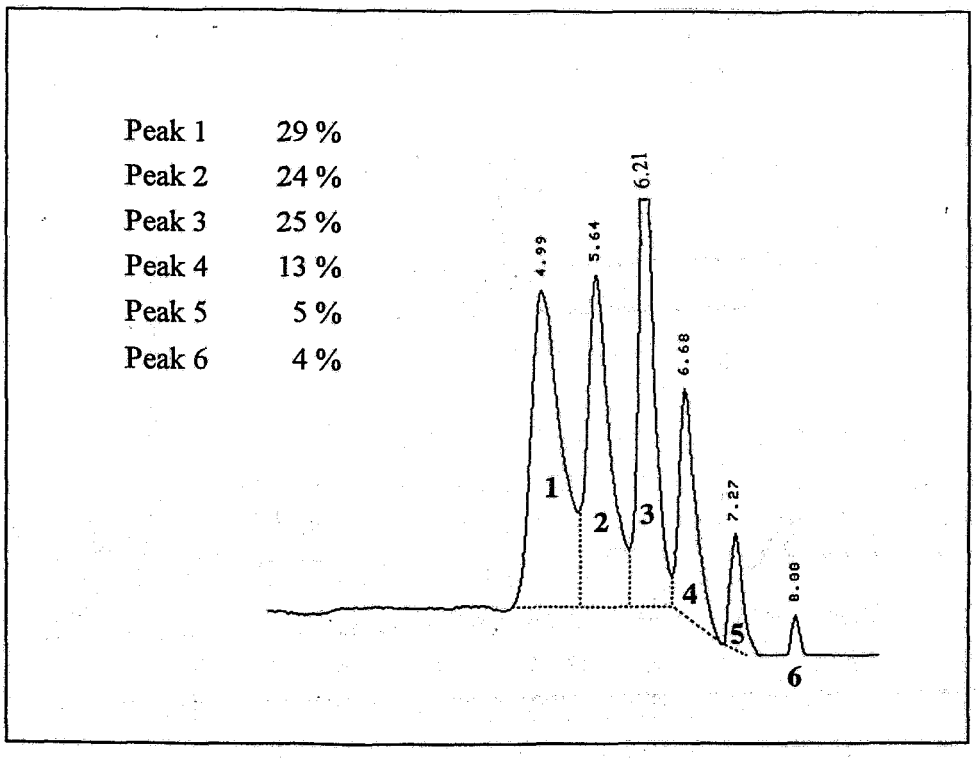

Fig. 6: HPLC chromatogram (UV detection) of a Tc(V)-rac.-DMSA complex solution

Tab. 2 shows the behaviour of the three isomers in these tests. It is evident, that the isolated isomers are stable for at least 30 minutes in the acidic solution. After heating or evaporation isomerization begins and the other two isomers are rebuilt (tests b and c). in different rates. The relative isomer concentrations slowly approach the known ratios indicated in Tab. 1.

Tab.2: The stability of individual isomer solutions under various conditions
(a): 20min, 25°C, pH 1; (b): 30min, 85°C, pH 1, (c): 10min, 85°C, evaporation

Isomer	(a)	(b)	(c)
I	100%	48% I (40% II, 12% III)	70% I(15% II, 15% III)
II	100%	51% II (42% I, 7% III)	84% II (11% I, 5% III)
III	100%	16% III (49% I, 35% II)	60% III (27% I, 13% II)

Fig. 7 clearly shows the behaviour of isomer II in these tests. Similar results were obtained for the two other isomers.

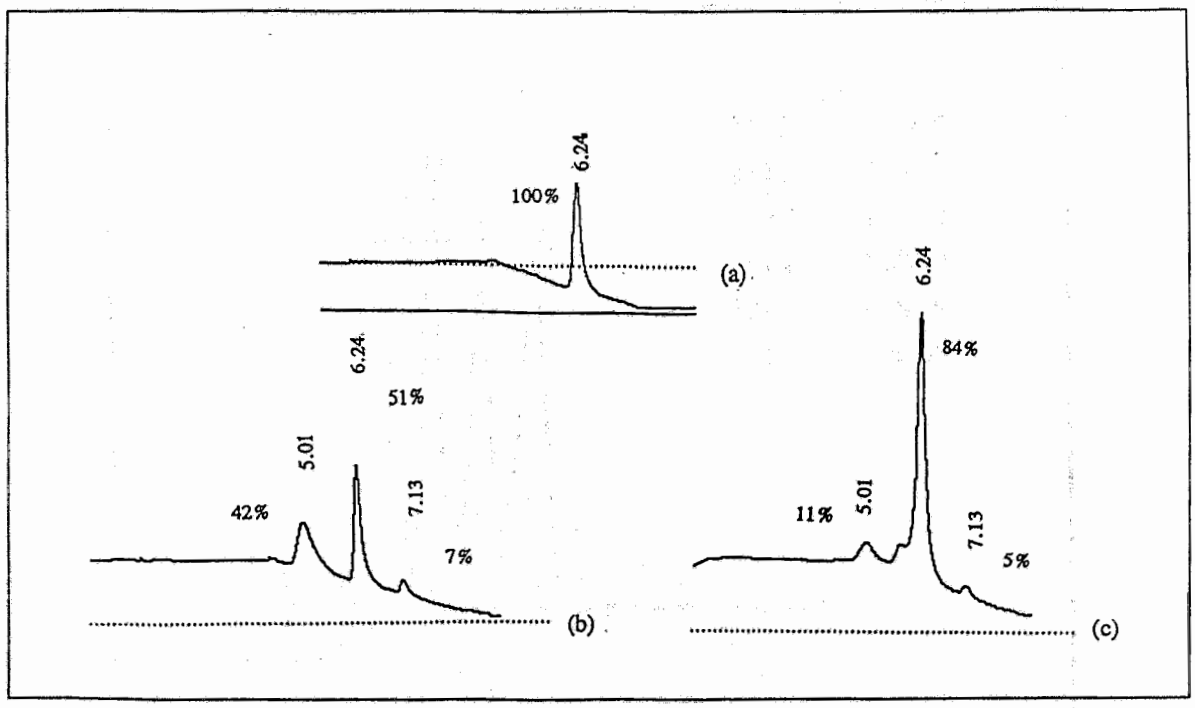

Fig. 7: HPLC stability studies of isomer II kept at different conditions (UV detection)
(a): eluate reinjection, (b): after heating, (c): after evaporation

References:

[1] Becker, W. et al., Horm. Metab. Res. Suppl. **21** (1989) 38
[2] Hoefnagel, C. A. et al., Clin. Nucl. Med. **13** (1988) 159
[3] Ohta, H. et al., Clin. Nucl. Med. **10** (1985) 855
[4] Blower, P. J. et al., J. Nucl. Med. **32** (1991) 845
[5] Spies, H. et al., Inorg. Chim. Acta **48** (1981) 255
[6] Davison, A. et al., Inorg. Chem. **19** (1980) 1988
[7] Spies, H. et al., Inorg. Chim. Acta **116** (1986) 1
[8] Westera, G. et al., Int. J. Radiat. Isot. **36** (1985) 311

10. RHENIUM(V) COMPLEXES WITH MESO AND RACEMIC DMSA PART I: PREPARATION AND IDENTIFICATION

S. Seifert, F. Schneider, H.-J. Pietzsch, H. Spies, B. Johannsen

Rhenium shows a close chemical similarity to technetium and is suitable for radiotherapy because of the ß-emitting radionuclides ^{186}Re ($t_{1/2}$ = 90h, E_β = 1.1MeV, E_γ = 137KeV) and ^{188}Re ($t_{1/2}$ = 17h, E_β = 2.1MeV). The γ-emission associated with decay of ^{186}Re is also useful in scintigraphy.

The so-called pentavalent $^{186/188}Re$-meso-DMSA proposed by Bisunadan et al. [1] represents a potential therapeutic analogue to the pentavalent ^{99m}Tc-meso-DMSA, which recently emerged as a useful radiopharmaceutical for imaging a range of tumours at low accumulation in normal tissues (except kidney) [2,3,4].

The chemical identity of $^{99m}Tc(V)$-meso-DMSA obtained from commercial "kit" preparations has recently been described in detail (Blower et al.) [5], and preparation of $^{99m}Tc(V)$DMSA by aqueous alkaline reduction of pertechnetate in the presence of DMSA has been shown to actually result in the formation of the $[TcO(DMSA)_2]^-$ complex, which contains the $[Tc{=}O]^{3+}$ core. Because of the chemical similarity of the two elements, the chemical structure of $^{186/188}Re(V)$DMSA should be $[ReO(DMSA)_2]^-$.

As found for technetium, rhenium complexes with meso and racemic DMSA result in three isomers each (Fig. 1).

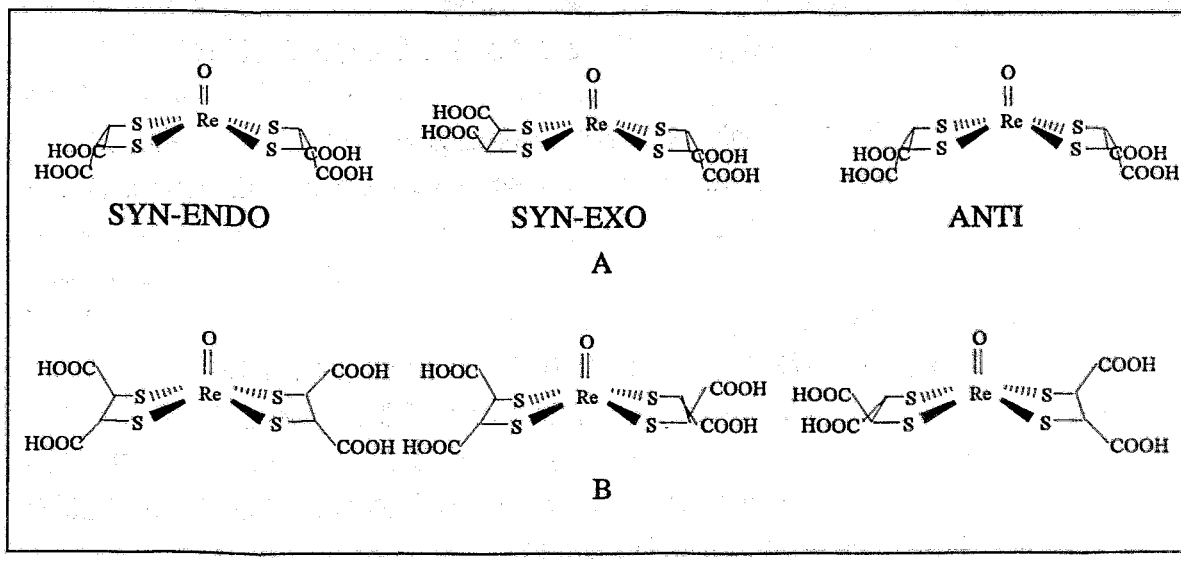

Fig. 1: A: Possible isomers of $[ReO(meso\text{-}DMSA)_2]^-$
B: Possible isomers of $[ReO(rac\text{-}DMSA)_2]^-$

Because the orientation of the carboxylic acid substituents of the more interesting meso-DMSA complex is not yet clear, we sought to isolate and characterize the individual isomers by chemical methods.

Preparation of the complexes

For preparation of the Re(V)DMSA complexes we used direct reduction of perrhenate by $SnCl_2$ in DMSA solution [1] as well as ligand exchange reactions of $Bu_4N[ReOCl_4]$ or $ReOCl_3(PPh_3)_2$ with DMSA.

Reduction of perrhenate by $SnCl_2$

For preparation of Re(V)DMSA complexes by reduction, stannous chloride (22mg, 0.1mmol) was added to a suspension of potassium perrhenate (20mg, 0.07mmol) and dimercaptosuccinic acid (27mg, 0.15mmol) in water (2.5ml) and heated under nitrogen in a boiling water bath for 30min. After cooling the capped vial was opened and the resulting suspension was filtered using a 0.2μm filter. $[Bu_4N]Br$ or $[Ph_4As]Cl$ was added to precipitate the complexes.

Fractional crystallization of the $[Ph_4As]$ salt from acetone results in two fractions. The first fraction contains pure orange crystals of the isomer II (see HPLC analysis). The second fraction, however, consists of a mixture of all three possible isomers of the Re(V)DMSA complex.

Anal. calc. for $Ph_4As[ReO(DMSA)_2]$ x 2 acetone (first fraction)

$C_{38}H_{40}O_{11}S_4ReAs$: C: 43.14%; H: 3.78%; S: 12.11%

Found: C: 43.07%; H: 3.80%; S: 12.12%.

It is also possible to obtain crystals of $K[ReO(DMSA)_2]$ by concentrating the original complex solution using a rotary evaporator. The red needles contain only the isomer II, but they are not suitable for X-ray analysis.

Anal. calc. for $K[ReO(DMSA)_2]$:

$C_8H_{12}O_{11}S_4ReK$: C: 15.07%, H: 1.88%, S: 20.09%.

Found: C: 15.33%, H: 1.72%, S: 20.15%

The potassium salt is readily soluble in water but only slightly soluble in other polar solvents like acetonitrile, methanol, ethanol or acetone.

After adding $[Ph_4As]Cl$ to the potassium salt and recrystallization from acetone, well-formed crystals suitable for X-ray studies were obtained.

IR-analysis: 3450, 1725, 1700, 1685, 1680, 1660, 1650, 1635, 1435, 960 (Re=O), 740, 680, 455cm^{-1}

Ligand exchange reaction

Ligand substitution reactions were carried out with DMSA (10mg, 0.05mmol) dissolved by heating in 1ml ethanol and dropwise addition of $Bu_4N[ReOCl_4]$ (10mg, 0.017mmol) or $ReOCl_3(PPh_3)_2$ (10mg, 0.012mmol) dissolved in 1ml ethanol or acetone. After stirring the mixture for 10 min the yellow solution was filtered and the isomer ratio was analyzed.

For chemical identification of the complex solutions HPLC and ^1H NMR methods were used.

The ^1H NMR analyses were carried out in D_2O or acetone-d_6 solutions using a Bruker AM 250 system at a ^1H frequency of 250MHz.

For HPLC analyses a PRP-1 column (Hamilton, 150 x 4.1mm) was used in conjunction with a linear gradient system of 0.1% trifluoroacetic acid in water / 0.1% trifluoroacetic acid in acetonitrile. The effluent from the column (flow rate 2ml/min) was monitored by UV absorbance at 340nm.

Results and discussion

We studied the heterogeneity of the complex formation with meso DMSA as well as the racemic form of DMSA.

Fig. 2 shows HPLC separation of the various Re-DMSA complexes prepared by stannous reduction of perrhenate in acidic aqueous solution.

For the preparation of Re-meso-DMSA the three peaks are considered to the three possible isomers in accordance with results obtained with Tc-meso-DMSA [5]. With racemic DMSA containing meso DMSA as an impurity, there are two additional peaks at 4.6 and 7.0 minutes, compared to meso DMSA on its own.

On the basis of HPLC and ^1H NMR studies of the complex solutions, this complex can be assigned to isomers I, II and III.

In acidic aqueous solution (Sn-reduction) a stable average isomer distribution of about 35% I, 60% II. and 5% III is found.

A similar result was obtained by ^1H NMR measurements of this solution. Fig. 3 shows the expected spectrum of two singlets and one dublet with a 1:1 integral ratio caused by the three isomers of the Re-meso-DMSA complex.

Further investigations concentrated on Re-meso-DMSA complexes because of the higher biological relevance of these compounds. An unexpected isomerization of the complexes was found as described in part II of this paper.

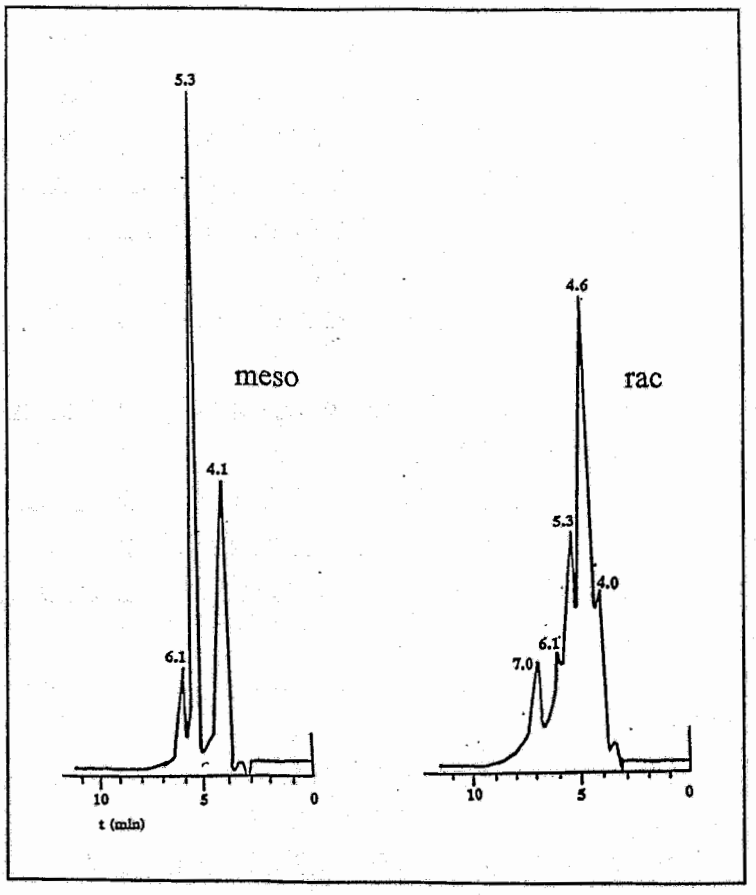

Fig. 2: HPLC separation of Re-complexes with meso and racemic DMSA (Sn-reduction method)

HPLC analysis of the aqueous solution of the red needles results in only one peak at 5.1min corresponding to the isomer II of the three possible $[ReO(meso\text{-}DMSA)_2]^-$ isomers.
^1H NMR studies of this compound made in D_2O showed that the isomer II represents in fact a syn configuration of the carboxylic groups of the two meso-DMSA ligand molecules (Fig. 4).

The symmetric isomer II is dominant in acidic solution, followed by isomer I. The analysis of the NMR spectrum reveals that the sum of the two singlets of 1:1 integral ratio corresponds to the yield of isomer I. That means that isomer I in HPLC represents the anti configuration of the carboxylic groups of the two meso-DMSA ligand molecules.
Identification of the other two singlets (syn-endo and syn-exo - peaks II and III in HPLC) requires crystallographic confirmation [6]. X-ray analysis of the isolated tetraphenylarsonium salt of isomer II is in progress.

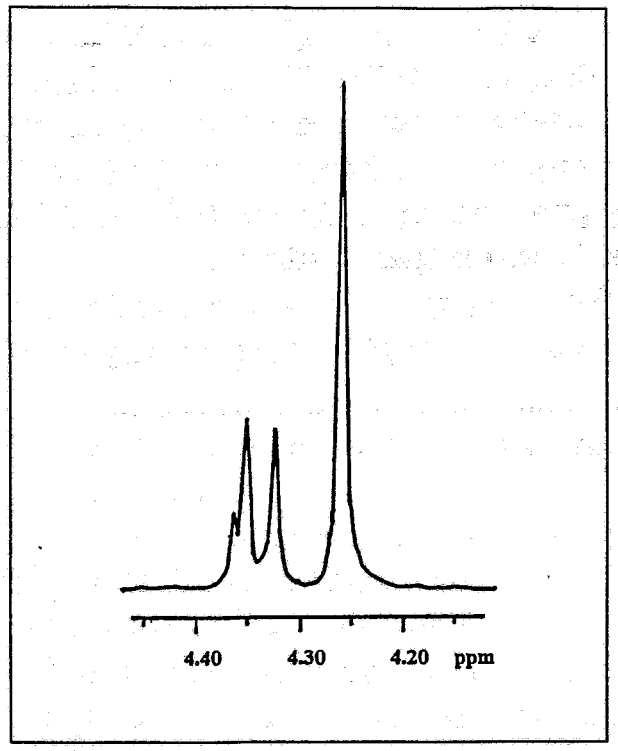

Fig.3: ^{1}H NMR spectrum of C-H proton region (4.2-4.6ppm) of $[ReO(DMSA)_2]^-$ in D_2O

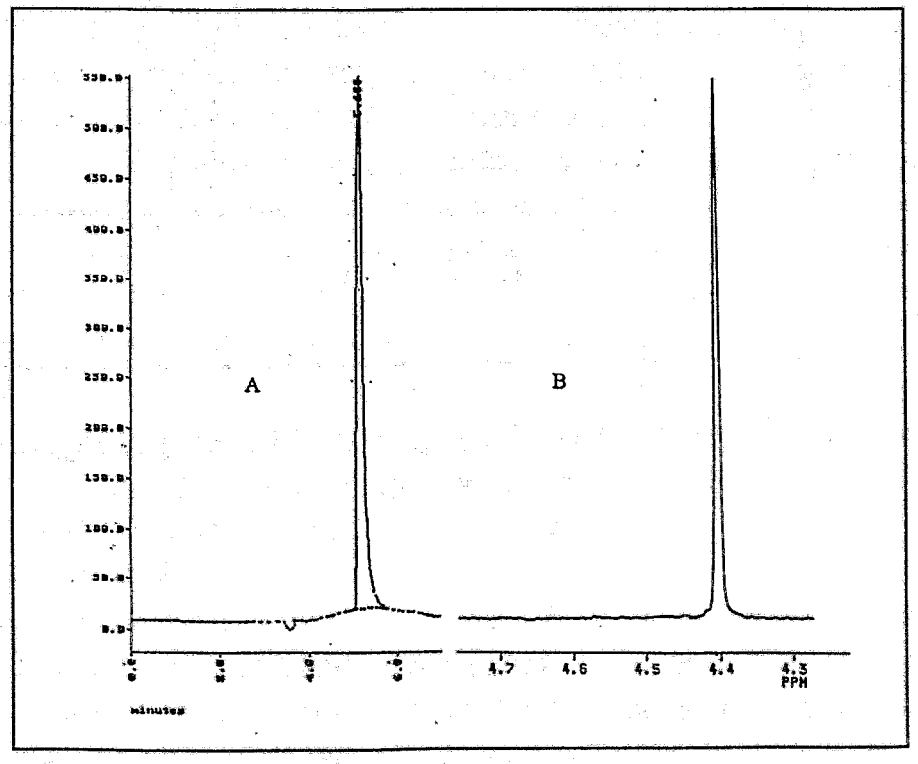

Fig. 4: HPLC (A) and ^{1}H NMR analyses (B) of $K[ReO(DMSA)_2]$ dissolved in D_2O

The three stereoisomers were also obtained by ligand exchange reaction with DMSA dimethylester or DMSA diethylester starting from $Bu_4N[ReOCl_4]$. HPLC analysis of the isolated DMSA dimethylester complex, obtained after crystallization by adding methanol and redissolved in acetone, shows one dominant isomer (peak I) and smaller yields of II and III. The chelate ring proton resonances observed in ^1H NMR analysis indicate that the dominant isomer is in the anti configuration (Fig. 5).

As expected, the elution order from the HPLC column is the same for the isomers of the Re(V)DMSA complexes as for the Re(V)DMSA diester complexes.

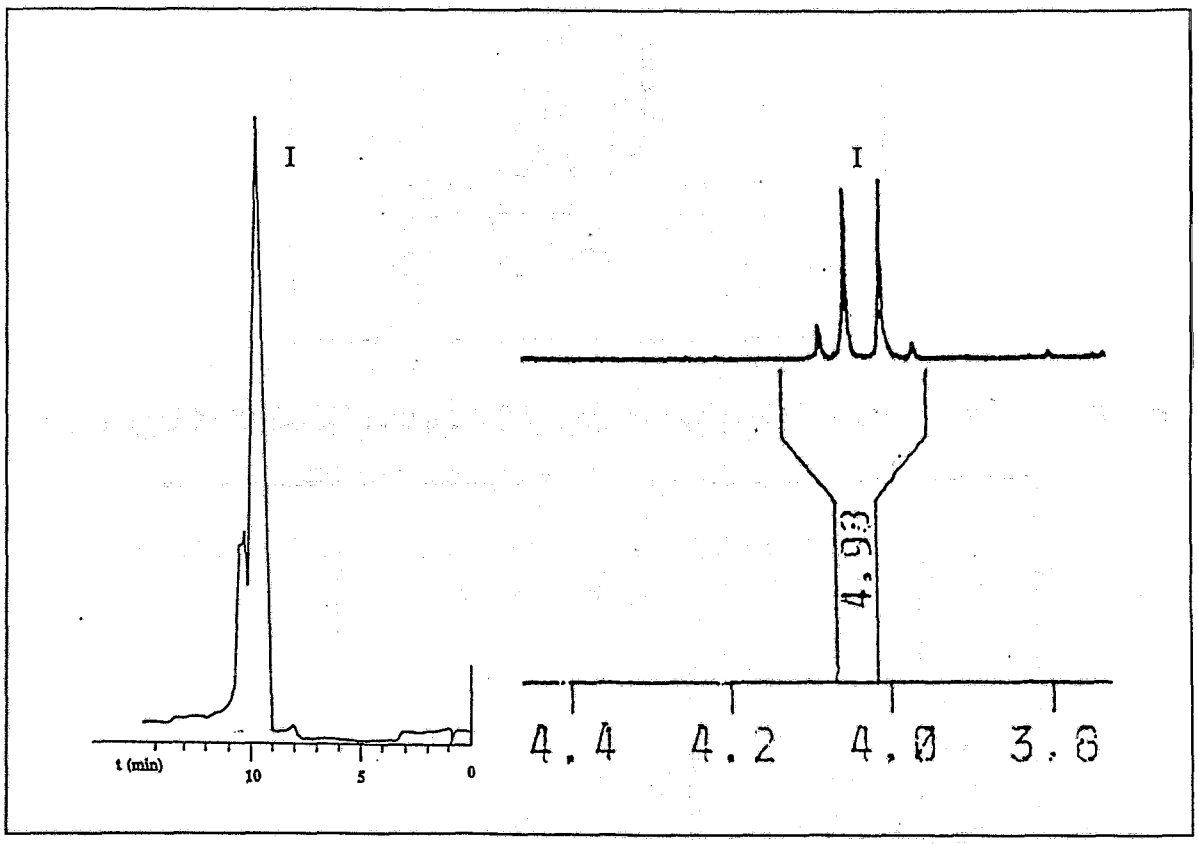

Fig. 5: HPLC and ^1H NMR analyses of $Bu_4N[ReO(DMSA\ dimethylester)_2]$ dissolved in acetone (d_6)

References:

[1] Bisunadan, M. M. et al., Appl. Radiat. Isot. **42** (1991) 167

[2] Ohta, H. et al., J. Nucl. Med. **25** (1984) 323

[3] Ohta, H. et al., Nucl. Med. Commun. **9** (1988) 105

[4] Clarke, S. E. M. et al., J. Nucl. Med. **29** (1988) 33

[5] Blower, P. J. et al., J. Nucl. Med. **32** (1991) 845

[6] Singh, J. et al., J. Chem. Soc., Chem. Commun. (1991) 1115

11. RHENIUM(V) COMPLEXES WITH MESO AND RACEMIC DMSA PART II: ISOMERIZATION EFFECTS

S. Seifert, F. Schneider, M. Findeisen[1], H.-J. Pietzsch, H. Spies, B. Johannsen
[1] Institut für Oberflächenmodifizierung Leipzig

Rhenium(V) and technetium(V) form three stereoisomeric complex compounds with meso dimercaptosuccinic acid as ligands. They are separable by HPLC and, in part, by chemical methods.

The isomers marked I, II, III are assigned to the anti, syn-endo and syn-exo forms according to the results described in part I.

The distribution pattern of the individual isomers depends on various parameters [1]. The studies revealed unexpected isomerization of the complexes. There are remarkable differences concerning the effect of solvent and time on distribution patterns.

In acidic aqueous solution (Sn-reduction) a stable average isomer distribution of about 35% I, 60% II, and 5% III is found, whereas in methanolic, ethanolic or acetonic solution (ligand exchange) the initial isomer ratio is about 55% I, 27% II, and 18% III.

There are remarkable differences concerning the effect of solvent and time on the distribution patterns.

In acidic aqueous solution the isomer ratio does not change for weeks. In methanolic or ethanolic solution it changes after only a few hours (Fig. 5), but not so in acetonic or acetonitrilic solution, where it remains stable for some days at least.

In further studies, the isomer mixture as obtained in acetonic solution with the order of portion I > II > III was evaporated to dryness and redissolved in water (pH 2). As a result the isomer ratio changed to II > I > III, thus indicating the possibility of a conversion of isomers.

To find out whether the pH of the aqueous solution has any influence on the distribution patterns, the acidic solution of the complexes (35% I, 60% II, 5% III) was neutralized. This resulted in a slow change of the isomer ratio at room temperature.

At about 100°C (boiling water bath) the reaction is completed after about three hours and has then an isomer distribution of 47% I, 25% II, and 28% III.

The change is reversible.

Fig. 1 shows that isomer II decreases in neutral solution, while I and III increase. After heating at pH 2, isomer II is rebuilt from III and I.

These results indicate a dependence of isomer distribution on the preparation conditions (aqueous or non aqueous) and the possibility of changing the isomer ratio by varying the pH-value of the solution.

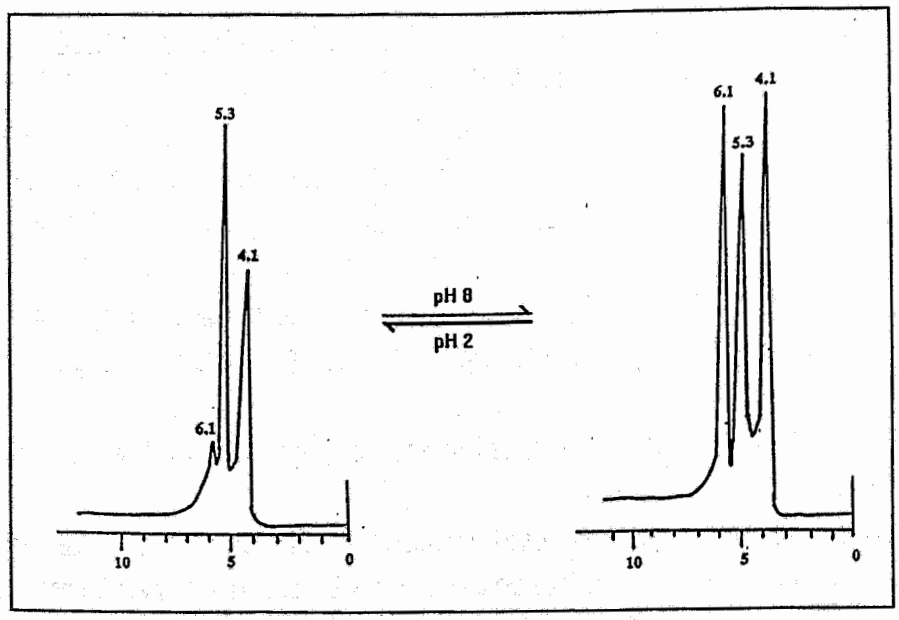

Fig. 1: HPLC chromatograms of $[ReO(DMSA)_2]^-$ showing the dependence of the isomer ratio in aqueous solution on pH value.

The stability of the individual isolated isomers in solution differs. While isomers I and III isomerize immediately after separation by HPLC, resulting in the typical isomer ratio II > I > III because of the acidic eluent, isomer II is stable at room temperature for 1 - 2 hours and can be kept stable for longer in a frozen solution.

Accordingly, the aqueous solution of the crystallized isomer II ($K[ReO(DMSA)_2]$) with a resulting pH 2 is also stable for some hours. Isomerization at room temperature proceeds very slowly as seen in Figs. 2 and 3.

After more than 100 hours the typical yields of all three isomers can be detected in the solution by HPLC and ^1H NMR.

The original solution shows only one strong singlet at 4.39ppm in ^1H NMR analysis after about 15min.

The yields of the other isomers (two singlets of 1:1 integral ratio at 4.42 and 4.45ppm and a weak singlet at 4.47ppm) increase in time up to the equilibrium isomer ratio for an acidic Re(V)meso-DMSA solution.

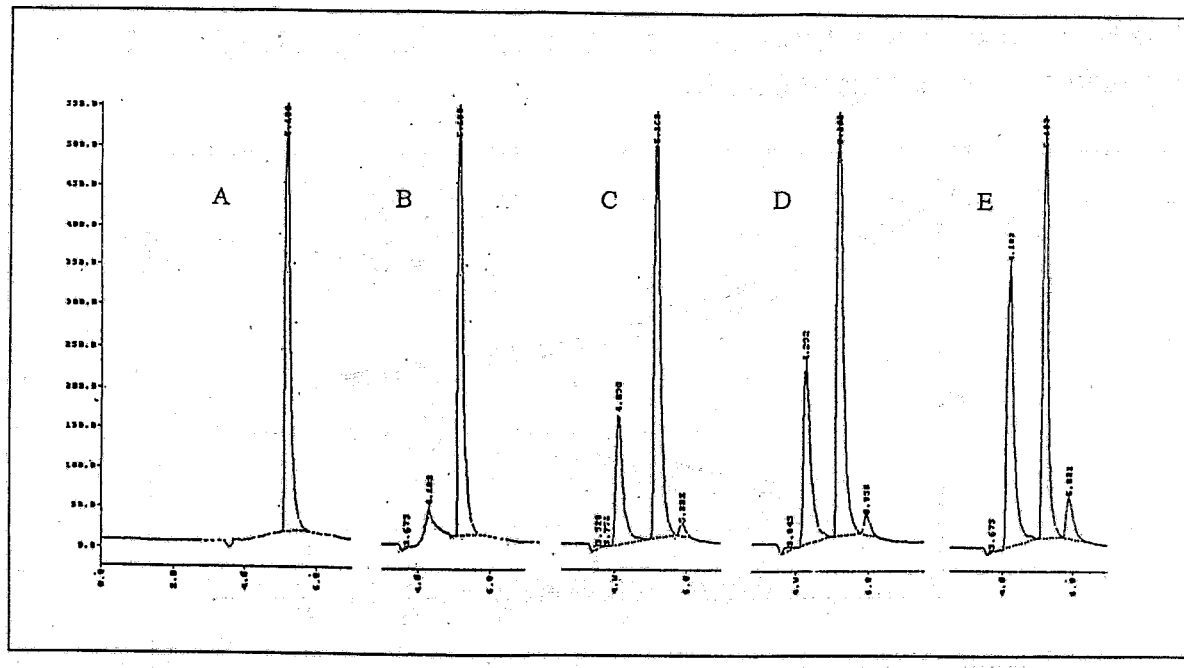

Fig. 2: HPLC analysis of $K[ReO(DMSA)_2]$ (isomer II) dissolved in water as a function of time after dissolution. A: 15min, B: 2.5h, C: 24h, D: 48h, E: 120h

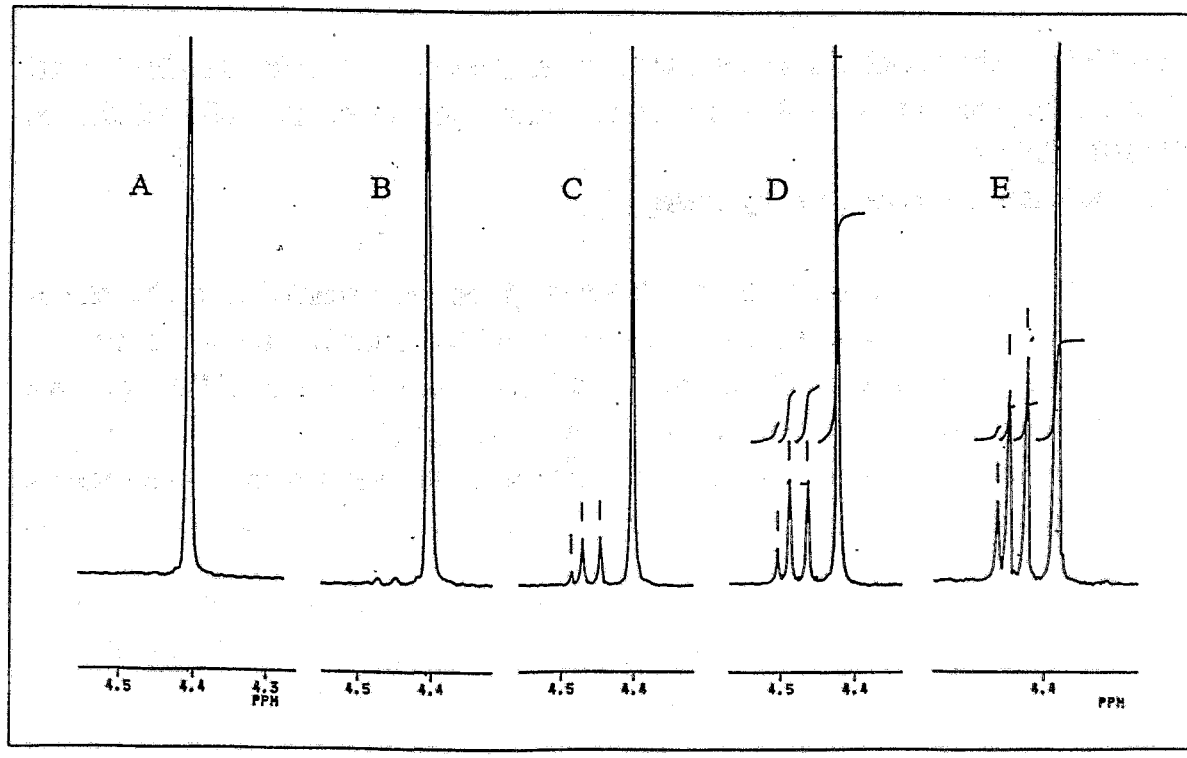

Fig. 3: ^1H NMR spectra of C-H proton region (4.3-4.6ppm) of $[ReO(DMSA)_2]^-$ as a function of time after dissolution in D_2O; A: 15min, B: 2.5h, C: 24h, D: 48h, E: 120h

The isomer ratios measured at different times by ^1H NMR correspond very well with those determined by HPLC analysis (Fig. 4).

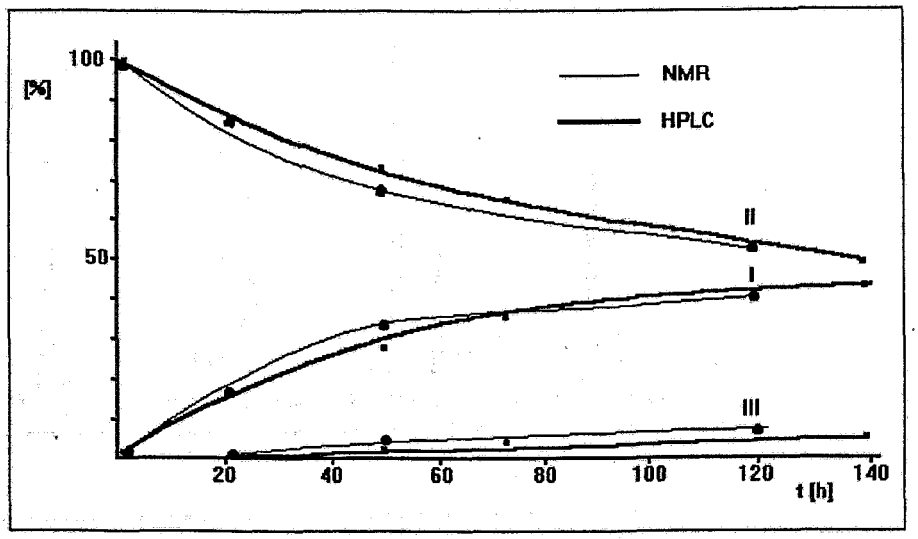

Fig. 4: Isomerization of K[ReO(DMSA)$_2$] dissolved in water as a function of time measured by HPLC and ^1H NMR studies

At pH 7 isomerization takes 1-2 days at room temperature (Tab. 1). After acidification (pH 2) about 20 hours are needed to restore the isomer pattern of an acidic solution of $[ReO(DMSA)_2]^-$.
The reactions can be accelerated by heating.

The above-mentioned change of the $[ReO(DMSA)_2]^-$ complex solution in methanolic or ethanolic solution seems to be a gradual esterification of the Re-DMSA complex isomers.
The products, observed in HPLC after more then 3 hours, with R_T values of between 6 and 9 minutes are probably isomers of meso-DMSA half-ester complexes.
Preparations of the DMSA monoester for the synthesis of the corresponding Re-complexes are in progress.

Tab. 1: Isomerization of $[ReO(DMSA)_2]^-$ (II) in water at pH 7 and room temperature

t [h]	I	II	III [%]
0	1.1	98.9	0
0.5	5.7	94.3	0
2.5	26.4	65.5	8.1
4.0	30.9	57.6	11.5
22.0	51.0	35.3	13.7
48.0	46.3	29.2	24.5
Acidified to pH 2			
3.5	34.5	47.8	17.7
19.0	33.7	57.5	8.8

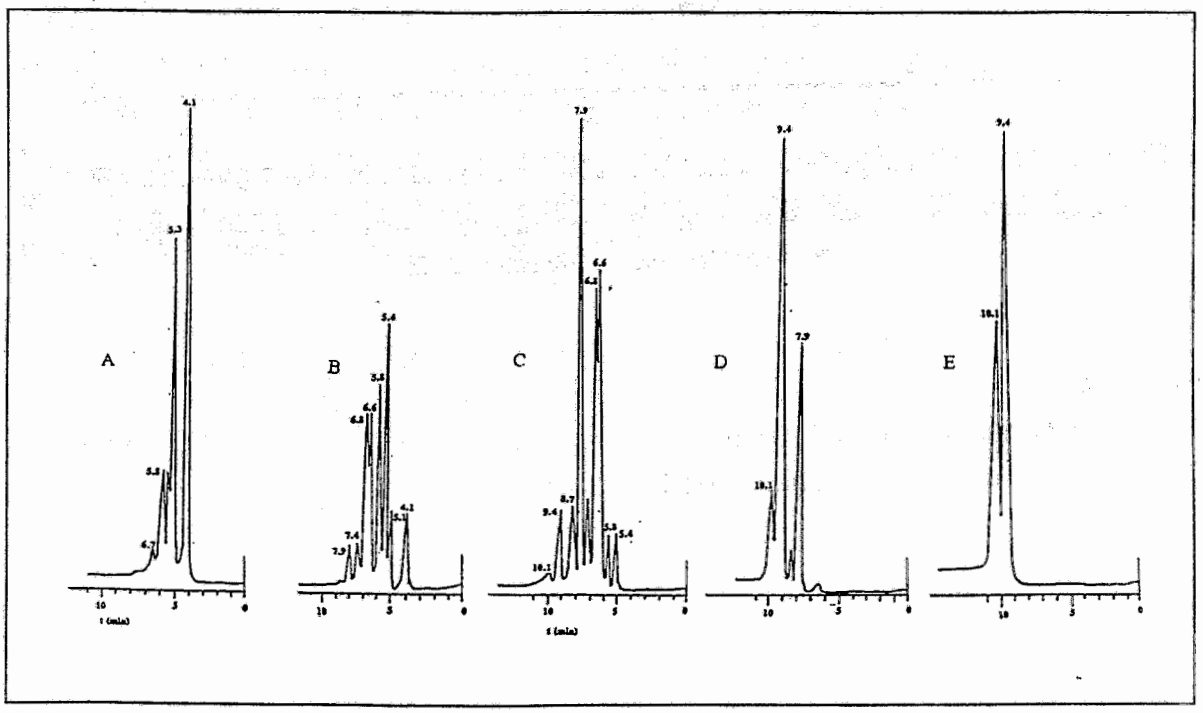

Fig. 5: HPLC chromatograms of complexes showing change of the $[ReO(DMSA)_2]^-$ isomers in methanol as a function of time after preparation, A: 5min, B: 3.5h, C: 24h, D: 6d, E: Re-meso-DMSA dimethylester

On the other hand, step-by-step hydrolyzation of the DMSA diester complex in alkaline solution results either in racemization (ammonia, amines) or in complete hydrolyzation and racemization into the $[ReO(rac\text{-}DMSA)_2]^-$complex isomers, as shown by [2] and in Fig. 6.

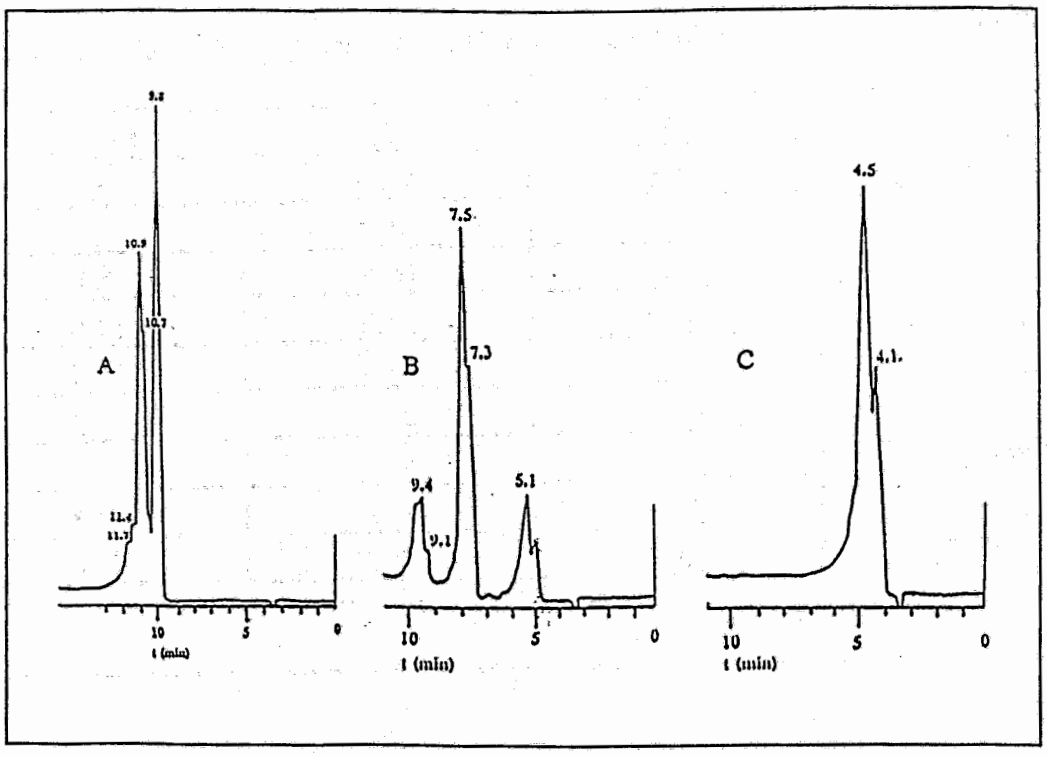

Fig.6: HPLC chromatograms of racemization (A) and hydrolyzation/racemization (B) of $Bu_4N[ReO(DMSA\ dimethylester)_2]$ by treating with ammonia (A) and heating with sodium hydroxide solution (B)

References

[1] Lindemann, L. et al., this report, p. 41

[2] Spies, H. et al., Inorg. Chim. Acta **116** (1986) 1

12. TECHNETIUM AND RHENIUM TRACERS WITH METABOLIZABLE ESTER FUNCTIONS

R.Syhre, S.Seifert, F. Schneider, H.-J.Pietzsch, H.Spies, B.Johannsen

The introduction of ester groups into appropriate moieties of technetium and rhenium complexes is considered a promising approach to Tc/Re tracers which should be trapped *in vivo* in the target organ. Built-in ester bonds also may help to improve target/nontarget ratios due to faster excretion of background radioactivity when enzymatic cleavage takes place in the blood. Cheesman et al. [1] succeeded in developing a brain perfusion imaging agent with ester derived diamine-dithiol ligand, which undergoes enzymatic hydrolyses in the brain. The technetium complex of N,N'-1,2-ethylenediyl-bis-L-cysteine diethyl ester, ECD, shows excellent uptake and retention characteristics.

We synthesized a number of technetium and rhenium complexes with sulphur donor ligands possessing metabolizable ester functions. Most of them belong to the class of oxotechnetium(V) complexes and involve both anionic complexes (I) derived from bi or tetradentate ligands and neutral complexes (II) with tridentate/monodentate coordination. In a first series all these compounds were functionalized so that the complex unit was bound to the carboxylic site of the ester group. Preparation of corresponding compounds with an inverse arrangement of the carboxylic and alcoholic parts is in progress.

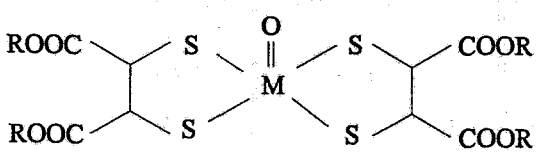

I

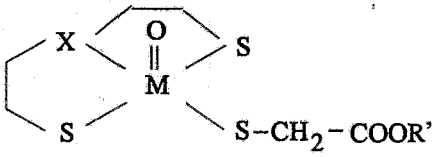

II

M = Tc, Re
R = Me, Et

X = O, S, NR'
R' = Alkyl (C_1...C_6)

Preliminary investigations on enzymatic hydrolysis of the ester group in anionic oxotechnetium(V) complexes were carried out with methyl and ethyl esters of *meso*-2,3-dimercaptosuccinic acid as ligands (I).

The Re-DMSA ester complexes were prepared by ligand exchange reaction starting with $Ph_4As[ReOCl_4]$. After dissolving in acetone a slight excess of the desired DMSA ester ligand was added and the solution was allowed to stand for some minutes. After reducing the volume, the compounds crystallize and can be isolated.

To determine whether the ester bond in Re-DMSA ester complexes is susceptible to cleavage by esterases, incubation experiments with tissue homogenates and plasma were carried out.

Experiments

6-7mg of the complex compound was dissolved in 1ml ethanol/water (50/50).

Generally, 0.1ml of the complex solution (6-9x10^{-3}mol/l) was added to 0.9ml of the esterase containing samples.

For incubation experiments homogenates from the liver, lungs and brain of rats, diluted 1:20 with phosphate buffer of pH 7.4, as well as blood plasma of rats and humans, diluted 1:1 with phosphate buffer of pH 7.4, and phosphate buffer only, for reference, were used.

The incubation of complexes took place at 37°C for 60 minutes. After incubation the samples were centrifuged and analyzed by HPLC.

For HPLC analyses the system for separation of Re-DMSA complexes as described in [2] was used.

Results and discussion

Fig. 1 shows chromatograms of Re-DMSA dimethylester and diethylester complex solutions after dilution with phosphate buffer as a reference for the esterase-containing samples (Figs. 2 and 3).

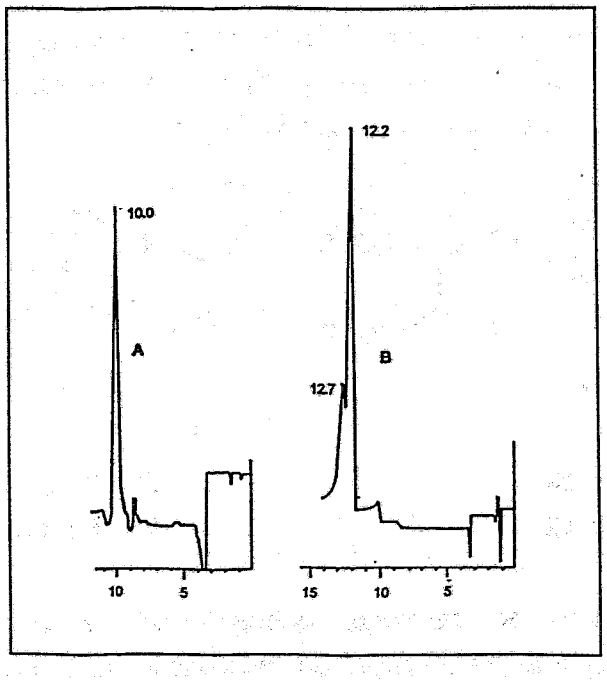

Fig. 1: HPLC chromatograms of [ReO(DMSA dimethylester)$_2$]$^-$ (A) and [ReO(DMSA diethylester)$_2$]$^-$ (B) after incubation in phosphate buffer (pH 7.4, 37°C, 60min.)

A complete separation of the three stereoisomers of the diester complexes was not possible with the HPLC system used. The analysis showed one peak of 10.0 for the dimethylester complex and two peaks of 12.2 and 12.7 for the diethylester complex.

Both complex compounds do not change significantly in buffer solution, but variations were observed in esterase containing samples of rats.

According to the HPLC chromatograms the enzymatic effect is qualitatively similar in blood plasma, liver, lungs and brain.

About 80% of Re-DMSA dimethylester was changed in blood plasma and liver homogenate and about 50% in lung homogenate (Fig. 2).

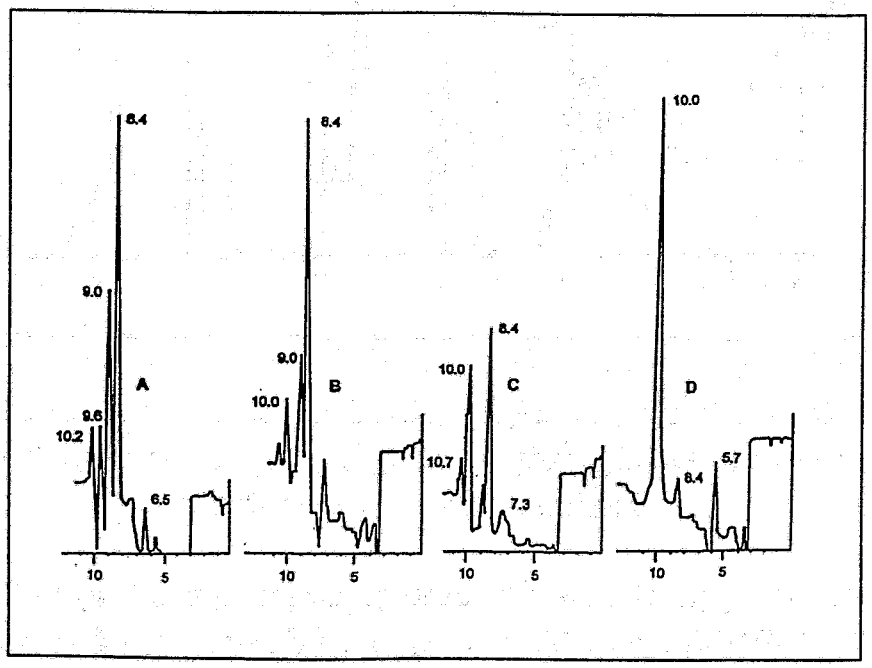

Fig. 2: HPLC chromatograms of $[ReO(DMSA\ dimethylester)_2]^-$ after incubation in plasma(A),and homogenates of liver (B), lungs (C) and brain (D) of rats, (phosphate buffer pH 7.4, 37°C, 60min)

After incubation of Re-DMSA diethylester in plasma and liver homogenates, about 50% of the complex was changed (Fig. 3).

However, only low variations of <10% of both *anionic* complexes were found in brain homogenates of rats.

The enzymes, responsible for cleavage of the tracers, and the nature of the metabolites still have to be identified.

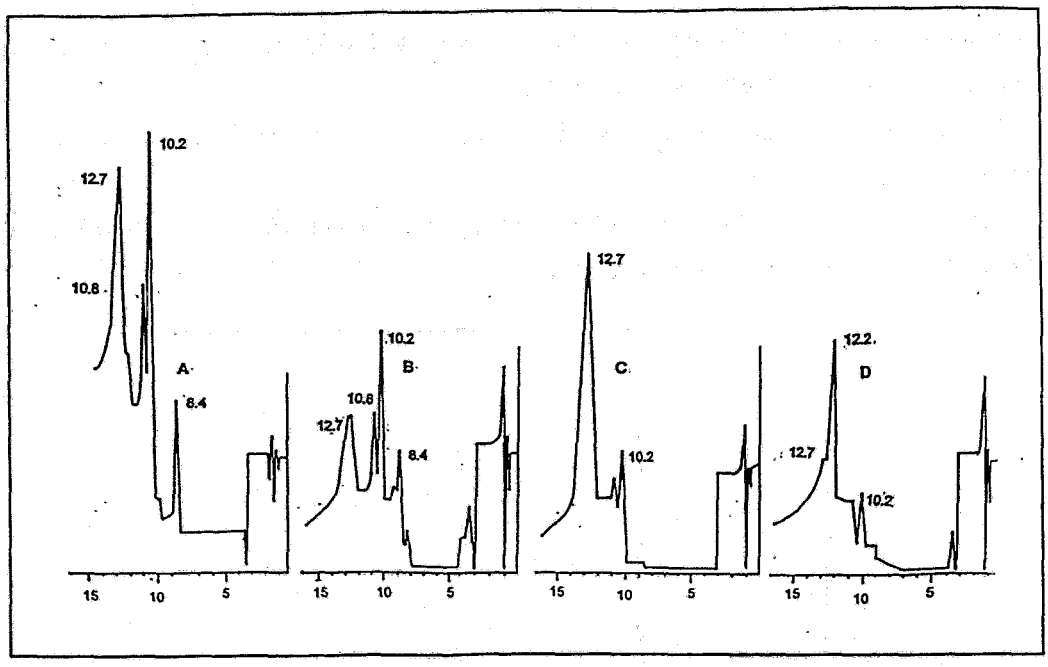

Fig. 3: HPLC chromatograms of $[ReO(DMSA\ diethylester)_2]^-$ after incubation in plasma(A),and homogenates of liver (B), lungs (C) and brain (D) of rats, (phosphate buffer pH 7.4, 37°C, 60min)

Preliminary results suggest that the ester cleavage proceeds gradually up to the monoester complex. The Re-DMSA monoethylester complex prepared by ligand exchange reaction of $[ReOCl_4]^-$ shows R_T values of 8.2, 8.4 and 9.0 in HPLC. These R_T values are also observed in incubation studies (Figs. 3 and 4) in addition to R_T values of 10.2 and 10.8 possibly arising from cleavage of only one ester group of the complex compound.
Apart from the possible monoester complexes (R_T 8.4 and 9.0), the incubated solutions of the Re-DMSA dimethylester complex already contain small amounts of the completely hydrolyzed tracer $[ReO(DMSA)_2]^-$ showing the known R_T values between 4.6 and 6.2 [2].

Interestingly, this studies also indicate that the metabolization behaviour of diester complexes might be dependent on species. While in rat plasma 50-80% of the Re-DMSA diester complexes are metabolized, in human plasma only the blank value is found (Fig. 4).

Cleavage of the DMSA diethylester complex isomers in plasma and liver homogenates of rats is also influenced by stereo-specific factors. As shown in Fig. 3, the isomer with R_T 12.2 is chiefly metabolized, while that with R_T 12.7 is not changed significantly.

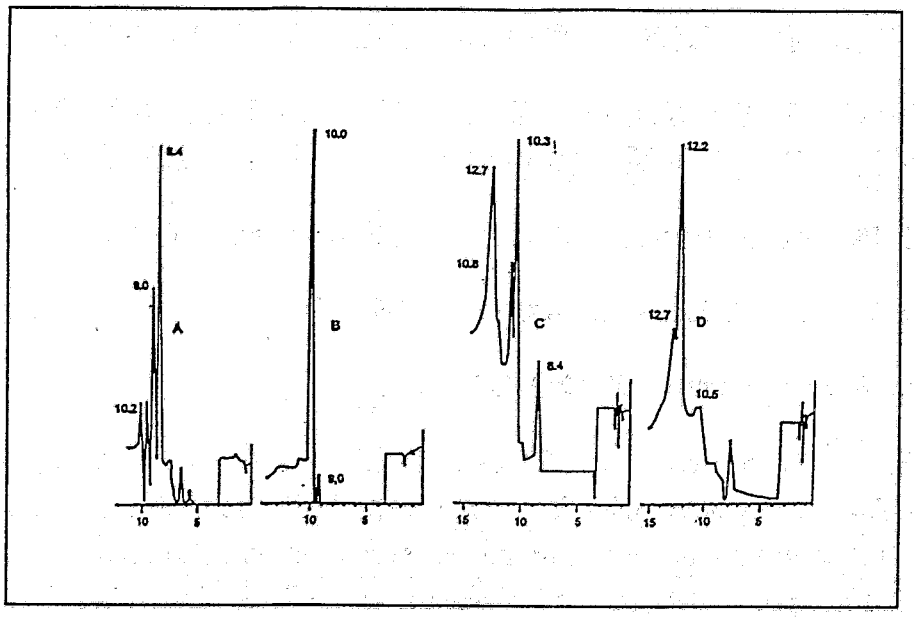

Fig. 4: HPLC chromatograms of $[ReO(DMSA\ dimethylester)_2]^-$ (A,B) and $[ReO(DMSA\ diethylester)_2]^-$ (C,D) after incubation in rat plasma (A,C), and human plasma (B,D), (phosphate buffer pH 7.4, 37°C, 60min)

References:

[1] Walovitch, R. C. et al., J. Nucl. Med. **30** (1989) 1892

[2] Seifert, S. et al., this report, p. 50

13. TECHNETIUM COMPLEXES WITH THIOETHER LIGANDS

2. SYNTHESIS AND STRUCTURAL CHARACTERIZATION OF NEUTRAL OXOTECHNETIUM(V) COMPLEXES WITH DITHIOETHERS

H.-J. Pietzsch, H. Spies, P. Leibnitz[1], G. Reck[1], J. Beger[2], R. Jacobi[2]

[1]Bundesanstalt für Materialforschung, D-1199 Berlin

[2]Bergakademie Freiberg, D-9200 Freiberg,

Neutral, bidentate thioethers such as 5,8-dithiadodecane, 3,6-dithiaoctane ("S_2") as well as the dithia-diol 1,8-dihydroxy-3,6-dithiaoctane ("$S_2(OH)_2$") react with tetrachlorooxotechnetate ($TcOCl_4^-$) in acetone to form binuclear oxo species of the type [TcO("S_2")$Cl_2]_2O$ with dithiaalkanes and [TcO("$S_2O(OH)$")Cl_2] with the dithia-diole, respectively. The complexes have been characterized by elemental analysis and spectroscopic methods.
The crystal structures of [TcO(5,8-dithiadodecane)$Cl_2]_2O$ (1) and [TcO(8-hydroxy-3,6-dithiaoctan-1-olato)Cl_2] (3) were determined from X-ray data [1].

Recently we found that cationic Tc(III) complexes containing neutral tetradentate thioethers and monothioles as co-ligands are formed when an appropriate technetium precursor is reduced by stannous chloride in the presence of both a tetrathiaalkane and a monothiole [2].
As observed earlier [3], reaction of pertechnetate with two equivalents of stannous chloride in the presence of e.g. R-S-CH_2CH_2-S-R ("S_2", R=alkyl) in acetone or acetic acid yields yellow-green coloured products. These species are reactive in ligand exchange reactions with e.g. 2,3-dimercaptosuccinic acid dimethylester, resulting in formation of the known bis(dithiolato)oxotechnetate(V) complexes [4]. We assume therefore our new species to be in the oxidation state +V. This prompted us to attempt the isolation and characterization of definite Tc(V) complexes with dithiaalkanes and related compounds. Preparation of new definite Tc(V) complexes was successful with tetrachlorooxotechnetate(V) as a precursor, not with the less reactive Tc(V) gluconate.
Dithiaalkanes as well as the potentially tetradentate 1,8-dihydroxydithiaoctane react with $TcOCl_4^-$ under partial exchange of chloride ligands by S atoms of dithia ligands.
3,6-dithiaoctane (R=C_2H_5) and 5,8-dithiadodecane (R=C_4H_9) produce in acetone/methanol analytically pure yellow-green oxo complexes of the [TcO("S_2")$Cl_2]_2O$ type, which precipitate from the reaction mixtures.

$$TcOCl_4^- \xrightarrow[\text{acetone/methanol}]{\text{"}S_2\text{"}} [TcO(\text{"}S_2\text{"})Cl_2]_2O$$

(1) "S_2": $C_4H_9SCH_2CH_2SC_4H_9$

(2) "S_2": $C_2H_5SCH_2CH_2SC_2H_5$

$$TcOCl_4^- \xrightarrow[\text{acetone/methanol}]{\text{"}S_2(OH)_2\text{"}} [TcO(\text{"}S_2O(OH)\text{"})Cl_2]$$

(3) "$S_2(OH)_2$": $HO\text{-}CH_2CH_2SCH_2CH_2SCH_2CH_2\text{-}OH$

The neutral complexes are stable on exposure to air and, except for acetone and acetonitrile insoluble in the common organic solvents. Elemental analyses are consistent with the proposed formulations (Tab. 1).

In the infrared spectra strong absorptions at 920cm^{-1} for (1), (2) as well as for (3) indicate the $Tc{=}O^{3+}$ core; ν(Tc-Cl) is not assigned owing to the absorption of other vibrations in the region 300-250cm^{-1}.

Tab. 1: Yields and analytical data of the complexes

Complex	Yield (%)	Elemental analysis (Calc./found (%))					melt. p. (°C)	UV/vis nm/lgε
		C	H	S	Cl	Tc		
(1)	45	30.0 30.2	5.5 5.4	16.0 15.9	17.7 17.5	24.8 25.1	174-175	400/3.9
(2)	40	20.9 21.1	4.1 4.3	18.6 18.4	20.6 20.2	28.8 29.1	193-194	400/3.8
(3)	60	19.6 19.5	3.5 3.3	17.4 17.6	19.3 18.7	27.0 27.2	148-149	405/3.8

In order to obtain an unambiguous structural assignment, the structures of the complexes (1) and (3) were determined by X-ray structure analyses. Suitable crystals were obtained from acetone/methanol. Drawings of (1) are shown in Figs. 1 and 2 and of (3) in Fig. 3. Selected bond angles and distances are listed in Tabs. 2 and 3.

In both complexes flip-flop mechanisms are observed in the ring Tc2, S4, C3, C4, S3 {complex (1)} and Tc, S1, C3, C4, S2 {complex (3)}. This causes smearing of the electron density of the C4 atoms of both molecules.

The crystal structure of (1) consists of two independent TcO("S_2")Cl_2 units bridged by an oxygen atom.

The characteristic feature is the presence of the O=Tc-O-Tc=O group. In this respect the structure of (1) is comparable to those of $[TcO(salpd)]_2O$ (salpd = N,N'-propane-1,3-diyl-

bis-(salicylideneiminate) [5], and $[TcO(N_2S_2)]_2O$ (N_2S_2 = N,N'-ethylene-bis(thio-acetylacetone-iminate) [6]

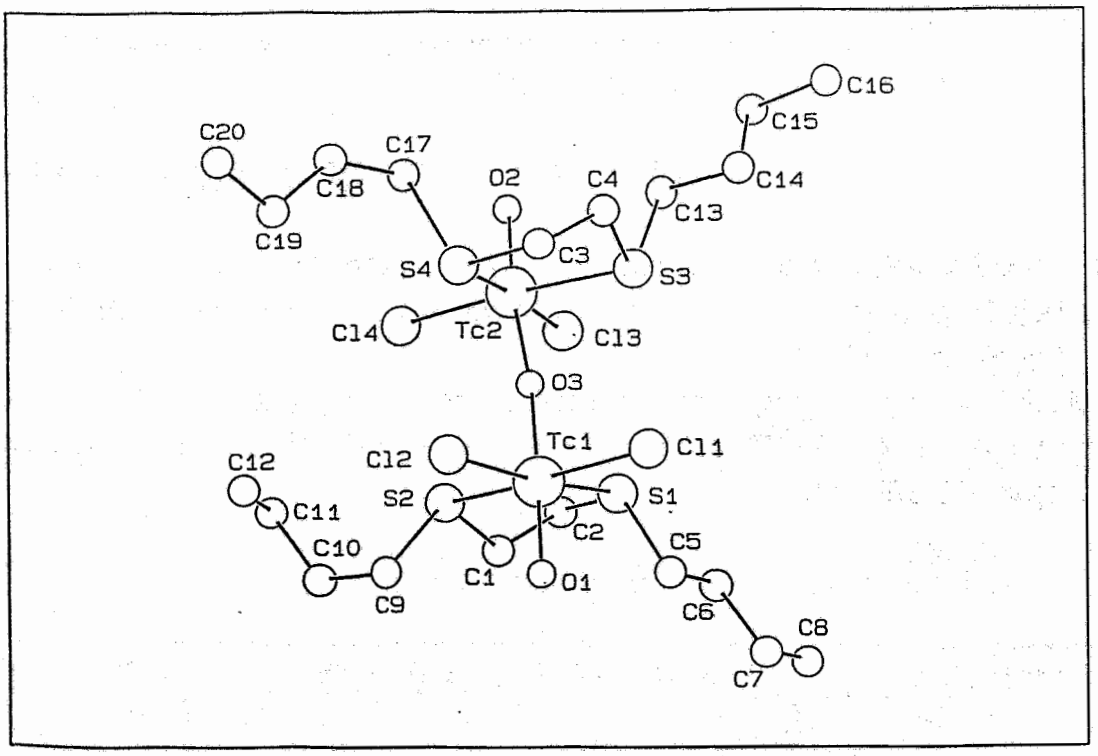

Fig. 1: CELLGRAF-drawing of $[TcO(5,8\text{-dithiadodecane})_2Cl_2]_2O$

The technetium atoms are centred in a flattened octahedron with the equatorial plane formed by a S_2Cl_2 donor set, in which the technetium atoms Tc1 and Tc2 are 0.12Å out of plane towards O1 and O2 respectively. The S_2Cl_2 planes are almost parallel with a small deviation of 0.013Å; the dihedral angle is 2.6°. The sulphur and chlorine donor atoms of the units are in the anti-position with respect to the bridging oxygen.

The bond lengths of the Tc=O cores with 1.665 and 1.674Å respectively, are in the range generally found for these units (1.61- 1.75Å), but they are in between those in the octahedral O=Tc=O compounds and in square-pyramidal Tc=O complexes. This corresponds to the relatively low value of Tc=O absorption in the infrared spectrum.

The bridging Tc-O distances (Tc1-O3 1.898Å and Tc2-O3 1.899Å) are intermediate between the average Tc=O length and the average Tc-O bond distance which are observed being in the range 1.98- 2.09Å [7-9].

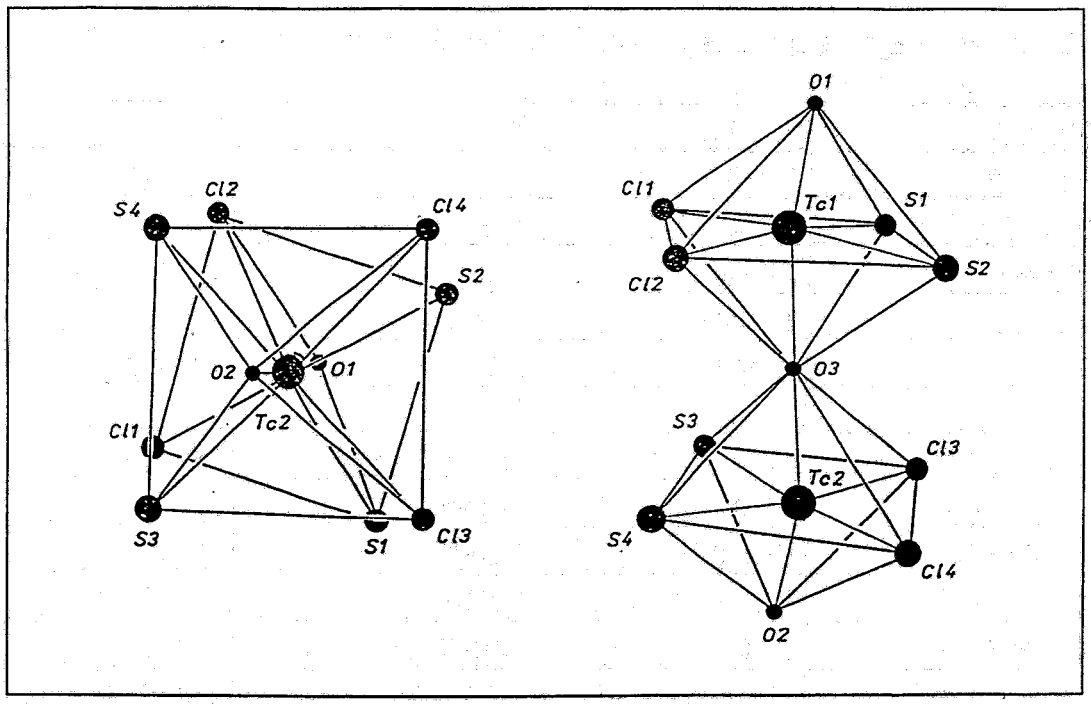

Fig. 2: Molecular geometry of [TcO(5,8-dithiadodecane)$_2$Cl$_2$]$_2$Oviewed perpendicular (on the left) and parallel to the O_1, Tc_1, O_3, Tc_2, O_2 axis

As illustrated in Fig. 3, complex (3) consists of discrete monomolecular units containing the O=Tc-O- core.

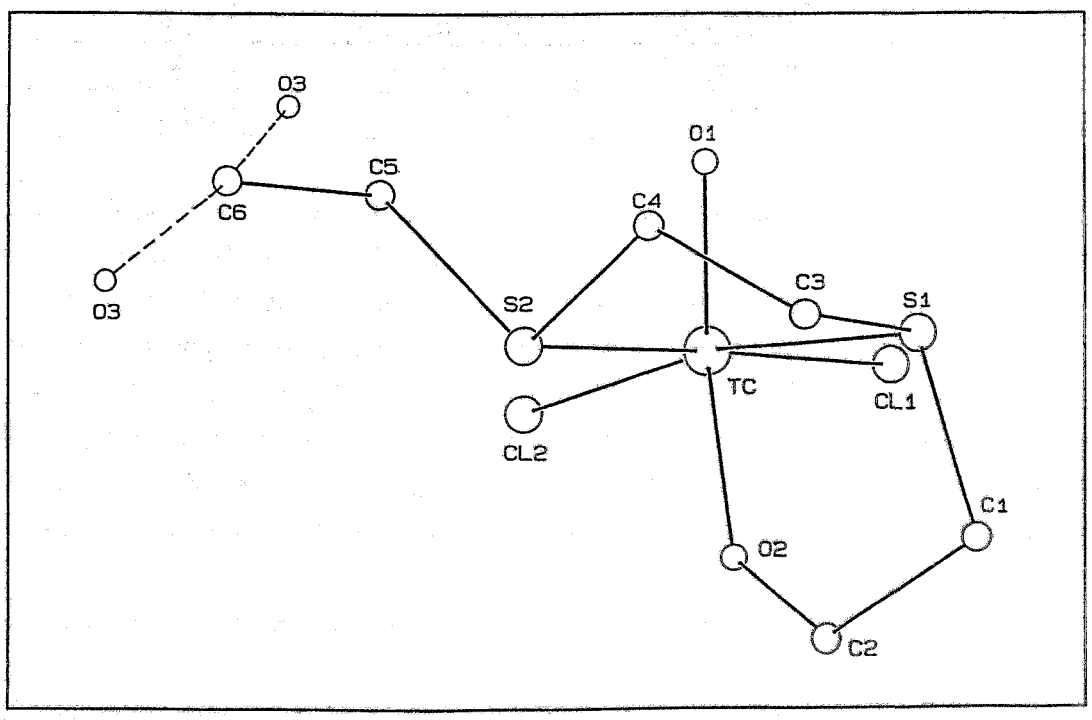

Fig. 3: CELLGRAF-drawing of [TcO{8-hydroxy-3,6-dithiaoctan-1-olato-(O,S,S)}Cl$_2$]

Tab. 2: Bond lengths (Å) and angles (deg) for $[TcO(5,8\text{-dithiadodecane})_2Cl_2]_2O$

Tc1-Cl1	2.396(2)	Tc2-Cl3	2.400(2)
Tc1-Cl2	2.418(2)	Tc2-Cl4	2.395(2)
Tc1-S1	2.464(2)	Tc2-S32.	2.433(2)
Tc1-S2	2.425(2)	Tc2-S4	2.445(2)
Tc1-O1	1.666(4)	Tc2-O2	1.674(4)
Tc1-O3	1.898(3)	Tc2-O3	1.899(3)
Cl1-Tc1-Cl2	91.03(7)	Cl3-Tc2-Cl4	90.69(8)
Cl1-Tc1-S1	90.28(7)	Cl3-Tc2-S3	92.10(8)
Cl1-Tc1-S2	173.40(7)	Cl3-Tc2-S4	173.65(6)
Cl1-Tc1-O1	98.0(2)	Cl3-Tc2-O2	98.4(2)
Cl1-Tc1-O3	92.4(1)	Cl3-Tc2-O3-	91.2(1)
Cl2-Tc1-S1	173.70(6)	Cl4-Tc2-S3	174.03(7)
Cl2-Tc1-S2	93.43(7)	Cl4-Tc2-S4	89.99(8)
Cl2-Tc1-O1	97.1(2)	Cl4-Tc2-O2	98.7(2)
Cl2-Tc1-O3	91.6(1)	Cl4-Tc2-O3	92.9(1)
S1-Tc1-S2	84.78(7)	S3-Tc2-S4	86.66(8)
S1-Tc1-O1	88.8(2)	S3-Tc2-O2	86.1(2)
S1-Tc1-O3	91.6(1)	S3-Tc2-O3	81.8(1)
S2-Tc1-O1	86.3(2)	S4-Tc2-O2	87.8(2)
S2-Tc1-O3	82.6(1)	S4-Tc2-O3	82.5(1)
O1-Tc1-O3	166.3(2)	O2-Tc2-O3	164.9(2)

In general, the structure strongly resembles that of the complex derived from dithiaoctane. However, while in the dinuclear species the trans-position is occupied by a bridging oxygen which may come from traces of water present in the reaction mix-ture, the trans position in complex (3) is occupied by an oxygen of one of the terminal hydroxy groups. The second hydroxy group remains "free". The CELLGRAF [10] drawing in Fig. 3 shows the two possible positions for the noncoordinated hydroxy group caused by a rotation disorder about the bond C5, C6. The S atoms of the dithioether and the two Cl atoms which remain at the metal due to the incomplete exchange at the tetrachlorooxotechnetium ion form a cis-arrangement in the equatorial plane.

Such compounds with a single bonded oxygen trans to the Tc=O core have been hardly described so far.

The length of the Tc-O bond (1.912Å) is comparable to that found in other trans-O=Tc-O$^-$ groups [11-13].

Tab. 3: Bond lengths (Å) and angles (deg) for [TcO{8-hydroxy-3,6-dithiaoctan-1-olato-(O,S,S)}Cl_2]

Tc-Cl(1)	2.461(1)	S(2)-C(4)	1.845(8)
Tc-Cl(2)	2.408(1)	S(2)-C(5)	1.814(7)
Tc-S(1)	2.446(2)	O(2)-C(2)	1.399(8)
Tc-S(2)	2.439(2)	O(3)-C(6)	1.389(0)
Tc-O(1)	1.680(4)	O(3)'-C(6)	1.286(0)
Tc-O(2)	1.895(4)	C(1)-C(2)	1.543(11)
S(1)-C(1)	1.799(8)	C(3)-C(4)	1.405(11)
S(1)-C(3)	1.854(8)	C(5)-C(6)	1.517(8)
Cl(1)-Tc-Cl(2)	92.03(6)	Tc-S(1)-C(1)	97.8(3)
Cl(1)-Tc-S(1)	89.40(6)	Tc-S(1)-C(3)	102.1(2)
Cl(1)-Tc-S(2)	173.72(6)	C(1)-S(1)-C(3)	102.9(4)
Cl(1)-Tc-O(1)	93.7(2)	Tc-S(2)-C(4)	98.4(3)
Cl(1)-Tc-O(2)	92.2(2)	Tc-S(2)-C(5)	106.0(2)
Cl(2)-Tc-S(1)	169.40(6)	C(4)-S(2)-C(5)	101.6(4)
Cl(2)-Tc-S(2)	93.60(5)	Tc-O(2)-C(2)	130.7(4)
Cl(2)-Tc-O(1)	104.4(2)	S(1)-C(1)-C(2)	107.2(5)
Cl(2)-Tc-O(2)	90.8(1)	O(2)-C(2)-C(1)	107.8(6)
S(1)-Tc-S(2)	84.56(6)	S(1)-C(3)-C(4)	113.0(5)
S(1)-Tc-O(1)	86.0(2)	S(2)-C(4)-C(3)	110.2(6)
S(1)-Tc-O(2)	78.7(1)	S(2)-C(5)-C(6)	114.8(4)
S(2)-Tc-O(1)	87.6(2)	C(5)-C(6)-O(3)	100.1(4)
S(2)-Tc-O(2)	84.9(2)	C(5)-C(6)-O(3)'	127.0(4)
O(1)-Tc-O(2)	163.5(2)	O(3)-C(6)-O(3)'	122.58(0)

This new class of technetium complexes is worthy of special interest as manifolde subsequent reactions can be anticipated. Diversity is given in ligand exchange reactions by vaious leaving groups in the coordination sphere. For complex (3) additional reactivity may be caused by the noncoordinated hydroxy group at the side chain. New radiopharmacologically relevant compounds may thus become accessible. Studies on the reactivity of the described complexes will follow.

Acknowledgements:
The authors thank Prof. E. Hoyer (Universität Leipzig) for the ligand 1,8-dihydroxy-3,6-dithiaoctane.

References:

[1] Pietzsch, H.J. et al., Polyhedron **12** (1993) 187
[2] Pietzsch, H.J. et al., Polyhedron **11** (1992) 1623
[3] Pietzsch, H.J. et al., Internal report, Rossendorf 1990
[4] Spies, H. et al., Inorg. Chim. Acta **116** (1986) 1
[5] Bandoli, G. et al., J. Chem. Soc. Dalton Trans. (1984) 2505
[6] Tisato, F. et al., J. Chem. Soc. Dalton Trans (1991) 1301
[7] Bandoli, G. et al., Coord. Chem. Rev. **44** (1982) 191
[8] Melnik, M. et al., Coord. Chem. Rev. **77** (1987) 27
[9] Mazzi, U. Polyhedron **8** (1989) 1683
[10] Reck, G. et al., CELLGRAF- a program for representation of organic and inorganic crystal structures, Analytical Centre, Berlin (1989/1991)
[11] Franklin, K. et al., Inorg. Chem. 1982, 21, 1941
[12] Jurisson, S. et al., Inorg. Chem. **23** (1984) 227
[13] Fackler, P. et al., Inorg. Chem. **23** (1984) 3968

14. TECHNETIUM COMPLEXES WITH THIOETHER LIGANDS: 3. SYNTHESIS AND STRUCTURAL CHARACTERIZATION OF CATIONIC TECHNETIUM COMPLEXES WITH THIACROWN ETHERS

H.J. Pietzsch, H. Spies, P. Leibnitz[1], G. Reck[1]
[1]Bundesanstalt für Materialforschung, D-1199 Berlin,

As part of our programme of studying the Tc/thioether chemistry and checking the suitabiltity of the resulting compounds for radiopharmacological purposes, we studied the capability of the TcN-core of being coordinated by thioether groups. The TcN-core shows a great capacity for stabilizing the metal in high oxidation states [1-3]. By now TcN complexes of the tetraaza macrocycles 1,4,8,11-tetraazacyclotetradecane (cyclam) [4], 1,4,8,11 tetraazacyclotetra-decane-5,7-dione [5] and the analogous aza/thia ligand 1,4-diaza-8,11-dithiacyclotetra-decane [6] have been fully characterized.
In order to gain an insight into the effects on coordination geometry and complex stabilities of factors such as ring size and functional group substituent in macrocyclic polythioether ligands we synthesized a number of technetium chelates with the thiacrown ethers 1,4,8,11-tetrathiacyclotetradecane (14S4), 1,5,9,13-tetrathiacyclohexadecane (16S4), 1,5,9,13-tetrathia-cyclohexadecane-3,11-diol (16S4-$(OH)_2$) and 1,4,7,10,13,16-hexathiacyclooctadecane (18S6). Some representatives were characterized by X-ray crystal structure determination.

The ligand exchange reactions on $NBu_4[TcNCl_4]$ proceeding in acetone/methanol solutions at ambient temperature result in the formation of cationic complexes $[TcNCl(S_4)]^+$.
The crystalline compounds precipitate from the reaction mixtures in analytically pure form. The elemental analyses correspond to the formulations $[TcNCl(S_4)]TcNCl_4$ for 14S4 (1), 16S4 (2) and 18S6 (3), $[TcNCl(S_4)]BPh_4$ (4) and [TcNCl(16S4-$(OH)_2$)]Cl (5) (see Tab. 1).

$TcNCl_4^-$ —(14S4/16S4/18S6 {$+BPh_4^-$}; acetone/methanol)→ $[TcNCl(S_4)]TcNCl_4$/$[TcNCl(S_4)]BPh_4$}

(1) S_4 : 14S4 (4) S_4 : 14S4
(2) S_4 : 16S4
(3) S_4 : 18S6

$TcNCl_4^-$ —(16S4-$(OH)_2$; acetone/methanol)→ [TcNCl(16S4-$(OH)_2$")]Cl (5)

From a mechanistic point of view it is interesting to note that the complexation reaction proceeds only after addition of methanol to the acetonic solution of the reaction participants.

This may be explained by the fact that the exchange reaction is coupled with a reduction of Tc(VI) to Tc(V), and methanol is assumed to be the reducing agent.

Tab. 1: Yields and analytical data of the complexes (1)-(5)

Compl.	Yield %	Elemental analysis[a] C	H	N	S	Cl	Tc	UV/vis nm/lgε
(1)	45	17.9 17.7	3.0 2.9	4.2 3.9	19.1 18.8	26.4 25.7	29.5 29.2	463/3.2
(2)	43	20.6 21.0	3.4 3.2	4.0 3.7	18.3 17.8	25.3 24.7	28.4 28.1	461/3.2
(3)	45	18.9 18.4	3.1 3.0	3.7 3.4	25.2 24.9	23.2 22.8	26.0 26.2	463/3.2
(4)	80	55.5 54.9	5.4 5.2	1.9 1.7	17.4 16.8	4.8 5.2	13.5 13.2	402/3.4
(5)	48	28.1 27.5	4.7 5.1	2.7 2.2	25.0 24.2	13.9 14.1	19.3 18.9	402/3.4

[a]Calc./found

The exchange rate for the ligands 14S4, 16S4 and 18S6 is about 50%. The complex cations obviously formed combine with the precursor to produce only slightly soluble salt, thus preventing further exchange. The reaction is practically quantitative in the presence of alternative counterions (e.g. BPh_4^-, PF_6^-).

The assumption that the solubility of the formed complexes in the reaction media governs the reaction route is supported by the reaction of 16S4-$(OH)_2$. The exchange reaction with this ligand, which bears two OH groups, is practically quantitative in the absence of additional counterions.

The UV/vis spectra of all complexes without alternative counterions (1)-(3) are characterized by the absorption band of the $TcNCl_4^-$ moiety (λ_{max}: 404nm, 460nm (sh) in acetone/methanol).

The infrared spectra show less characteristic bands in the range between 1000 and 1100cm^{-1} which we assigne to the TcN core of the complex cations and additional peaks at 1080cm^{-1} for compounds (1), (2) and (3) which contain the $TcNCl_4^-$ anion.

Structure of [TcNCl(14S4)]$TcNCl_4$ (1) and [TcNCl(18S6)]$TcNCl_4$ (3)

The molecular structures of compounds (1) and (3) together with the atomic numbering schemes are given in Figs. 1 and 2. Selected interatomic distances and angles are summarized in Tabs. 2 and 3.

(1) and (3) consist of couples of independent cations with the metal in the oxidation state +5 and hexavalent $TcNCl_4^-$ anions. In both complex cations the Tc atom is six-coordinated in a rather distorted octahedral geometry, being directly bound to four sulphur atoms of the macrocyclic ligand in the equatorial plane. The nitrido and the chlorine atoms occupy the axial positions.

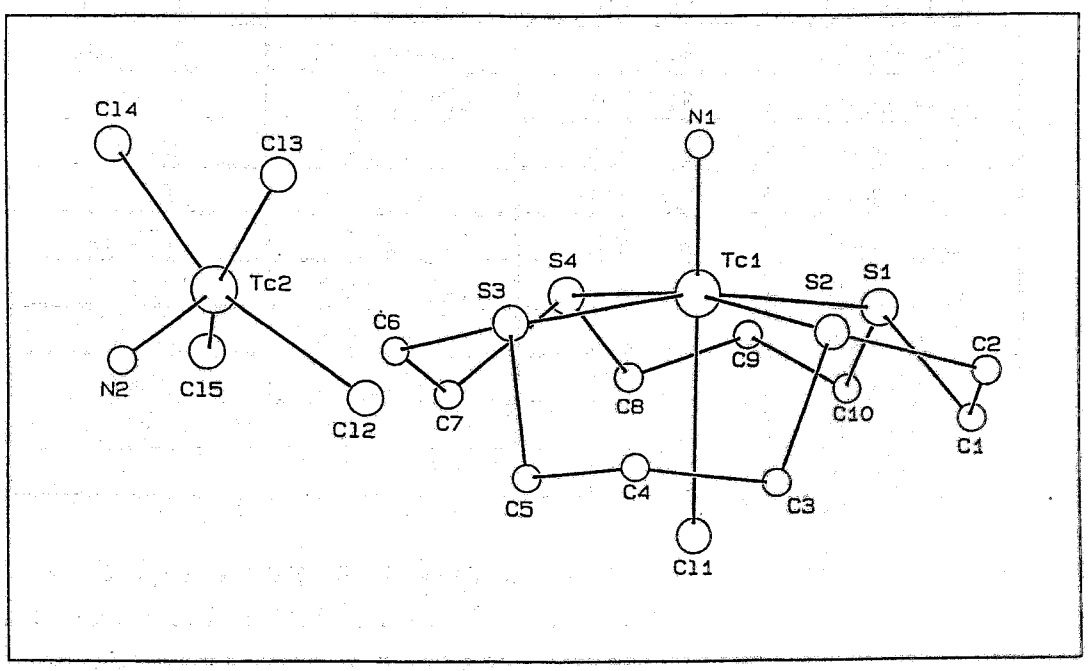

Fig. 1: CELLGRAF drawing of [TcNCl(14S4)]$TcNCl_4$ (1)

Tab. 2: Selected Bond lengths (Å) and angles (deg) for [TcNCl(14S4)]TcNCl4 (1)

Tc1-Cl1	2.718(1)	Tc2-Cl2	2.325(1)
Tc1-S1	2.414(1)	Tc2-Cl3	2.329(1)
Tc1-S2	2.411(1)	Tc2-Cl4	2.345(1)
Tc1-S3	2.405(1)	Tc2-Cl5	2.337(1)
Tc1-S4	2.408(1)	Tc2-N2	1.582(4)
Tc1-N1	1.615(3)		
Cl1-Tc1-S1	81.34(3)	S3-Tc1-N1	95.3(1)
Cl1-Tc1-S2	87.87(3)	S4-Tc1-N1	95.4(1)
Cl1-Tc1-S3	86.84(3)	Cl2-Tc2-Cl3	88.90(4)
Cl1-Tc1-S4	81.83(3)	Cl2-Tc2-Cl4	157.62(4)
Cl1-Tc1-N1	176.4(1)	Cl2-Tc2-Cl5	87.23(4)
S1-Tc1-S2	84.92(3)	Cl2-Tc2-N2	101.3(1)
S1-Tc1-S3	167.51(3)	Cl3-Tc2-Cl4	87.25(4)
S1-Tc1-S4	96.97(3)	Cl3-Tc2-Cl5	156.58(4)
S1-Tc1-N1	96.7(1)	Cl3-Tc2-N2	102.5(1)
S2-Tc1-S3	90.62(3)	Cl4-Tc2-Cl5	87.59(4)
S2-Tc1-S4	169.10(3)	Cl4-Tc2-N2	101.0(1)
S2-Tc1-N1	95.0(1)	Cl5-Tc2-N2	100.9(1)
S3-Tc1-S4	85.29(3)		

While the molecular cation (1) has a noncrystallographic mirror plane through Tc(1), N(1), Cl(1), C(4), C(9), a mirror plane through Tc(1), N(1), Cl(1) , S(5), and (S6) does not exist in (3). The noncrystallographic symmetry was disturbed by a dislocation of the atoms C(5) and C(6) caused by packing of the molecules in the unit cell.

The Tc atom is displaced from the plane formed by the four S atoms by 0.236Å toward the N(1) atom in compound (1) and by 0.209Å in compound (3). The Tc(1)=N bond distances of 1.615Å for (1) and 1.707Å for (3) are consistent with the triple-bond distances found in all Tc(V)-nitrido complexes structurally characterized [7].

The structure of (1) closely resembles that of the $[TcNCl(N_4)]^+$ cations (N_4 = 2 en, 1,5,8,12-tetraazadodecane) [8].

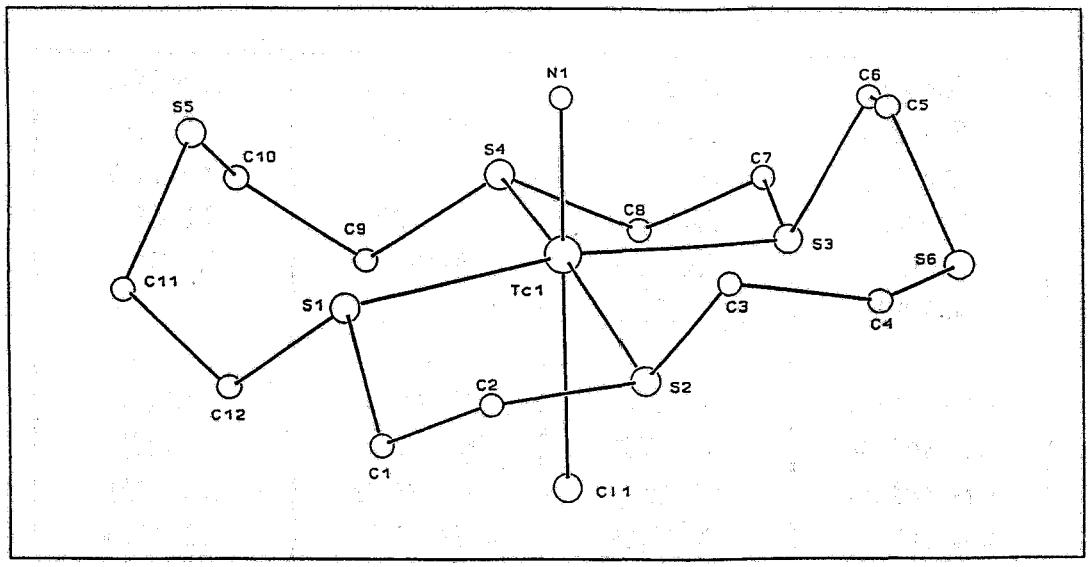

Fig. 2: CELLGRAF drawing of the molecular cation of [TcNCl(18S6)]$TcNCl_4$ (3)

Structure of [TcNCl(16S4-$(OH)_2$]Cl (5)

The octahedral molecular structure of (5) is comparable to that of $[TcNCl(14S4)]^+$: four S atoms of the thiacrown ether form the equatorial plane, the nitrido and Cl^- ligands are in the axial positions (Fig. 3, Tab. 4). The metal is displaced from the equatorial plane by 0.114Å toward the N atom. As found for (1) the complex cation has a noncrystallographic mirror plane through Tc, N, Cl(1), C(2), O(2), C(8), O(1).

In the crystal the cations and the Cl^- counterions are connected by two symmetry-independent hydrogen bonds O(1)-H---Cl(2) (3.045Å) and Cl(2)---H-O(2)'(2.973Å) forming chains in [1 1 0] direction.

[TcNCl(16S4-$(OH)_2$]Cl (5) deviates from (1) and (3) concerning the extremely long Tc-N bond distance.

Tab 3: Selected Bond lengths (Å) and angles (deg) for $[TcNCl(18S6)]TcNCl_4$ **(5)**

Tc1-Cl1	2.567(1)	Tc2-Cl2	2.352(1)
Tc1-S1	2.469(1)	Tc2-Cl3	2.334(1)
Tc1-S2	2.499(1)	Tc2-Cl4	2.345(1)
Tc1-S3	2.464(1)	Tc2-Cl5	2.338(1)
Tc1-S4	2.461(1)	Tc2-N2	1.611(4)
Tc1-N1	1.707(3)		
Cl1-Tc1-S1	87.82(4)	S3-Tc1-N1	95.2(1)
Cl1-Tc1-S2	81.65(4)	S4-Tc1-N1	90.6(1)
Cl1-Tc1-S3	83.96(4)	Cl2-Tc2-Cl3	87.87(5)
Cl1-Tc1-S4	86.82(4)	Cl2-Tc2-Cl4	161.22(5)
Cl1-Tc1-N1	177.4(1)	Cl2-Tc2-Cl5	85.81(4)
S1-Tc1-S2	82.76(3)	Cl2-Tc2-N2	100.5(2)
S1-Tc1-S3	171.30(4)	Cl3-Tc2-Cl4	90.57(5)
S1-Tc1-S4	99.99(3)	Cl3-Tc2-Cl5	160.08(4)
S1-Tc1-N1	93.1(1)	Cl3-Tc2-N2	99.7(1)
S2-Tc1-S3	93.21(4)	Cl4-Tc2-Cl5	89.39(5)
S2-Tc1-S4	168.05(4)	Cl4-Tc2-N2	98.3(2)
S2-Tc1-N1	100.9(1)	Cl5-Tc2-N2	100.0(1)
S3-Tc1-S4	82.42(3)		

For all three compounds studied by X-ray analysis, coordination of technetium by four sulphur atoms in the equatorial plane was found to be the common feature regardless of differences in ring size or the presence of two additional sulphur atoms in the ring of 18S6 or two hydroxy groups in $16S4\text{-}(OH)_2$.

The geometry of the distorted octahedral TcN complexes having a sixth, negatively charged ligand in trans position to the TcN bond may be explained in terms of balancing the strong influence of the nitrido group, which destabilizes the octahedral coordination, and by the demand for an effective neutralization of the residual charge on the TcN^{2+} group [9].

The trans influence of the nitrido ligand is, for example apparent in $[TcNCl_2(PMe_2Ph)_3]$ in the cis and trans Tc-Cl bond lengths of 2.441 and 2.665Å, respectively.

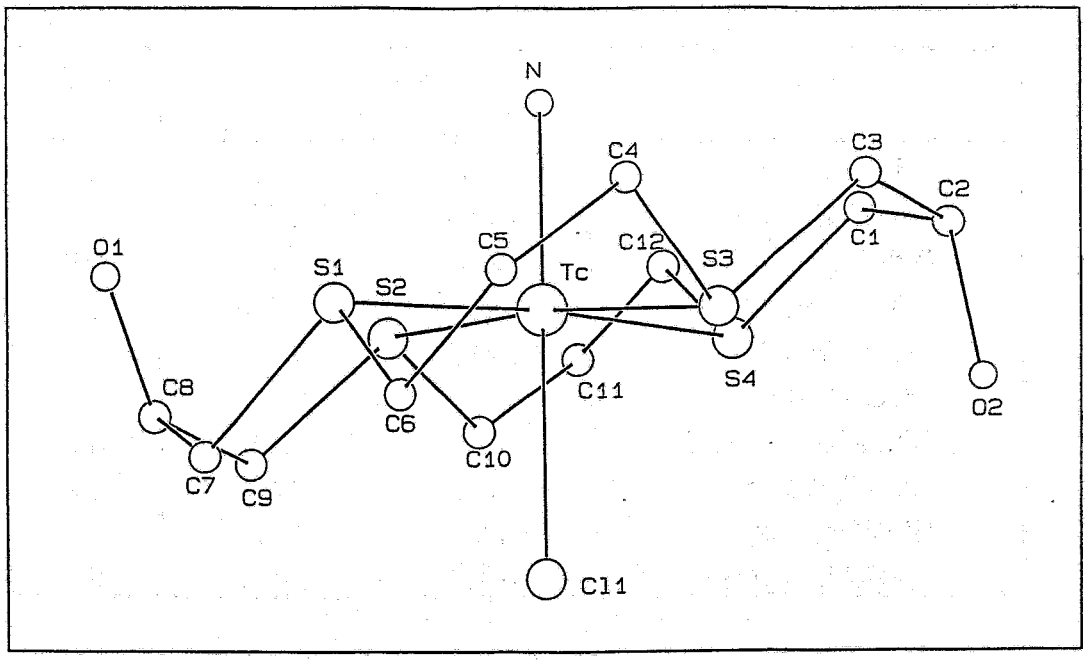

Fig. 3: CELLGRAF drawing of the molecular cation of [TcNCl(16S4-$(OH)_2$)]Cl (5)

Tab. 4: Selected bond lengths (Å) and angles (deg) for [TcNCl(16S4-(OH)2)]Cl (5)

Tc-Cl1	2.469(4)	Tc-S3	2.430(4)
Tc-S1	2.431(5)	Tc-S4	2.446(5)
Tc-S2	2.447(4)	Tc-N	1.95(1)
Cl1-Tc-S1	87.2(2)	S1-Tc-N	91.5(3)
Cl1-Tc-S2	89.0(2)	S2-Tc-S3	174.3(2)
Cl1-Tc-S3	85.3(1)	S2-Tc-S4	89.1(2)
Cl1-Tc-S4	87.8(2)	S2-Tc-N	91.6(3)
Cl1-Tc-N	178.6(4)	S3-Tc-S4	90.3(2)
S1-Tc-S2	90.7(2)	S3-Tc-N	94.1(3)
S1-Tc-S3	89.4(2)	S4-Tc-N	93.5(3)
S1-Tc-S4	175.1(2)		

As shown in Tab. 5 for previously described complexes as well as for compounds reported here, both the Tc-N and Tc-Cl bond lengths vary over a wide range. The same is true for the congener rhenium.

Tab. 5: Bond lengths of Tc/Re nitrido complexes with trans-coordinated Cl

complex	bond length [Å]		Ref.
	Me=N	Me-Cl	
$[TcNCl(en)_2]^+$	1.603	2.732	14
$[TcNCl(tad)]^+$	1.626	2.663	14
$[TcNCl_2(PMe_2Ph)_3]$	1.624	2.665	15
$[TcNCl(dmpe)_2]^+$	1.854	2.608	17
$[TcNCl(14S4)]^+$	1.615	2.718	this paper
$[TcNCl(18S6)]^+$	1.707	2.567	this paper
$[TcNCl(16S4\text{-}(OH)_2]^+$	1.950	2.469	this paper
$[ReNCl_2(PMe_2Ph)_3]$	1.660	2.633	19
$[ReNCl_2(PEt_2Ph)_3]$	1.788	2.563	20
$[ReNCl(dpae)_2]^+$	1.839	2.451	21

Abbreviations:
en: ethylenediamine
tad: 1,5,8,12-tetraazadodecane
dpae: 1,2-bis(diphenylarsino)ethane
dmpe: 1,2-bis(dimethylphosphino)ethane

Considerable Tc-N bond lengthening was found for $[TcN(dmpe)_2Cl]^+$ (dmpe = dimethylphosphinoethane; Tc-N bond distance: 1.85Å) /10,11/ and attributed to steric interactions between the nitrido group and the co-planar phosphorus atoms [12].
While the Tc-N bond lengths of (1) and (3) fall in the range between about 1.60 to 1.854Å, the distance of 1.950Å observed in the preliminary X-ray structural analysis of $[TcNCl(16S4\text{-}(OH)_2]Cl$ (5) is exceptionally long.
Marchi et al. [8] have already pointed out that the lengths of the TcN and Tc-Cl bonds are inversely related. On the one hand, the strong trans influence of the nitrido ligand in $[TcNCl(en)_2]^+$ causes a considerable lengthening of the Tc-Cl bond distance at 2.732Å, the longest Tc-Cl bond distance ever observed in Tc complexes [8]. On the other, the extremely long Tc-N bond distance in $[TcNCl(16S4\text{-}(OH)_2)]^+$ (5) is accompanied by a decrease of the Tc-Cl bond to a distance normally found for equatorially bound chlorine (2.469Å).
This is also true of the TcN complexes contained in Tab. 5. The sums of the appropriate Tc-N and Tc-Cl bond lengths are relatively constant.
The differences observed for (5) may be indicative of a tendency to adopt a less distorted octahedral geometry. Accordingly, technetium is closer to the S_4 plane (0.114Å) than found for (1) (0.236Å) and (3) (0.209Å).

References:

[1] Baldas, J. et al., J. Chem. Soc. Dalton Trans. (1984) 2395

[2] Baldas, J. et al., J.Chem. Soc. Dalton Trans. (1991) 2441

[3] Pietzsch, H.J. et al., Z. Chem. **27** (1987) 265

[4] Zuckman, S. et al., Inorg Chem. **20** (1981) 2386

[5] Marchi, A. et al., J. Chem. Soc. Dalton Trans. (1990) 19

[6] Ianoz, E. et al., Inorg. Chim. Acta **156** (1989) 235

[7] Melnik, M. et al., Coord. Chem. Rev. **77** (1987) 275

[8] Marchi, A. et al., Inorg. Chem. **29** (1990) 2091

[9] Batsanov, A.S. et al., Z. Anorg. Allg. Chem. **564** (1988) 129

[10] Archer C.M. et al., Polyhedron **8** (1989) 1879

[11] Archer, C.M.et al., J.C.S. Dalton Trans. (1992) 183

[12] Dilworth, J.P. et al., Inorg. Chim. Acta **71** (1982) 21

[13] Forsellini, E. et al., Acta Cryst. Sect. B **38** (1982) 3081

[14] Corfield, P.W.R. et al., Inorg. Chem. **6** (1967) 197

[15] Yam, V.W. et al., J.C.S. Dalton Trans. (1992) 1717

15. TECHNETIUM COMPLEXES WITH THIOETHER LIGANDS: 4. CATIONIC Tc(III) COMPLEXES WITH TETRADENTATE THIOETHERS AND MONODENTATE THIOLS: PREPARATION AND PRELIMINARY BIOLOGICAL EVALUATION

H.J. Pietzsch, S. Seifert, R. Syhre, H. Spies

Recently we found that cationic Tc(III) complexes, $[Tc("S_4")(SR)_2]^+$, are formed when pertechnetate is reduced by stannous chloride in the presence of both a tetrathiaalkane and a monothiol [1]:

$$TcO_4^- + "S_4"/RSH \xrightarrow{Sn^{2+}} [Tc("S_4")(SR)_2]^+$$

"S_4": R´-CH_2CH_2-(S-CH_2CH_2-S-CH_2CH_2)$_n$-R´ (n=2; R´=H, ethyl)
RSH.: R=alkyl, aryl

The lipophilic compounds are extractable from the reaction mixtures by chloroform and can be isolated as PF_6^- salts.
The complexes are interesting as potential myocardium affine agents with their positive charge and in analogy to cationic diphosphine/thiolate Tc(III) complexes [2].
In this paper we are reporting on the preparation of the cationic species at carrier-added level and on the preliminary evaluation of their biobehaviour in the rat.

For biodistribution studies the complexes (see Tab. 1) were prepared with 10^{-4}mol/l $^{99}TcO_4^-$ in aqueous-acetonic solution according the following standard procedure:

0.5mg of the tetrathiaalkane and 2.5mg of the thiol were dissolved in 1.5ml acetone. This mixture was added to a solution of 20mg mannitol in 0.5ml $^{99/99m}$Tc-pertechnetate (10^{-4} mol/l). After addition of 2.0mg $SnCl_2$ in 0.1ml ethanol the reaction mixture was allowed to stand for 10 minutes.
To obtain injectable solutions acetone was evaporated under nitrogen, the residues were diluted with propyleneglycol/saline and filtered through a 0.2μm filter.

The products formed were characterized by HPLC (RP 18, THF/0.5m NH_4OAc (40/60), 1ml/min) and TLC (silica gel, methanol/THF/0.5m NH_4OAc (50/5/40)). A typical product distribution pattern is shown in Fig. 1.

Tab. 1: Tc complexes for in-vivo studies

complex	R`-$S_4$-R` R`	R-SH R
(1)	ethyl	ethyl
(2)	ethyl	isopropyl
(3)	ethyl	isobutyl
(4)	ethyl	phenyl
(5)	ethyl	p-OCH_3-phenyl
(6)	butyl	isopropyl

At lower Tc concentrations the yield of the desired product decreases and becomes $<10\%$ at n.c.a. level. It was found that the R_T values of the cationic complexes correlate with the partition coefficients in octanol/saline (see Tab. 2).

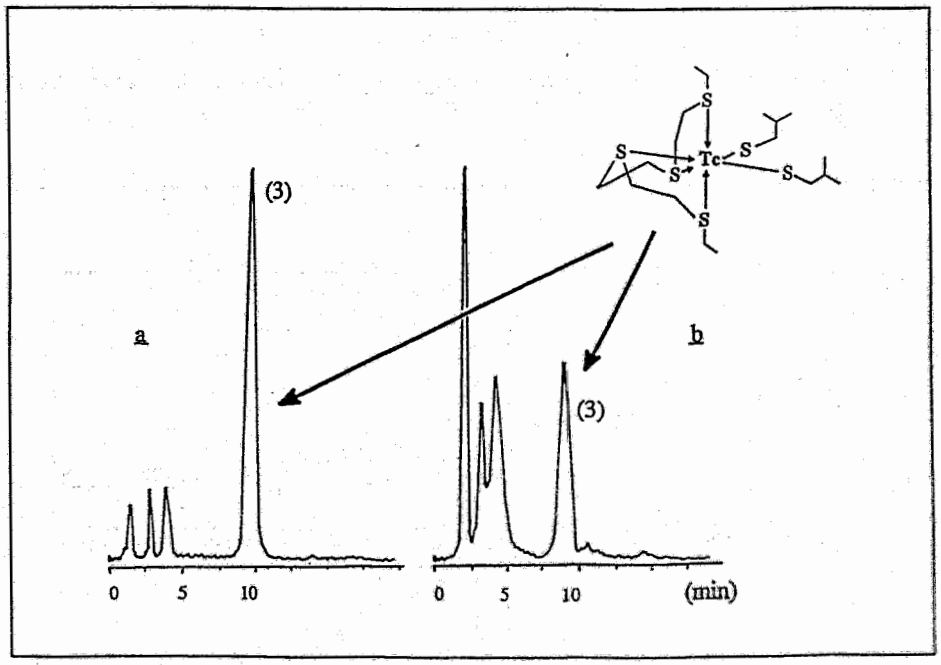

Fig. 1: HPLC product distribution pattern of a preparation of complex (3) at different Tc-concentrations (yields in %) [a: $c_{Tc} = 2x10^{-4}M$ (80-90); b: $c_{Tc} = 2x10^{-5}M$ (20-30)]

Tab. 2: Correlation of the R_T-values of complexes (1), (2) and (3) with their lipophilicity

complex	R_t(min)	lg p.c. (octanol/saline)
(1)	5	1.4
(2)	7	2.1
(3)	10	3.6

Biological evaluation

Animal studies were performed on male Wistar rats (150g BW) after intravenous administration of the $^{99/99m}$Tc-compounds. The animals were killed at intervals ranging from 5 minutes to 2 hours after the injection

All complexes studied show similar biodistribution patterns with significant myocardial uptake. This uptake is most pronounced with the complexes (2) and (5). Blood elimination is faster than the myocardial washout (see Fig. 2).

The lipophilic nature of the complexes causes a high hepatobiliary uptake and excretion (50-70% dose p.i.). as shown in Fig. 3.

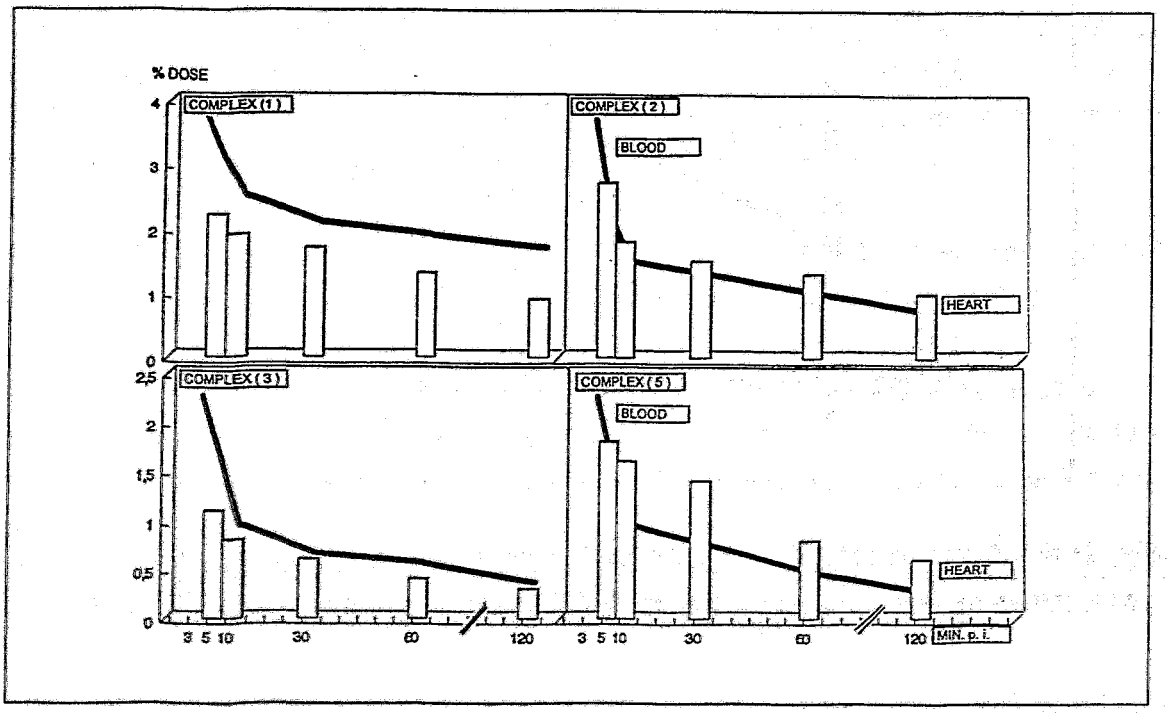

Fig. 2: Blood elimination and myocardial washout of complexes (1), (2), (3) and (5) in % dose/gram

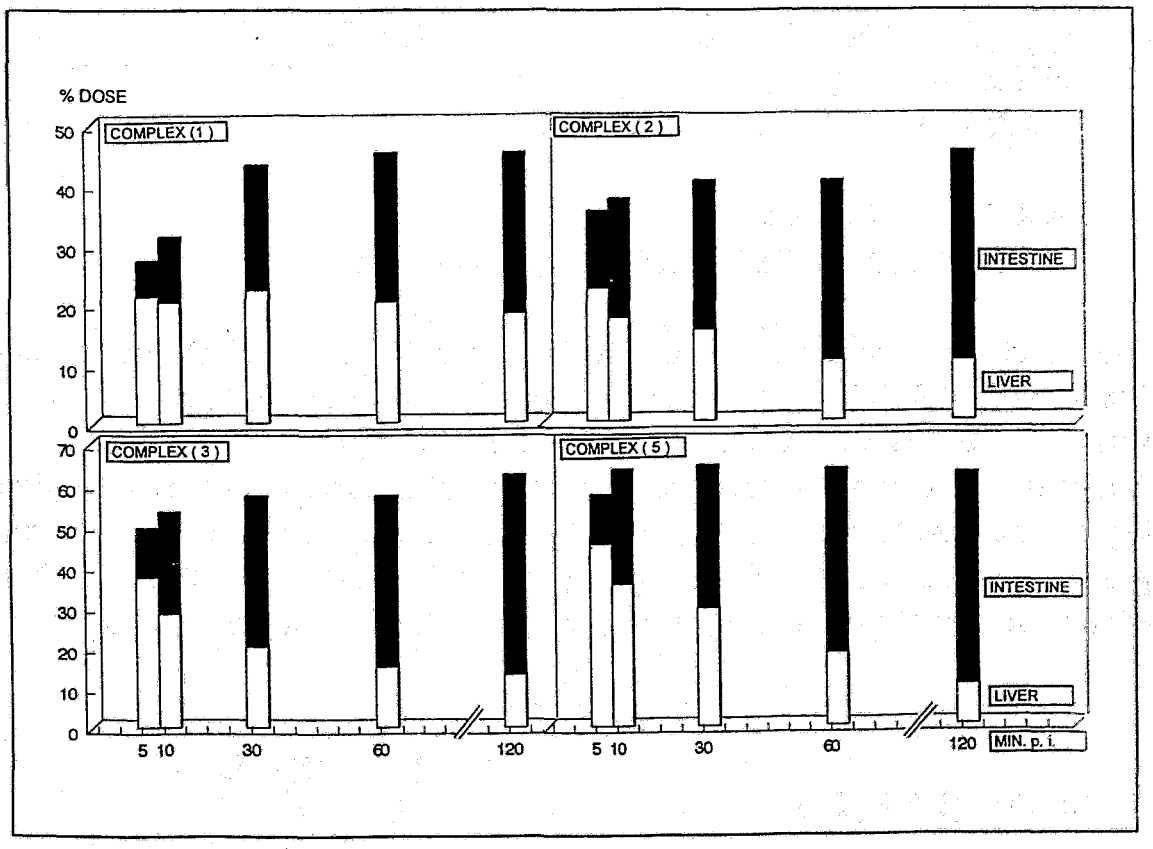

Fig. 3: Hepatobiliary pool of complexes (1), (2), (3) and (5) in % dose

The myocardium affinity of the new lipophilic and positively charged complexes is not surprising in view of their analogy to the well-known diphosphine/thiolato compounds [1]. In contrast to them, thioether complexes appear to be less susceptible to reduction in vivo. As such susceptibility is blaimed for undesired washout from the myocardium [2], thioether complexes may be advantageous. Until now, their preparation is restricted to the carrier-added level. To overcome this obstacle, we will focus our investigations on less steric constrained bidentate thioethers R-S-CH_2CH_2-S-R.

References:

[1] Pietzsch, H.J. et al., Polyhedron **11** (1992) 1623

[2] Konno, T. et al., Inorg. Chem. **28** (1989) 1694 and lit. loc. cit.

[3] Deutsch, E. et al., Nucl. Med. Biol. **16** (1989) 191 and lit. loc. cit.

16. SYNTHESIS AND CHARACTERIZATION OF NEUTRAL TECHNETIUM(III) COMPLEXES WITH THE TRIPODAL LIGAND TRIS(2-MERCAPTOETHYL)AMINE

H. J. Pietzsch, H. Spies, F. E. Hahn[1]
[1]Freie Universität Berlin, Institut für Anorganische Chemie

The trianionic tetradentate ligand tris-(2-mercaptoethyl)-amin (NS_3) reacts with $TcCl_3(PPh_3)_2(CH_3CN)$ in a 1:1 ratio to produce neutral lipophilic Tc(III) complexes. Depending on the polarity of the solvent two different compounds were observed:
In a polar mixture of methylene dichloride/methanol (1:4) three chlorine and one phosphine li-gands are substituted, forming $TcNS_3(PPh_3)$ (1). In pure methylene dichloride both phosphines are retained and $TcNS_3(PPh_3)_2$ (2) is formed. Complex (1) is obtained in form of violett crystals (λ_{max}: 541 nm), whereas complex (2) is a blue powder (λ_{max}: 597 nm).

$$TcCl_3(PPh_3)_2(CH_3CN) \xrightarrow{CH_2Cl_2/MeOH} TcNS_3(PPh_3)\ (1)$$

$$TcCl_3(PPh_3)_2(CH_3CN) \xrightarrow{CH_2Cl_2} TcNS_3(PPh_3)_2\ (2)$$

Both compounds were characterized by elemental analysis, infra red, UV/visible and NMR spectroscopy
An X-ray single-crystal structure determination of $TcNS_3(PPh_3)$ (1) shows that the complex has a trigonal-bipyramidal geometry with the nitrogen and the phosphorus in the axial positions and the sulphurs bound in the equatorial plane (Fig. 1 and Tab. 1).
In this respect the structure is comparable to that of $Tc(P(o\text{-}C_6H_4S)_3)(CNC_3H_7)$ [1]. A similar coordination geometry is found in the neutral Tc(III) complexes $TcPR_3(SXS)(SR)$, formed by reduction of the [3+1]-complexes TcO(SXS)(SR) with an excess of phosphine in acidic solution (R=alkyl, aryl; SXS=tridentate ligand of the type $HSCH_2CH_2\text{-}X\text{-}CH_2CH_2SH$, X=O,NR, S) [2].
Owing to the reducing power of the phosphine and the thiol compound, (1) can also be prepared directly from pertechnetate with an excess of triphenylphosphine and tris-(2-mercaptoethyl)amine; in this reaction $TcNS_3(PPh_3)_2$ (2) was not be observed in significant amounts:

$$TcO_4^- \xrightarrow{+\ NS_3/PPh_3/H^+} TcNS_3(PPh_3)\ (1)$$

This makes the procedure very easy and gives access to a new class of Tc^{3+} complexes for radiopharmaceutical studies with Tc-99m at c.a. and n.c.a. level.

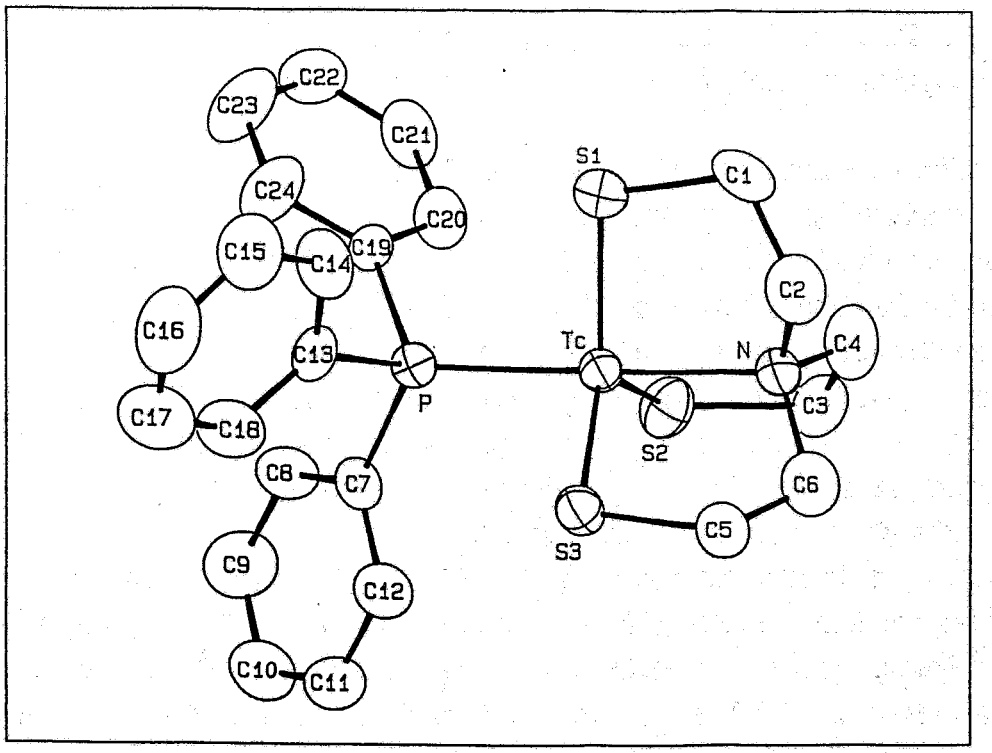

Fig. 1: ORTEP-drawing of $TcNS_3(PPh_3)$ (1)

Tab. 1. Bond lengths (Å) and angles (deg) for $TcNS_3(PPh_3)$ (1)

Tc-S1	2.227(2)	Tc-P	2.325(2)
Tc-S2	2.225(2)	Tc-N	2.192(5)
Tc-S3	2.227(2)		
S1-Tc-S2	119.30(7)	S2-Tc-P	95.59(7)
S1-Tc-S3	119.91(7)	S2-Tc-N	85.44(15)
S1-Tc-P	93.84(6)	S3-Tc-P	94.92(6)
S1-Tc-N	85.01(15)	S3-Tc-N	85.20(14)
S2-Tc-S3	118.73(7)	P-Tc-N	178.7(2)

References

[1] De Vries, N. et al., Inorg. Chem. **30** (1991) 2662

[2] Pietzsch, H.J. et al., Inorg. Chim. Acta **168** (1990) 7

17. RHENIUM COMPLEXES WITH TRIPODAL TETRADENTATE LIGANDS CONTAINING SULPHUR DONORS

H.-J. Pietzsch, M. Glaser , H. Spies, J. Beger[1], R. Jacobi[1]
[1]Bergakademie Freiberg , Institut für Organische Chemie

Our studies of technetium and rhenium complexes with tripodal ligands are aimed at designing mixed ligand compounds $M(XY_3)Z$ where the monodentate co-ligand Z may be structurally varied in a wide range and should be capable of being functionalized by reactive groups. So far, Tc/Re complexes of tripodal ligands with oxygen [1], phosphorus [2], isonitrile [3] and sulphur donors [4] are known.

After having synthesized $Tc(NS_3)PPh_3$ as a typical representative of the desired complex type, we are now investigating the formation of rhenium complexes with tris(2-mercaptoethyl)amine "NS_3" and tris(3-mercaptopropyl)amine as tripodal ligands and triphenylphosphine as a monodentate co-ligand.

Ammonium perrhenate, trans-oxotrichlorobis(triphenylphosphine)rhenium(V) **1**, benzyl-tri(ethyl)ammonium oxotetrachlororhenium(V) **2** and trichloro(acetonitrile)bis-(triphenylphosphine)rhenium(III) **3** were used as precursors. The Re^{V} and Re^{III} complexes **1-3** shown in Fig. 1 should allow chlorine substitution at a definite oxydation state. Initial ligand exchange experiments have been carried out in order to obtain neutral ,lipophilic compounds.

Reaction of "NS_3" with **1** in toluene furnished a grey powder of low solubility in common solvents. Its infrared spectrum showed broad bands indicating a polymer. Similar results have been obtained by the reaction of "NS_3" with **2** in MeOH/MeCN/triethylamine.

3 reacted with "NS_3" in the presence of triphenylphosphine in $MeCl_2$ a formed violet compound **4** [λ_{max} = 500.2nm ($MeCl_2$)]. It was purified by column chromatography (silica, $CHCl_3$). The elemental analysis revealed 1:1 units of triphenylphosphine/"NS_3" and additional chlorine. The structure of compound **4** cannot yet be interpreted with certainty on the basis of elemental analysis and ^1H NMR.

The reduction route starting directly from NH_4ReO_4 with an excess of ligand in EtOH was more sucessful. Two different products **5** and **6** are formed as illustrated by Fig. 1. Compound **5** appears as a violet species in solution (EtOH), but it decomposes slowly. Appearantly, chlorine was attached to the rhenium ion, thus making **5** instable due to the presence of "native" chlorine. In order to avoid this effect, further experiments were carried out in MeCN. However, similar products were obtained which are good soluble in polar solvents to give a violet colour occured.

The green compound **6** was formed under similar conditions but in the presence of an excess of triphenylphosphine. Polar by-products were removed by column chromatography

(silica, toluene). After recrystallization from toluene, dark green needles (m.p. 234°C, decomp.) of **6** were obtained.

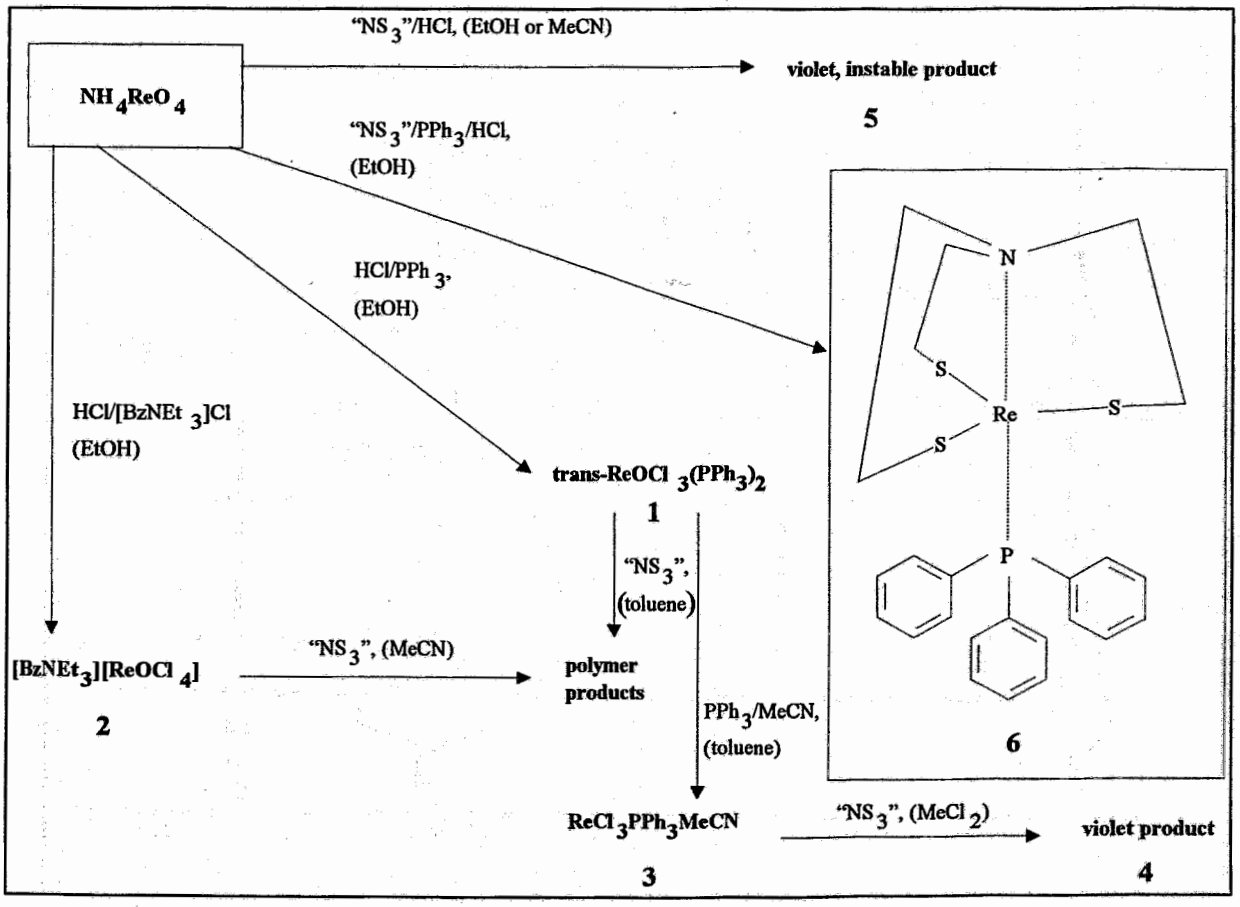

Fig. 1: Some products obtained from Re^{VII}, Re^{V} and Re^{III}.

The UV/vis spectrum of **6** showed absorptions at 247, 306 and 461nm in $MeCl_2$. In the infrared spectrum no band of νRe=O was observed. The ^1H NMR spectrum supported formula **6** (Fig. 2). Here the shape of the methylene multiplet suggested 6 equivalent CH_2 groups. Elemental analysis supplied a further evidence for the structure assumed.
Up to now tris(3-mercaptopropyl)amine has generally yielded ambiguous products .Its deviant behaviour may be due to the steric conditions.

Elemental analysis of **6** :

$C_{24}H_{27}NPS_3Re$		C	H	N	S
M: 642,35	calc. (%)	44,84	4,20	2,17	14,97
	found (%)	44,76	4,31	2,19	14,73

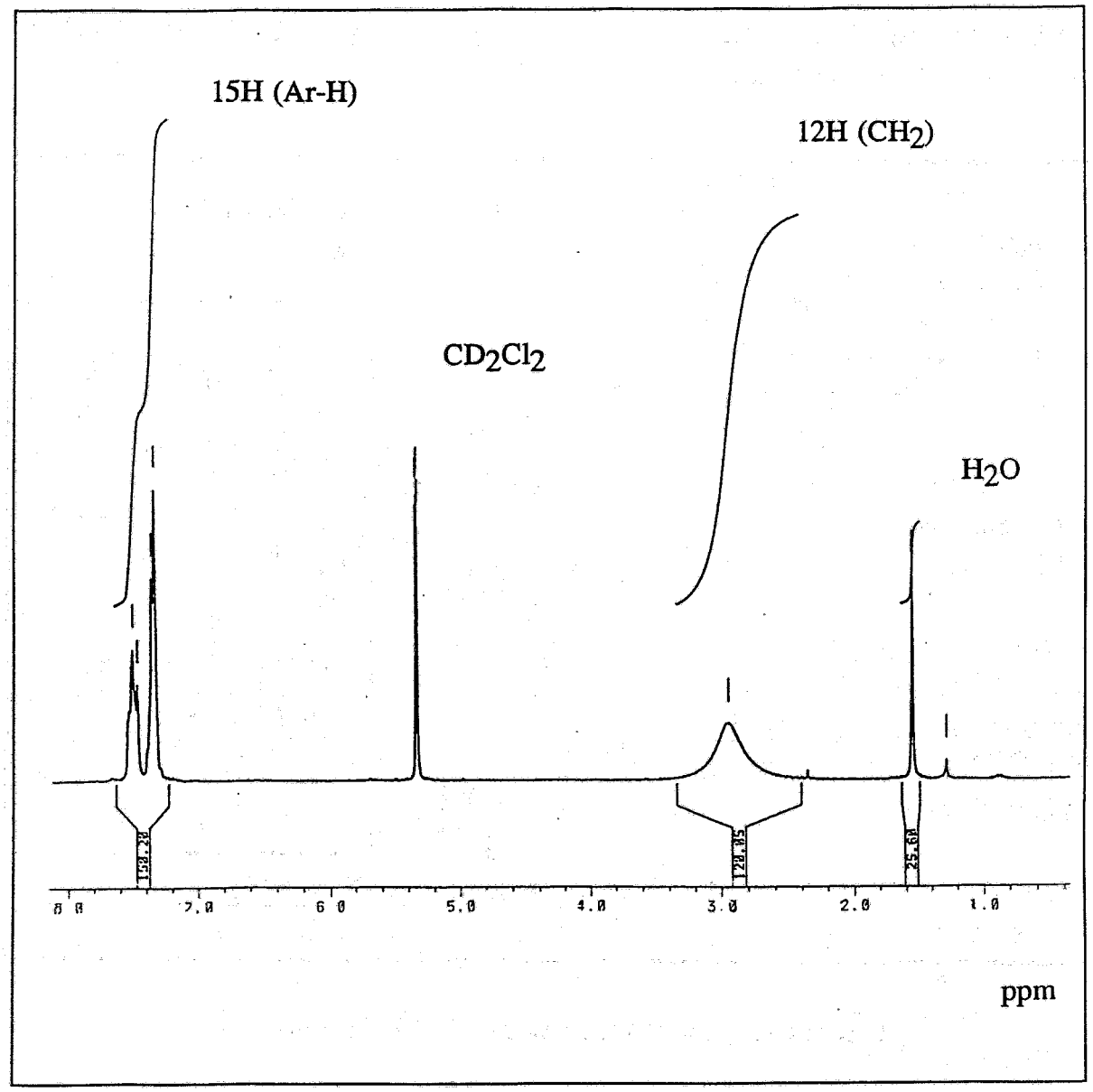

Fig. 2: ^1H NMR spectrum of **6** (CD_2Cl_2)

References:

[1] Hahn, F. E. et al., B. **124** (1991) 481

[2] Dilworth, J. R. et al., Inorg. Chim. Acta **195** (1992) 145

[3] Hahn, F.E. et al., Angew. Chem. **104** (1992) 1218

[4] de Vries, N. et al., Inorg. Chem. **30** (1991) 2662

Blower, P. J. et al., Trans. Met. Chem. **7** (1982) 353

18. A ROUTE TO ALKYLAMMONIUM SUBSTITUTED Re(V) AND Tc(V) COMPLEXES

H.Spies, M.Glaser, G.Görner, Th.Fietz

Cationic technetium complexes attract considerable attention as potential tracers for radiopharmacological studies, e.g. as myocardium affine agents [1]. In view of this background, experiments have been undertaken to introduce a positive charge into the side chain of neutral rhenium and technetium complexes.

A tertiary amino group in the side chain of neutral Tc [2] and Re complexes obtained according to our so-called 3+1 procedure [3], may be alkylated to produce the corresponding alkylammonium substituted complexes.

The reaction route for (2-(diethylmethylammonium)ethanthiolato)(3-thiapentane-1,5-dithiolato)oxorhenium(V) iodide **2** as a typical representative is described in Fig. 1.

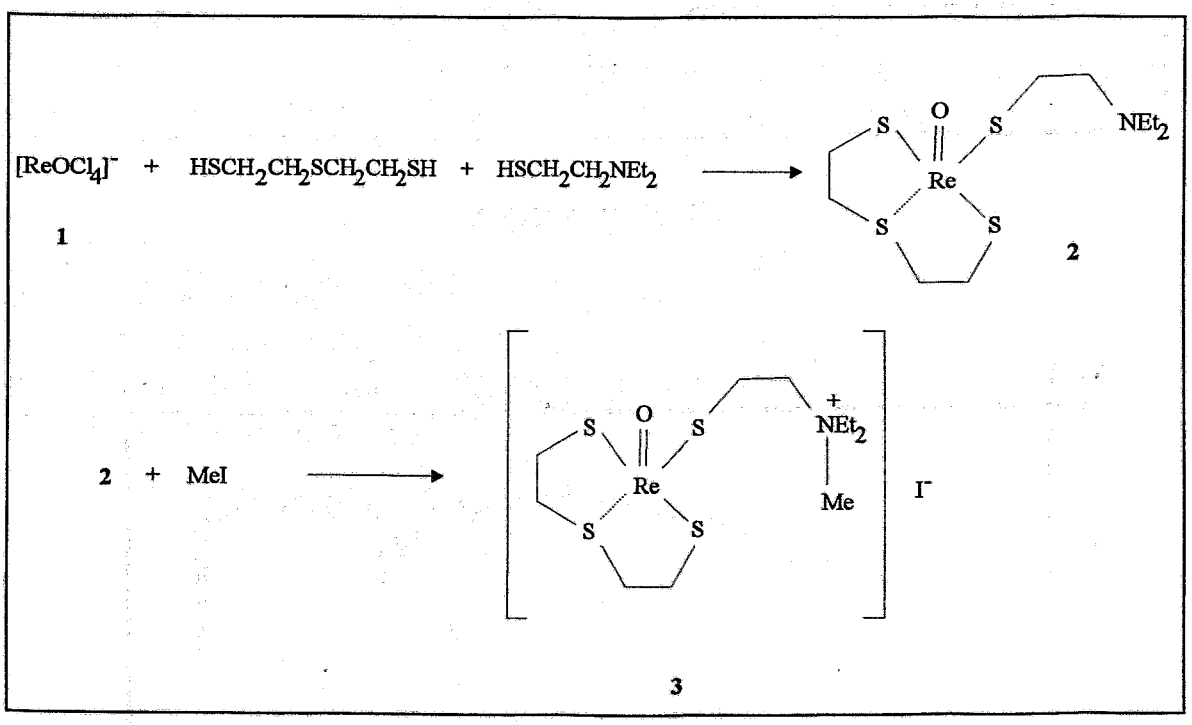

Fig. 1: Synthesis of **3**

A 1:1:1.5 mixture of benzyltriethylammonium tetrachlorooxorhenate(V) **1**, 3-thiapentane-1,5-dithiol, and 2-(diethylamino)ethanthiol in acetonitrile/methanol is allowed to react for 1h at 0°C to form (2-(-diethylamino)ethanthiolato)(3-thiapentane-1,5-dithiolato)oxo rhenium(V).

The product was separated from the reaction mixture by diluted hydrochloric acid in the form of a hydrochloride. The amine **2** liberated by sodium hydroxide solution and extracted by $MeCl_2$ was subsequently quaternated by addition of an excess of methyl iodide. Product **3** was precipitated by cooling and recrystallized from EtOH. The yield of the red crystals, m.p. 170-181°C, amounted to about 38%. The salt is soluble in polar solvents such as water or ethanol.

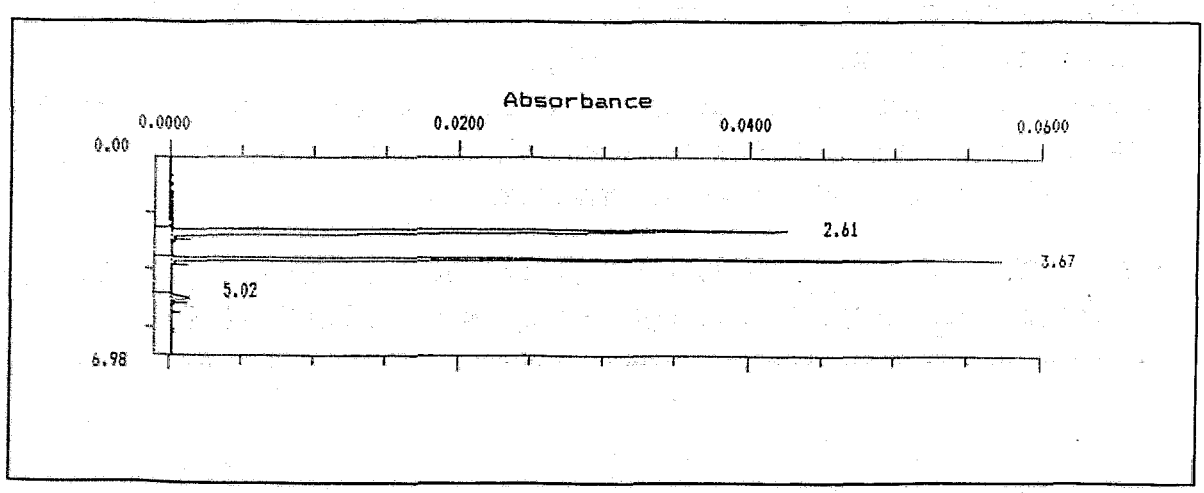

Fig. 2: Electropherogram of **3**

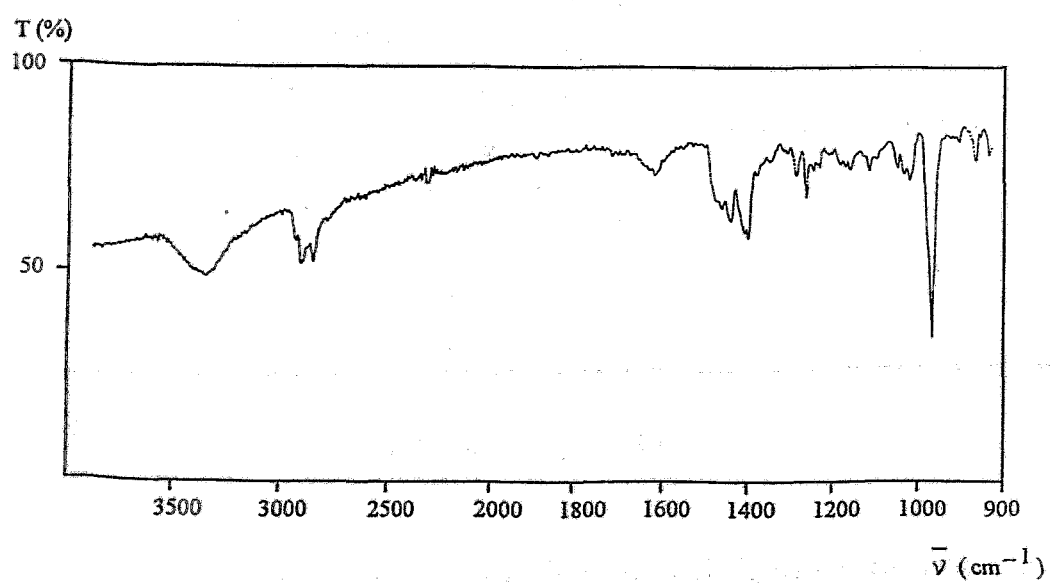

Fig. 3: Infrared spectrum of **3**

The cationic nature of the new compound was confirmed by capillary electrophoresis (Fig. 2). The electropherogram (15kV, 40cm, 214nm, 0.01m sodium phosphate buffer, pH 7) shows a sharp peak at retention time 2.61min assigned to the cationic species, the peak of acetone used as neutral a reference substance at 3.67min and a low signal at 5.02min caused by iodide.

The infrared spectrum of **3** clearly shows the νRe=O band at 968cm^{-1} (Fig. 3). The UV/Vis spectrum has bands at 226, 260(sh) and 364nm, similar to those found in corresponding neutral oxorhenium complexes with SSS/S coordination [4]. The values confirm that the coordination sphere is not attacked by alkylation.

The ^{1}H NMR spectrum has a relatively complex shape due to the presence of different methylene groups in the molecule. The spectrum is consistent with the formula, even if not all the intensities can be assigned to corresponding protons.

Thus, alkylation of the amino group is a suitable route for preparation of "Tc/Re-labelled" ammonium salts. Furthermore, the exclusive alkylation of the amine moiety underlines the high stability of Re-S bonds in this special type of sulphur coordinated complexes.

References:

[1] Li, Q.-S. et al., J. Nucl. Med. **29** (1988) 1539
[2] Spies, H. et al., Plzen.lek.Sborn., Suppl. **62** (1990) 85
[3] Pietzsch, H.J. et al., Inorg.chim.Acta, **165** (1989) 163
[4] Spies, H. et al., this report, p. 94

19. NEUTRAL OXORHENIUM(V) COMPLEXES WITH MONOTHIOL/ TRIDENTATE DITHIOL COORDINATION

H. Spies; Th. Fietz; H.-J. Pietzsch

In view of the fact that the rhenium nuclides ^{186}Re and ^{188}Re emit beta particles with therapeutically useful energies, rhenium is included in our efforts to design and evaluate new radiotracers for radiodiagnostic and radiotherapeutic purposes.

With the aim of obtaining a series of homologous substituted Re compounds for systematical studies, e.g. for investigating the dependence of lipophilicy of the complexes on the length of alkyl chains linked to the complex core, we examined the usefulness of the "3+1" principle for preparation of new lipophilic Re complexes. This synthesis route, which involves simultaneous action of a tridentate dithiol ligand and a monodentate thiol on an appropriate metal centre, has already shown its suitability for preparation of neutral mixed-ligand complexes of Tc(V) [1].

Alkyl- and aryl-substituted oxorhenium(V) complexes ReO(SXS)(SR) with HSXSH=HS-CH_2CH_2-S-CH_2CH_2-SH or HS-CH_2CH_2-O-CH_2CH_2-SH and R= alkyl, (substituted) aryl, have been prepared by reaction of $NBzEt_3[ReOCl_4]$ (1) with HSXSH and RSH according to Fig.1.

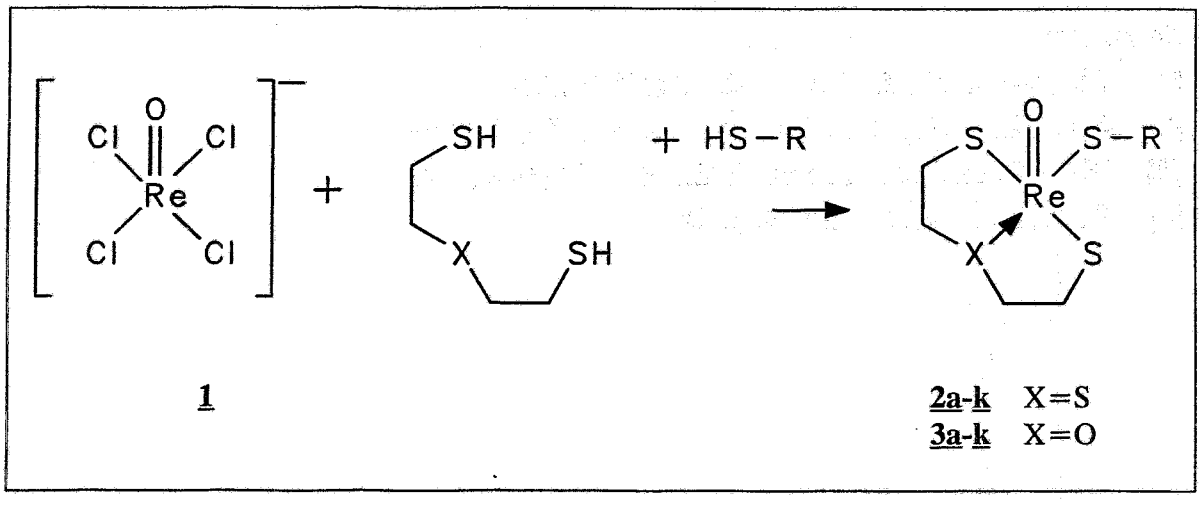

1

2a-k X=S
3a-k X=O

Fig. 1: Reaction scheme.

The aryl-substituted complexes 2a-d and 3a-d can be obtained directly from the reaction mixture when stoichiometrical amounts of (substituted) thiophenols and of HS-CH_2CH_2-X-CH_2CH_2-SH (X=S;O) are mixed and added to stirred solutions of the corresponding amount of 1 in a small volume of methanol at 0°C. The complexes, which precipitate very soon, are isolated and purified by being dissolved in hot chloroform, drop-by-drop addition of ethanol and subsequent reduction of the solvent to a small volume.

The aliphatic substituted compounds **2e-k** and **3e-k** do not directly precipitate under these conditions. The complexes are purified by column chromatography (silica gel, 20x2cm, methanol) which removes colorless by-products. On evaporating most of the solvent, crystals of **2e-k** and **3e-k** are formed. However, when using long-chained mercaptanes, crystallisation may prove impossible due to formation of oils.

Analytically pure, crystalline compounds **2a-k** and **3a-k** are listed in Tab. 1. The yields of pure compounds differ widely from 20 to 55%.

Tab. 1:

Compound	R	Fp.	Re=O in IR
2a	C_6H_5	193-199°C	960 cm^{-1}
2b	4-CH_3O-C_6H_4	202-205°C	952
2c	4-CH_3-C_6H_4	>310°C	960
2d	4-Cl-C_6H_4	>310°C	960
2e	CH_3	157-158°C	966
2f	C_2H_5	152-154°C	960
2g	n-C_4H_9	95-100°C	960
2h	n-C_8H_{17}	91-96°C	956
2i	n-$C_{12}H_{25}$	102-106°C	960
2j	C_6H_5-CH_2	174-177°C	960
2k	C_6H_5-CH_2CH_2	161-164°C	956
3a	C_6H_5	190-194°C	976
3b	4-CH_3O-C_6H_4	190-192°C	976
3c	4-CH_3-C_6H_4	193-197°C	972
3d	4-Cl-C_6H_4	189-193°C	976
3e	CH_3	133-135°C	974
3f	C_2H_5	104-107°C	976
3g	n-C_3H_7	87-89°C	
3h	i-C_3H_7	157-159°C	
3i	CH_3-$CH(CH_3)$-CH_2	80-82°C	
3j	n-$C_{12}H_{25}$	44-48°C	
3k	C_6H_5-CH_2CH_2	105-107°C	968

The composition of the compounds follows from their elemental analysis, ^1H NMR and infrared spectra. The IR recording of 4-methoxyphenylthiolato-3-oxapentanedithiolato-

oxorhenium(V) (**3b**), which was chosen as a typical example of the class of complexes covered herein, shows a strong Re=O stretching band at 976cm^{-1} (see Fig. 2). In IR recordings of all Re(V) complexes examined, we found the Re=O bands to differ from 952 to 976cm^{-1} whereas the wavenumbers of the respective bands of complexes **2** were generally lower than in complexes **3**. In comparision to that values, the Re=O stretching band in $ReOCl_4^-$ is found at about 1000cm^{-1}. Analogous examinations of Tc=O complexes show the respective band at 920-980cm^{-1} [1].

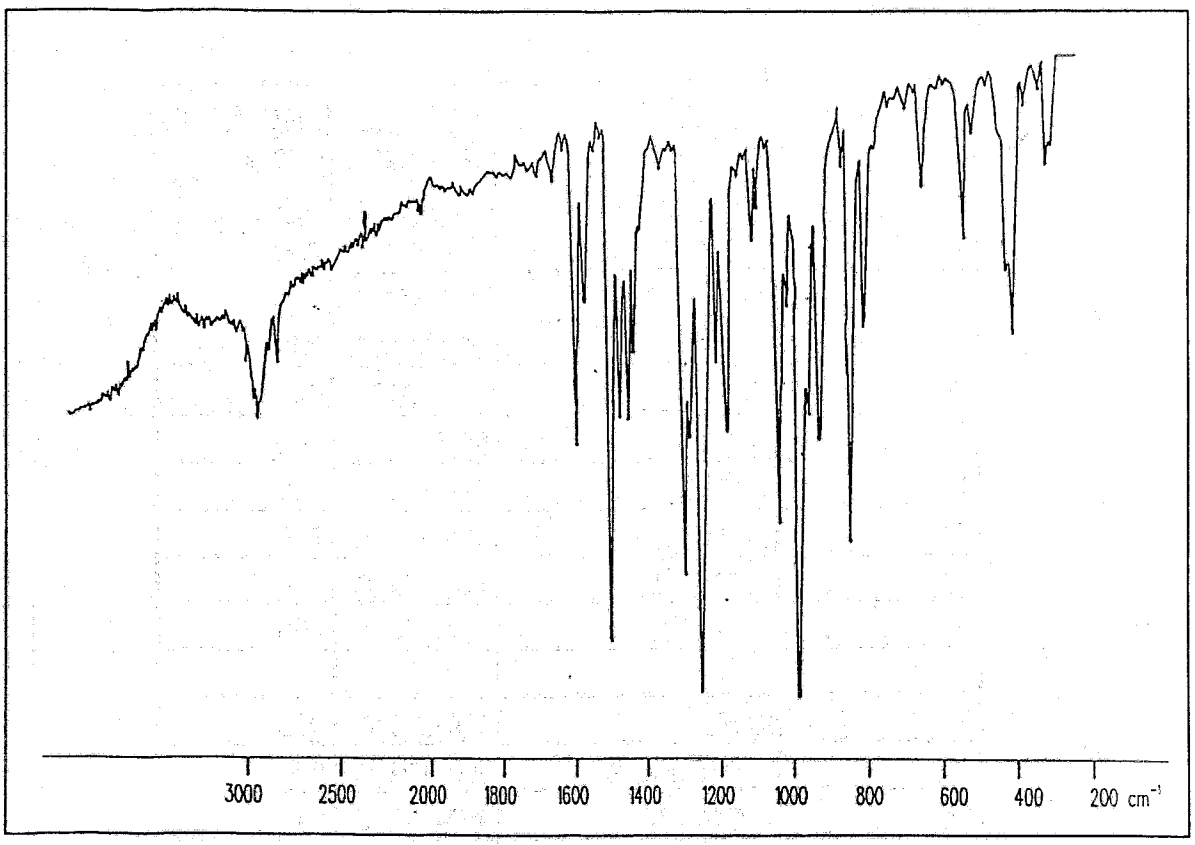

Fig. 2: IR spectrum of **3b** in KBr

In the ^{1}H NMR study (Fig.3; solvent peaks omitted), the spectrum of **3b** in $CDCl_3$ exhibits an assembly of three broad signals for the protons of -S-CH_2CH_2-O-CH_2CH_2-S- at 4.68, 3.72 and 3.25-3.50 ppm, which is not, however, symmetrical as expected. The monodentate ligands proton NMR signals are seen at 7.50 ppm, 6.95 ppm (2 aromatic protons each) and 3.85 ppm (CH_3O). The patterns of the methylene protons in the NMR spectra of the series **2** (X=S) can be clearly distinguished from those of **3b** (X=O). Within the sulphur series, the patterns do not differ so much. In this respect the rhenium compounds behave much like to the analogous technetium compounds [1].

The UV/vis spectrum of **3b** shows a broad maximum at λ_{max}=357nm (lgε=3.83).In the UV/vis spectrum of the respective sulphur compound **2b** two sharper maxima at 344nm (lgε=3.92) and 410nm(lgε=3.94) can be detected.

X-ray crystal analysis of both **3b** and an alkyl-substituted example of the compound class is in progress.

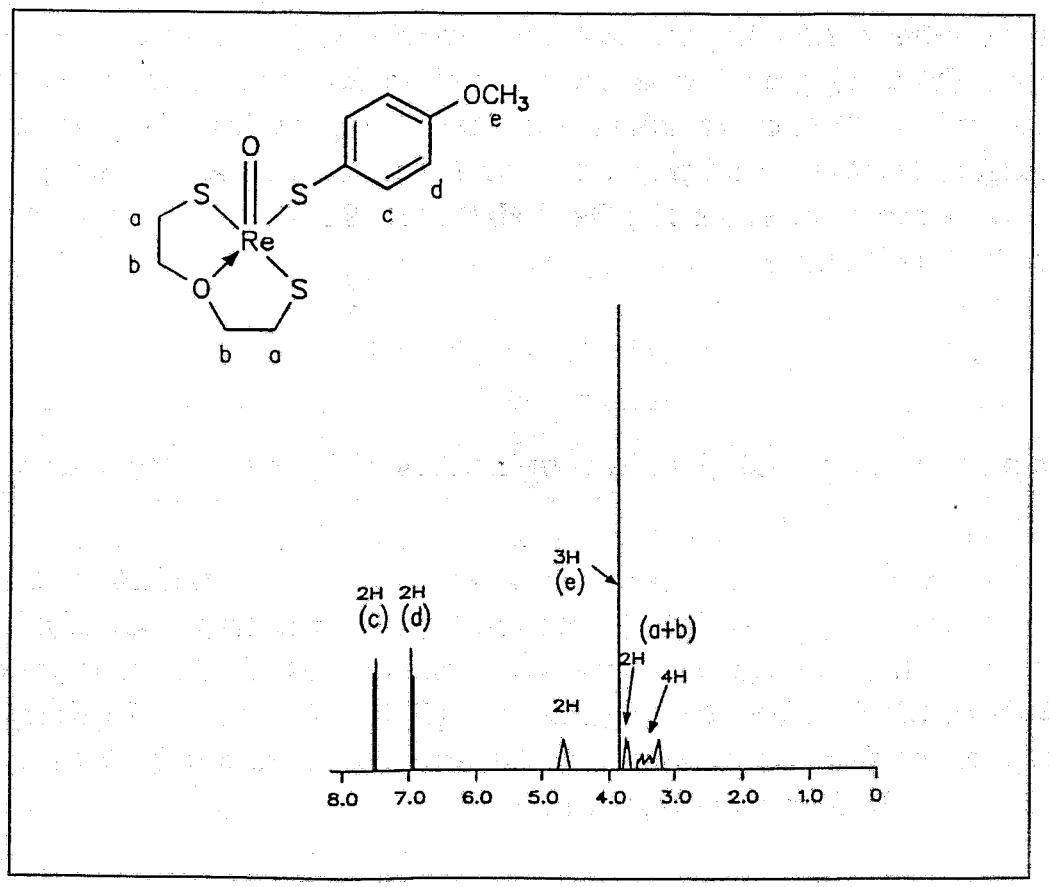

Fig. 3: ^{1}H NMR spectrum of **3b** in $CDCl_3$

Reference:

[1] Pietzsch; H.-J. et al., Inorg.Chim.Acta **161** (1989) 15

20. CHARACTERIZATION OF TECHNETIUM-99 COMPLEXES WITH MERCAPTOACETYL PEPTIDES (MAG_3, MAG_2, MAG_1)

B. Johannsen, B. Noll, St. Noll, H. Spies, P. Leibnitz[1], G. Reck[1]
[1]Bundesanstalt für Materialforschung, D-1199 Berlin

Having studied in detail the preparation of the oxotechnetium(V)complex of mercaptoacetyl-triglycin (MAG_3) [1], which is an important renal function agent, we wanted to learn and understand the effects of shortening the peptide chain (going from MAG_3 via MAG_2 to MAG_1) on the structure and properties of the Tc complexes. Shortening the peptide chain alters the donor atom set from S N_3 O to S N_2 O and to S N O, which may cause a different coordination of technetium.

Experiments

Complexes were prepared by ligand exchange reactions starting from Tc(V) gluconate.

Methods

The influence of the molar ratio of the reactants on the occurrence of products was studied by UV/vis spectroscopy (Specord M40). The chromatographic behaviour was determined by thin-layer chromatography with 95% ethanol as the solvent and by HPLC on an RP 18 column (Nucleosil, 25cm) with 0.05M phosphate buffer pH 7.4 as the eluent. The charge of the complexes obtained was determined by thin-layer electrophoresis with phosphate buffer solution pH 7.0 and glycine buffer pH 2 and pH 10.

Variation of the ligand/Tc-gluconate molar ratio

100µl 0.01M potassium pertechnetate, 0.5ml ^{99m}Tc-generator eluate and 100µl 0.01M stannous chloride in 0.01M HCl are added to 1.5ml 0.05M sodium gluconate.
$1*10^{-5}$mole MAG_3, MAG_2 or MAG_1 as the ligand is dissolved in 100µl water and the molar equivalents according to the molar ratio are added to the Tc-gluconate solution, for the ligand/Tc molar ratio 100/1 $1*10^{-4}$mol ligand is dissolved in 1ml 0.1M NaOH.

Preparation of $Ph_4As[TcO(MAG_2)]$

$9{,}7*10^{-5}$mol MAG_2, dissolved in 1ml 0.1N NaOH, is added to 3ml Tc gluconate solution ($1*10^{-4}$ mol). After addition of $8.4x10^{-5}$mol tetraphenylarsonium chloride, dissolved in 200µl water, a dark coloured solid precipitates, which is collected and washed with ether/ethanol. Recrystallization from ethanol yields 45mg (0.064mmol = 64%) of a brown crystalline compound, m.p. 190°C.

Anal. Calc. for $C_{32}H_{32}N_2O_6SAsTc$: C: 51.43; H: 4.32; N: 3.75%

Found: C: 51.57; H: 4.91; N: 3.21%

IR: 960cm^{-1} νTc=O

UV/vis (ethanol) (λmax (log ε)): 345nm (3.16)

^{1}H NMR: 7.80ppm (m, 20H) phenyl; 4.66/4.25ppm (AB, 2H) and 4.07ppm (s, 2H) 2 x N-CH_2, 3,85/3.66ppm (AB, 2H) S-CH_2.

Results and Discussion

Studies of complex formation

Various Tc-species are obtained, depending on the ligand/Tc molar ratio (Tab.1). Complex 1 (r_f=0.6-0.7) is obviously the 1:1 complex because of its identity with the r_f of the ^{99m}Tc radiopharmaceutical preparation for MAG_3 and with the r_f of the isolated Tc-MAG_2. Complexes 2 and 3 (r_f = 0.3-0.4 and r_f = 0-0.1) occurring during the radiopharmaceutical preparation of Tc-MAG_3 too [1] can be considered to be Tc complexes with a higher ligand/Tc ratio. With increasing pH value >11 they can be transformed into the kinetically stable complexes 1 (MAG_3 and MAG_2) as well as into complex 2 (MAG_1).

Tab. 1: Ligand exchange of Tc gluconate with MAG_3, MAG_2 and MAG_1 at various ligand/Tc ratios. The species were separated by TLC on silica gel with 95%ethanol as the eluent.

	Content [%]			
Molar ratio	**complex 1 r_f=0.6-0.7**	**complex 2 r_f=0.3-0.4**	**complex 3 r_f=0-0.1**	**Tc-gluconate r_f=0**
Tc/MAG_3				
1:1	70.5	12.0	4.0	13.5
1:2	23.0	65.0	12.0	-
1:4	3.0	67.5	29.5	-
1:5	2.5	60.5	37.0	-
Tc/MAG_2				
1:1	83.0	-	4.5	12.5
1:2	84.0	-	16.0	-
1:7	51.0	31.0	18.0	-
1:100	-	39.0	61.0	-
Tc/MAG_1				
1:1	-	49.5		50.5
1:2	-	91.0	9.0	-
1:7	-	90.0	10.0	-
1:100	-	85.0	15.0	

Tab. 2: Electrophoretic behaviour - anionic migration of the kinetically stable complexes related to TcO_4- as an internal standard.

Complexes	pH 2	pH 7
$TcMAG_3$ (1:1)	0.35	0.65
$TcMAG_2$ (1:1)	0.55	0.55
$TcMAG_1$ (1:2)	0.30	0.55

Tc-MAG_1

It is of interest to obtain information about the relative reactivity of the donor atoms, which changes when the MAG_3 ligand is changed, e. g. by shortening the length of the peptide chain.

Vandebrouck et al. [2] have already shown an increase in the complexation strength from MAG_3 to MAG_6 as well as the prominence of MAG_2, having the highest ability to form a complex with ^{99m}Tc.

It is obvious that no 1:1 complex can be formed with MAG_1 as a ligand. In neutral solution a $TcOL_2$ complex is formed, which is extractable into methylene dichloride after adding a lipophilic cation (NBu_4^+). The anionic mobility is the same at pH 7 and 2. Therefore, the carboxylic groups of both ligand molecules are involved in binding technetium. In alkaline solution MAG_1 possibly acts as both a tridentate S, N, O ligand and a monodentate S ligand, since the electrophoretic migration of the Tc complex depends on pH (Tab. 2), one free carboxylic group in the complex molecule is assumed.

Tc-MAG_2

Reaction of MAG_2 with technetium(V) gluconate in neutral aqueous solution results in a spectrum of different compounds. The ratio of compounds changes with the ligand to metal molar ratio, which is qualitatively seen in a change of colour after addition of various amounts of the ligand to the precursor. The maxima in the UV spectrum of the reaction mixture are found as 345nm for 1:1, 370nm for 8:1 and about 400nm for a 100:1 ligand:technetium molar ratio. In TLC, up to three species were detected at ratios greater than 1:1.

The 1:1 Tc-MAG_2 complex differs from that of MAG_3 by being formed at even a slight excess of ligand, which indicates that O-donors may play a remarkable role in stabilizing the Tc(V)O core. When the reaction of MAG_2 with technetium(V) gluconate is carried out in an alkaline medium, a pure component occurs regardless of the molar ratio. It was isolated as a tetraphenylarsonium salt.

Further support for the structure of $AsPh_4[TcO(MAG_2)].C_2H_5OH$ was given by X-ray crystallography. A perspective view of the complex anion is shown in Fig. 1 and emphasizes that the compound belongs to the well-known group of square-pyramidal oxotechnetium(V) complexes. (Selected bond distances and angles are summarized in Tab. 3).

Tc-MAG_3

With MAG_3 as the ligand, the well-known anionic 1:1 complex possessing a free carboxyl group is formed in alkaline solution, or the ligand/Tc ratio in ligand exchange reactions is kept low. Any excess of ligand over Tc favours the 2:1 ligand/Tc complex and, at a higher excess, the 4:1 species. In the latter case MAG_3 only reacts as a monodentate thiol. Intermediates occur due to the high reactivity of the free mercapto group in the ligand, favouring complexes with ligand/Tc ratios higher than 1. This is true of any excess of ligand over Tc in the reaction solution. Both a 1:2 and 1:4 MAG_3 species were identified and separated from the 1:1 complex by HPLC (Fig. 2).

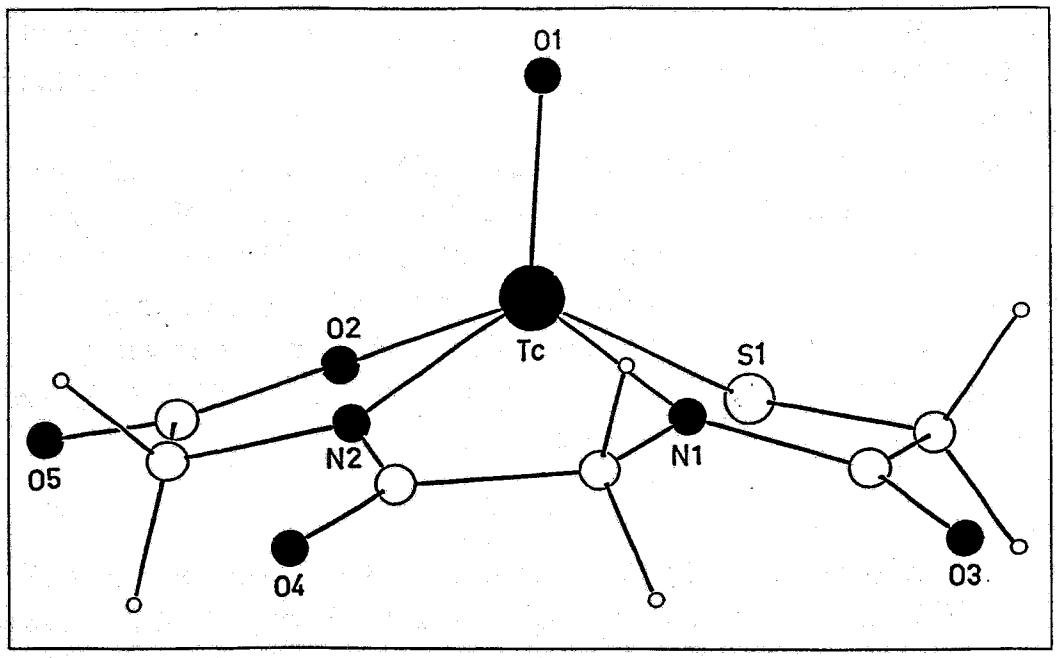

Fig. 1: Molecular anion of $AsPh_4[TcO(S\text{-}CH_2CONH\text{-}CH_2\text{-}CONH\text{-}CH_2\text{-}COO)]$

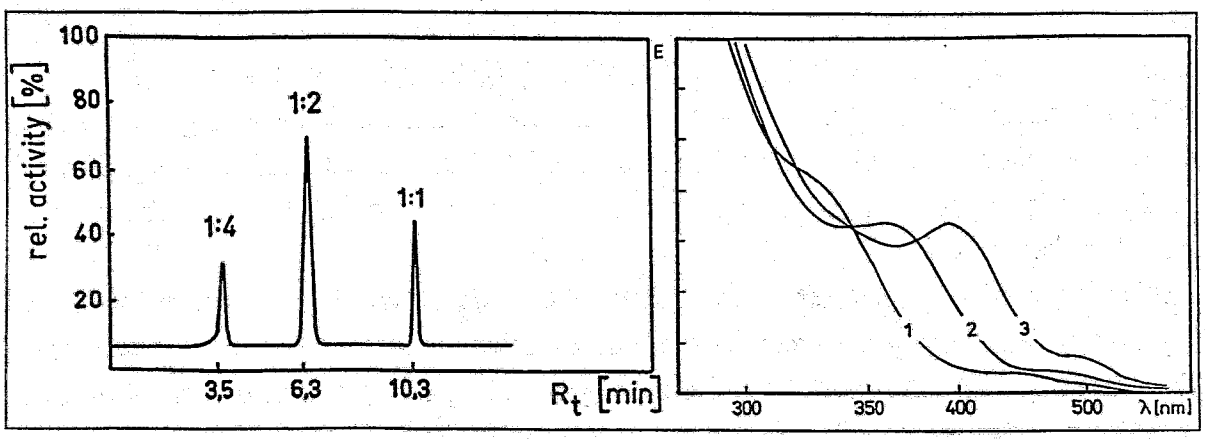

Fig. 2:
Separation by HPLC of three Tc-MAG_3-complexes on an RP-18 column with 15% methanol in 0.05M potassiumdihydrogen-phosphate, pH 5.85

Fig. 3:
UV/vis spectra of Tc-MAG_3-species
1 predominant 1:1 complex
2 predominant 1:2 complex
3 predominant 1:4 complex

Tab. 3: Selected bond angles and distances for [TcO(MAG_2)]

Bond lengths (Å)					
Tc-O_1	1.644	Tc-N_1	1.968	C_1-S	1.828
Tc-O_2	2.016	Tc-N_2	1.968	C_6-O_2	1.314
Tc-S	2.271			C_6-O_5	1.230
Bond Angles (deg)					
O_1-Tc-S	110.4	S-Tc-N_2	133.7		
O_1-Tc-N_1	109.4	S-Tc-O_2	88.3		
O_1-Tc-N_2	115.8	N_1-Tc-N_2	78.9		
O_1-Tc-O_2	110.2	Tc-S-C_1	98.5		
S-Tc-N_1	83.6	Tc-O_2-C_6	117.6		

Conclusions

MAG_n ligands (n = 1, 2, 3) easily form various Tc^Voxo complexes. Depending on the reaction conditions, such as Tc/ligand ratio and pH, they may act as monodentate, bidentate or tetradentate (except n = 1) ligands. The good donor quality of the mercapto group, which outbalances the amide-N and carboxyl-O atoms, triggers the initial formation of $TcOL_4$ under excess ligand conditions. The chelate effect ultimately leads to 1:1 complexes. This process can be facilitated by activiation of the amide-N at pH >11 as well as by low ligand/Tc ratios.

MAG_2 differs from MAG_3 in that it provides interesting S, N_2, O coordination.

[TcO(MAG_2)] is a Tc compound with sulphur-containing ligands within the well-known group of square-pyramidal oxotechnetium(V) complexes in which a carboxylic group is involved in the equatorial plane. The distance of the Tc-O(carboxylate) bond is relatively short (2.010Å) compared, for example, to that of the trans-coordinated carboxylic group in TcO($pen)_2$ (pen = penicillamine) (2.214Å) [3], which is in accordance with the high stability of Tc-MAG_2 observed in the above experiments.

Shortening the peptide chain length and blocking the carboxylic group in the ligand molecule is expected to make 2:1 complexes the main products. This has been confirmed for MAG_1. In alkaline solution MAG_1 possibly acts as both a tridentate S, N, O ligand and a monodentate S ligand.

References

[1] Noll, B., et al., Appl. Radiat. Isot. **43** (1992) 899

[2] Vandebrouck, T. et al., Eur. J. Nucl. Med. **18** (1991) 674

[3] Franklin, K. H. et al., Inorg. Chem. **21** (1982) 1941

21. COMPLEX FORMATION OF TECHNETIUM WITH THE METHYL ESTERS OF MAG_2 AND MAG_1

B. Noll, St. Noll, B. Große, B. Johannsen, H. Spies

Mercaptoacetylglycine methyl ester (MAG_2 ester) and mercaptoacetyldiglycine methyl ester (MAG_1 ester) were included in our investigation on complex formation of SH/amide ligands with technetium and rhenium. Our studies are aimed at finding out how blocking the carboxylic groups influences the complexation reaction, with a view to finding an approach to new lipophilic species.

Experimental

Methods

The influence of the molar ratio of the reactants on the occurrence of Tc- complexes was studied by UV/vis spectroscopy (Specord M40). The chromatographic behaviour was determined by thin-layer chromatography with 95% ethanol as a solvent and by HPLC on an RP 18 column (Nucleosil, 25cm) with 0.05M phosphate buffer pH 7.4 as an eluent. The charge of the complexes obtained was determined by thin-layer electrophoresis with phosphate buffer solution pH 7.0 and glycine buffer pH 2 / pH 10.

TLC of the ligands and their precursors was performed on silica gel sheets (Silufol) with n-butanol/acetic acid/water 4:1:1, spots were detected by iodine or ninhydrin under a UV lamp.

Synthesis of mercaptoacetyl diglycine ester (MAG_2 ester)

Chloroacetyl-diglycine (modified procedure of [1]):

To a solution of 10g (0.09mol) of glycine anhydride dissolved in 50ml of 2N sodium hydroxide, 7.8ml of chloroacetyl chloride and 24ml of 5N sodium hydroxide were added over 45min while stirring in an ice bath. After acidification with 40ml of 5N hydrochloric acid chloroacetyl-diglycine crystallized while cooling. The product was separated, washed with ice-water and recrystallized from water.

Yield: 7.5g (41%)

Mp 174°C, r_f 0.70 (iodine)

IR(KBr): ν_{NH} 3350; ν_{COOH} 1730; $\nu_{C=O}$ 1675,1630; δ_{NH} 1550 cm^{-1}

Benzoylmercaptoacetyl diglycine:

5.7g (0.04mol) thiobenzoic acid was dissolved in 20ml methanol and neutralized with sodium methylate. This solution was dropped to 5.2g (0.025mol) of chloracetyl-diglycine in

1 litre of dry methanol while stirring under nitrogen. After 12h the reaction was completed and the solvent was removed by rotary evaporation. To the residue 2N hydrochloric acid was added, the solid was separated and washed with warm water, followed by chloroform, acetonitrile and diethylether.

Yield: 6.9g (89%)

Mp 194°C, r_f 0.80 (iodine)

IR(KBr): ν_{NH} 3450; ν_{COOH} 1730; $\nu_{C=O}$ 1660,1640,1580; δ_{NH} 1540cm^{-1}

Benzoylmercaptoacetyl diglycine methyl ester:

To 1g (3.2mmol) benzoylmercaptoacetyl diglycine dissolved in 200ml methanol, 5g methanolic cation exchange resin DOWEX 50WX8 and 5g ZEOSORB 4A were added and the mixture was refluxed for 19h while stirring vigorously. After cooling the resin was filtered off and the methanol was distilled on a Rotavapor. The viscous yellow oily residue crystallized at 4°C.

Yield: 857mg (83%), r_f 0.8 (uv)

IR (KBr) $\nu_{C=O}$ 1640; ν_{COOR} 1680; δ_{NH} 1550cm^{-1}

Mercaptoacetyl diglycine methyl ester:

0.857g (2.65mmol) of benzoylmercaptoacetyl diglycine methyl ester was dissolved in 68ml methanol. Under an N_2 atmosphere, 286mg (5.3mmol) sodium methylate was dropped to the solution while stirring. Stirring was continued for 60min, and after neutralization with methanolic DOWEX 50WX8, the mixture was filtered and methanol was distilled on a Rotavapor. 25ml water was added to the residue and the solution was extracted twice with 15ml benzene. The volume of the aqueous solution was reduced to 10ml and introduced onto a column filled with DOWEX 50WX8. The eluted product was obtained by freeze-drying.

Yield: 176mg (30%)

20mg of this product was purified by liquid chromatography on Sephadex G10 with water as an eluent and a pump speed of 20ml/h. Detection was carried out by a flow-through analyzer measuring the refractometric index.

Yield: 16.4mg (82%), Mp. 129°C, r_f 0.5 (ninhydrin)

IR (KBr) $\nu_{C=O}$ 1650; ν_{COOR} 1750; δ_{NH} 1575 cm^{-1}

^{1}H NMR (DMSO) TMS δ 3.2 (-CH_2-SH,2H); δ 3.6 (-OCH_3-,3H); δ 3.7 (-SH,1H); δ 3.8-3.9 (-CH_2,4H); δ 8.3 (-CO-NH,2H)

Mercaptoacetyl glycine ester (MAG_1 ester)

Chloroacetyl glycine(modified procedure of [2]):

7ml (1.2 equiv.) chloroacetyl chloride and 110ml 1N sodium hydroxide were added to a solution of 5g (0.07mol) of glycine in 67ml of 1N sodium hydroxide over 30min, while stirring in an ice bath. Then the mixture was acidified with 20ml 5N hydrochloric acid and the product was dried by rotary evaporation. The residue was three times extracted with acetone and the acetonic solution was reduced to a volume of 15ml. After addition of 30ml chloroform, a viscous oil was obtained which was separated and extracted with 300ml of hot diethyl ether. The ether solution was reduced to a volume of 50ml and the product crystallized while cooling to yield chloroacetyl glycine.

Yield: 3.9g (39%), Mp 81°C, r_f 0.75 (iodine)

IR(KBr): ν_{NH} 3320; ν_{COOH} 1730; $\nu_{C=O}$ 1620; δ_{NH} 1540 cm^{-1}

Benzoylmercaptoacetyl glycine:

5.7g (0.04mol) thiobenzoic acid was dissolved in 20ml methanol and neutralized with sodium methylate. This solution was dropped to 3.2g (0.021mol) of chloroacetyl glycine in 750ml dry methanol while stirring under nitrogen. Stirring was subsequently continued for 12h and then the methanol was removed by rotary evaporation. 2N hydrochloric acid was added to the residue, yielding a brown oil, which was separated and dissolved in 80ml chloroform. While cooling and stirring vigorously, the product crystallized and after separation it was washed with water, chloroform and diethylether.

Yield: 1.5g (27%), Mp 136°C, r_f 0.85 (iodine)

IR(KBr): ν_{NH} 3380; ν_{COOH} 1740; $\nu_{C=O}$ 1675,1620; ν_{NH} 1540 cm^{-1}

Benzoylmercaptoacetyl glycine methyl ester:

To 3.2g (0.0126mol) benzoylmercaptoacetyl glycine dissolved in 275ml methanol, 6ml of methanolic cationic exchange resin DOWEX 50WX8 and 3g Zeosorb 4A were added and the mixture was refluxed for 30h and then filtered. The methanol was distilled on a Rotavapor and the viscous red oily residue was allowed to crystallize at 4°C.

Yield: 1.8g, r_f 0.75 (UV)

Mercaptoacetyl glycine methyl ester:

334mg benzoylmercaptoacetyl glycine ester was dissolved in 25ml methanol in a round bottle. After addition of 2mg of $Pd/CaCO_3$ the bottle was connected to a vacuum apparatus, evacuated and then hydrogen was added to a pressure of 66kPa. The reaction mixture was stirred vigorously for 30min while adding 0.7ml sodium methylate in 5ml methanol. The mixture was neutralized with cationic exchange resin DOWEX 50 WX8 and the reaction

product separated by freezing dry. The residue was extracted twice with 3ml benzene and purified by liquid chromatography on a Sephadex G10 with a flow-through analyzer measuring the refractometric index. The eluent was water, the pump speed was 20ml/h and the final product was isolated by freeze-drying.

r_f 0.7 (ninhydrin)

Anal.: MG 163 $C_5H_9O_3NS$

calc.: C 36.80, H 5.55, N 8.58, S 19.65%

found: C 36.15, H 5.70, N 8.25, S 19.51%

^{1}H NMR(DMSO) TMS δ 3.5(-CH_2-SH,2H); δ 3.6(O-CH_3,3H); δ 3.2(-SH,1H); δ 3.9(-CH_2,2H); δ 8.3(-CO-NH,1H)

Preparation of the Tc complexes:

Complexes were prepared by ligand exchange reaction starting from a Tc-gluconate complex. The ^{99}Tc-gluconate complex is prepared by addition of $1*10^{-6}$mol stannous chloride to $1*10^{-6}$mol potassium pertechnetate in 2ml 0.05M sodium gluconate solution. $1*10^{-5}$mol ligand is dissolved in 100μl water and the molar equivalents according to the ligand/Tc molar ratio are added to the Tc-gluconate solution.

Results and discussion

Tc-MAG$_2$-methyl ester

As indicated by the UV/vis spectra, variation of the ligand/technetium ratio results in various complexes of Tc-MAG$_2$-methyl esters. At a 1:1 ligand/technetium ratio the maximum occurs at 360nm, an increase to 2:1 doubles the extinction at the same wavelength. At a higher molar ratio a second maximum occurred at 400nm, which vanished at pH > 10.

Complex solutions contain two species separable by thin-layer electrophoresis. The portions of both components in the 1:2 and 1:4 reaction mixtures are listed in Table 1. When the complex solutions are adjusted alkaline, only component 2 is detectable. A pH 2 it has the same relative electrophoretic mobility $u_{rel.}$ = 0.30-0.35 as at pH 10.

HPLC on an RP 18 column with 82% phosphate buffer pH 7.4 and 18% acetonitrile as an eluent permits separation of the neutral reaction mixture into four components, whereas the alkaline solution shows only one component (Fig. 1).

Tab. 1: Proportions of anionic products in the Tc-MAG_2-methyl ester system depending on the Tc / ligand molar ratio as determined by thin-layer electrophoresis (u_{rel} = relative electrophoretic mobility of Tc-components with respect to pertechnetate)

Molar ratio Tc/Ligand	component 1 [u_{rel} 0.10-0.15]	component 2 [u_{rel} 0.30-0.35]
1 : 2	30%	70%
1 : 4	57%	31%

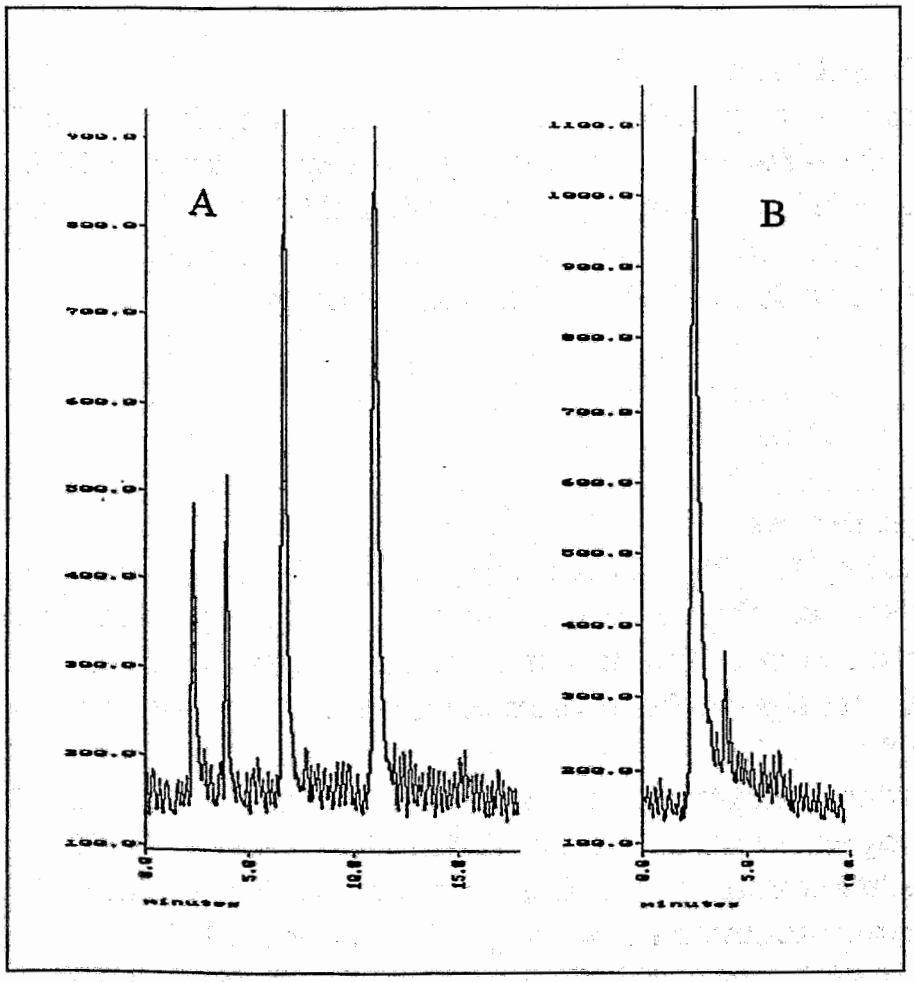

Fig.1: Separation of the Tc-MAG_2-methyl ester reaction mixture by HPLC on RP 18 (Nucleosil) with 82% phosphate buffer pH 7.4 and 18% acetonitrile as an eluent
A - neutral solution, B - alkaline solution

Tc-MAG$_1$-methyl ester

In the UV/vis spectrum there is an absorption at 370nm, the maximum of extinction is achieved at the molar ratio of 1:4. With a much higher ratio (1:50) a second maximum is observed at 400nm. The reaction mixture of the molar ratio 1:4 was separated into two anionic complexes by electrophoresis at pH 7 with the relative electrophoretic mobilities of 0.20 and 0.45 (Fig. 2).

The proportions of the two species depending on the molar ratio of the reaction mixture are shown in Table 2.

Tab. 2: Distribution of Tc-complex species in Tc/MAG$_1$-ester reaction mixture determined by thin-layer electrophoresis, phosphate buffer pH 7, field strength 20V/cm.

	Distribution of activity[%]		
MV	Tc-gluc. (u_{rel} ~0.35)	complex 1 (u_{rel} ~0.2)	complex 2 u_{rel} (0.45)
1 : 1	~100	-	-
1 : 2	50	30	20
1 : 4	-	61	39
1 : 8	-	47	43

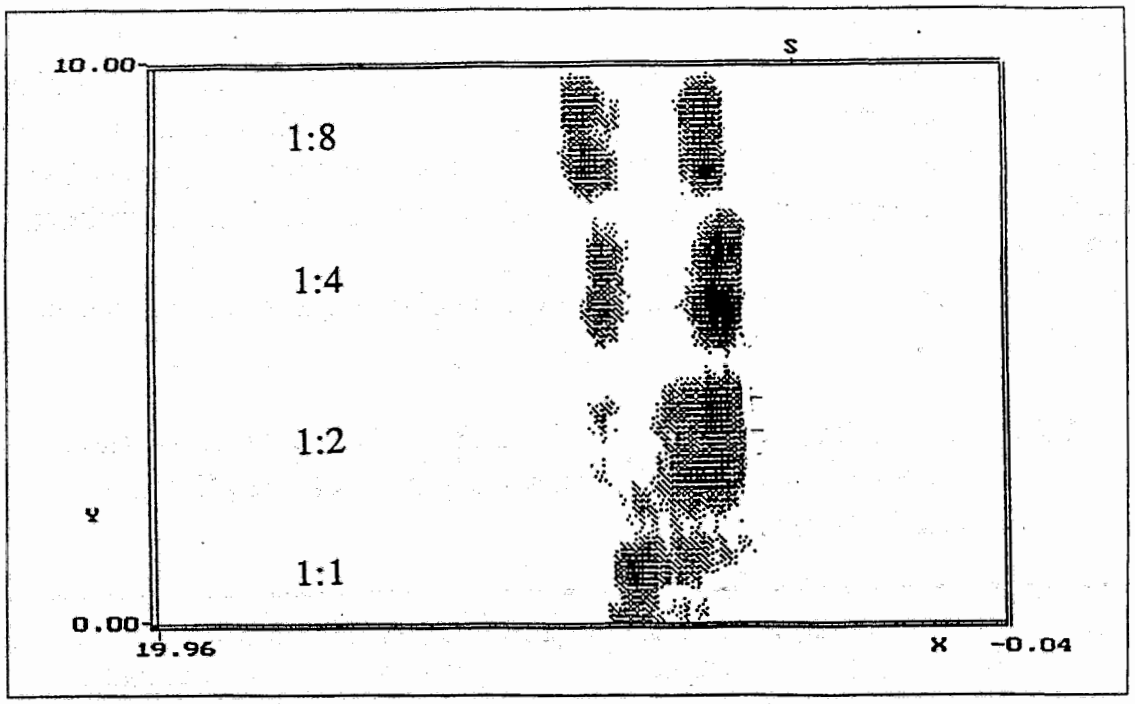

Fig.2: Electropherogram of the Tc-MAG_1-methyl ester reaction mixture in phosphate buffer pH 7, field strength 20V/cm, electrophoresis time 45min.

Conclusion

In neutral solution more than one Tc-species were detected by several analytical methods in the Tc-MAG_2 and Tc-MAG_1-methyl ester reaction mixtures. These are formed directly by ligand exchange, starting from the Tc gluconate. According to the results obtained by HPLC, four different species are formed in the Tc-MAG_2-methyl ester system, in alkaline solution only one species was found, which differs in its analytical behaviour from those obtained in neutral solution.

References:

[1] Fischer, E., Ber. **39** (1906), 2931

[2] Levene, P. A. et al., J. Biolog. Chem. **61** (1924)

22. HPLC AND CAPILLARY ELECTROPHORESIS OF S-PROTECTED MAG_n-ALKYL ESTERS

B. Noll, K. Landrock, St. Noll, G. Görner

For synthesis of alkyl ester of S-benzoyl-MAG_n (n = 1, 2, 3) by reaction of the corresponding carboxylic acid, a method is required for analytical determination of both compounds.

The content of the S-benzoyl-MAG_n ester in the reaction mixture was determined by HPLC and by capillary electrophoresis. The methyl esters of the S-benzoyl-MAG_n glycines were prepared as described by [1]. The purified S-benzoyl-MAG_n derivatives and the corresponding acids were used as reference substances.

HPLC separation of S-benzoyl-MAG_n from the S-benzoyl-MAG_n ester was performed on an RP18 column (Hypersil ODS, 250x4.6mm) with phosphate buffer pH 7.0/methanol 70/30 (v.v) as an eluent, a better resolution of the S-benzoyl-MAG_n-derivatives is obtained by using 0.1% phosphoric acid / methanol 70/30.

The dependence of the retention time on the separation conditions is shown in Fig. 1.

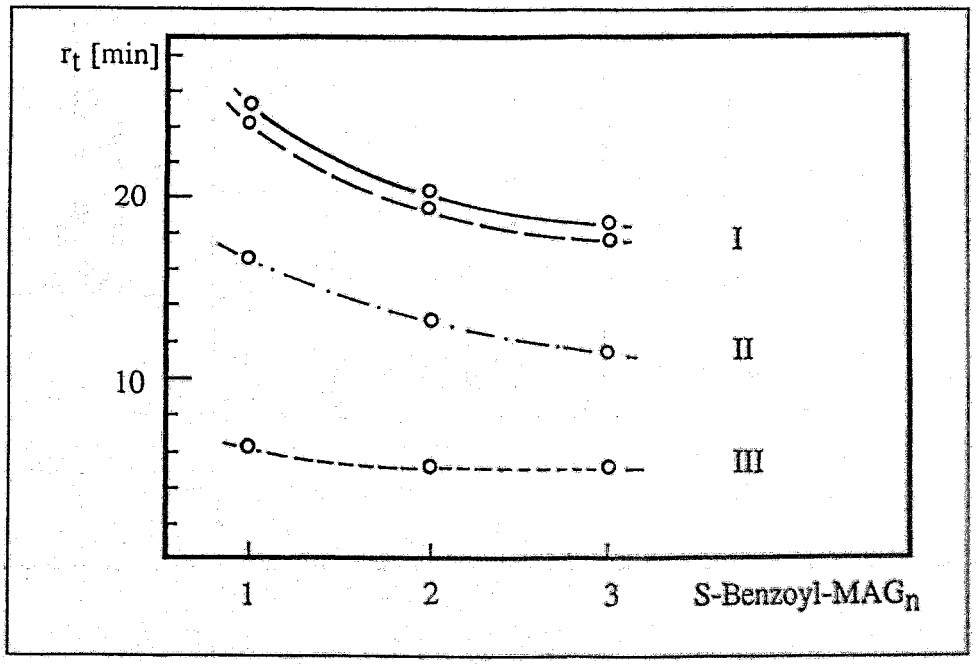

Fig. 1: HPLC separation of S-benzoyl-MAG_n derivatives and the corresponding methyl esters using various eluents.

I- S-benzoyl-MAG_n-ester —— eluent: 0.1% phosphoric acid / methanol 70 / 30
---- phosphate buffer pH 7.0 / methanol

II- S-benzoyl-MAG_n eluent: 0.1% phosphoric acid / methanol 70 / 30

III- S-benzoyl-MAG_n eluent: phosphate buffer pH 7.0 / methanol

The capillary electrophoresis experiments were carried out with a P/ACE instrument from Beckman using untreated fused silica capillaries of 40 cm length, 0.01M phosphate buffer pH 7 as an electrolyte and working with a voltage of 15 kV.

The results obtained by HPLC are in good agreement with those obtained by capillary electrophoresis (Fig. 2).

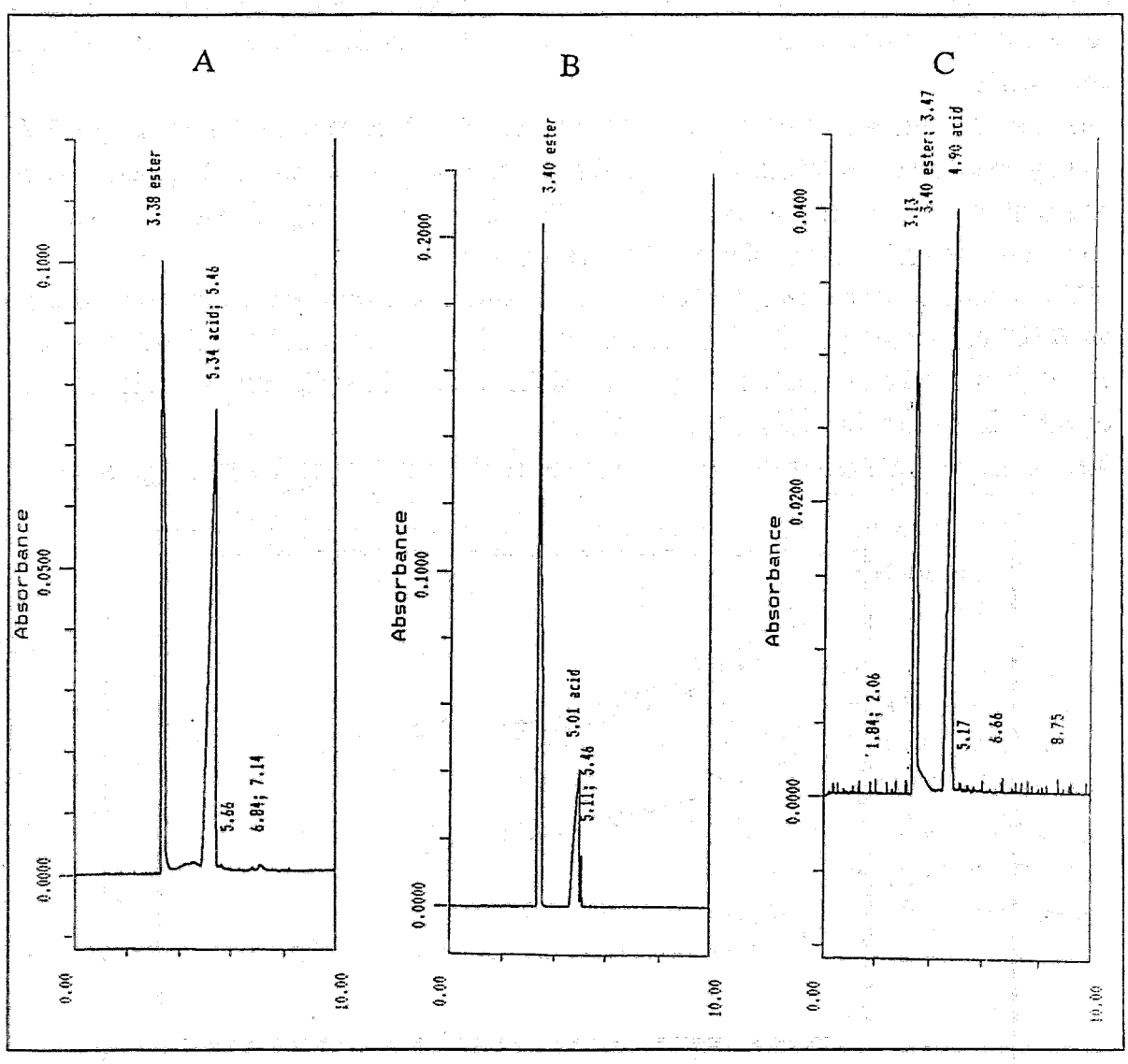

Fig.2: Separation of S-benzoyl-MAG_n derivatives and the corresponding methyl esters by capillary electrophoresis, A: S-benzoyl-MAG_3 /S-benzoyl-MAG_3 methyl ester, B: S-benzoyl-MAG_2 /S-benzoyl-MAG_2 methyl ester, C: S-benzoyl-MAG_1 /S-benzoyl-MAG_1 methyl ester

Reference:

[1] Noll, B. et al., this report, p. 107

23. TRITIATION OF BENZOYL-MAG$_3$-ERGOLINE AND ERGOLINE

St.Noll, B.Große, M.Findeisen[1], P.E.Schulze[2]
[1]Institut für Oberflächenmodifizierung, Leipzig
[2] c/o Schering Aktiengesellschaft, Berlin

Benzoyl-MAG$_3$-ergoline and ergoline were tritiated by catalytic hydrogen isotope exchange and investigated by radio thin-layer chromatography and ^{3}H NMR spectroscopy.
The tritiation of benzoyl-MAG$_3$-ergoline (Fig. 1) results in 20% of tritiated MAG$_3$-ergoline, 50% "acetyltriglycine-ergoline" and 30% undefinable by-products. The experiments reveal that under conditions of a catalytic hydrogen exchange, not only is the protection substituent of the molecule split off but the sulphur-carbon bond is also partially split. This can be demonstrated by radio thin-layer chromatography, UV and NMR spectroscopy and by comparison with reference substances.

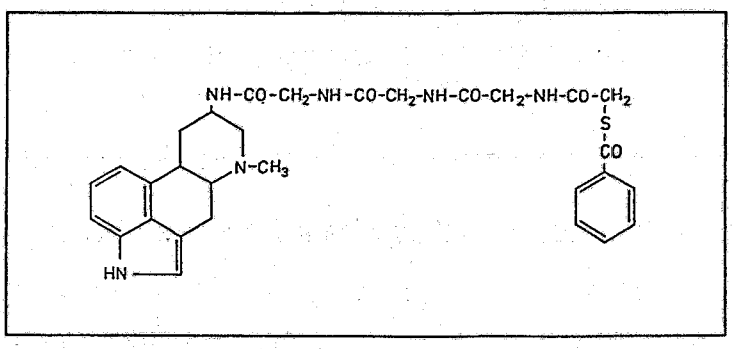

Fig. 1: Structure of the benzoyl-MAG$_3$-ergoline molecule

It was important to know whether ergoline in MAG$_3$-ergoline remained unchanged under the conditions of labelling and which positions of the molecule were labelled with tritium.
For this reason ergoline was labelled by catalytic isotope exchange under the same conditions as MAG$_3$-ergoline. The tritium labelled ergoline obtained with a radio-chemical purity of 95% was investigated by ^{3}H NMR spectroscopy.
The measurements were carried out with a BRUKER AM-250 system at a ^{1}H frequency of 250MHz and a ^{3}H frequency of 266MHz using a 5mm ^{3}H selective probe head with ^{1}H decoupling coils. The solvent was DMSO-D$_6$ (calibration at 2.51ppm in both spectra). Fig. 2 shows the ^{3}H NMR spectrum (I) and the ^{1}H NMR spectrum (II) of the labelled ergoline.
The fact that ergoline remains unchanged during the labelling process is demonstrated by its ^{1}H NMR spectrum, which is identical with that of an unlabelled reference substance. Fig. 2 also indicates the labelling positions in the ergoline molecule as described by the ^{3}H NMR spectrum.

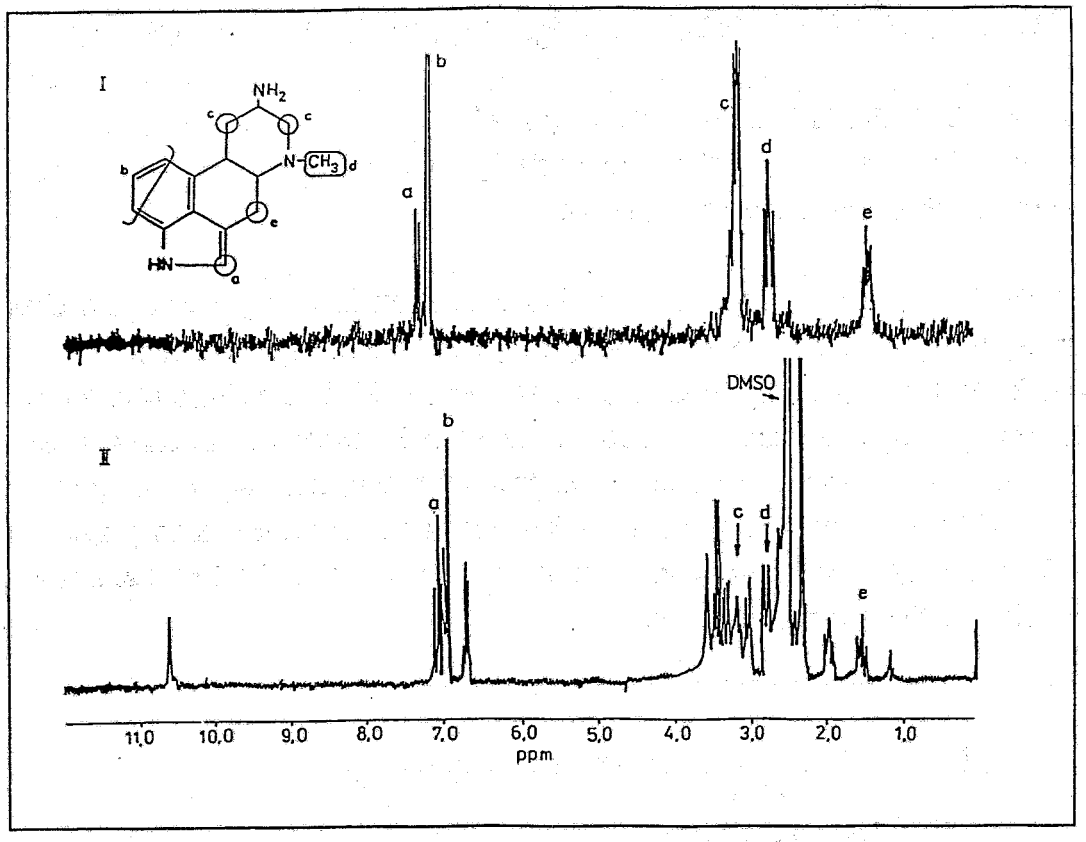

Fig. 2: ^{3}H and ^{1}H NMR spectrum of ergoline and structure of ergoline molecule

Experiments:

1. Tritiation of benzoyl-MAG$_3$-ergoline:

3.0mg benzoyl-MAG$_3$-ergoline was dissolved in 0.25ml water and 0.25ml ethanol in a 5ml round bottle. After addition of 148mg Pd-black, the bottle was connected to a vacuum apparatus, evacuated and then tritium gas (50% tritium, 50% hydrogen) was added up to a pressure of 55kPa. The reaction mixture was stirred vigorously for 3h. The catalyst was separated by centrifugation and washed with water several times. The solvent was freeze dried and labile tritium was separated by dissolving the residue in aqueous ethanol and lyophilizing it three times.

The product obtained has a radioactivity of 1.60GBq and a radiochemical purity of 20% as found in a Silufol//n-butanol/acetic acid/water chromatographic system.

2.Tritiation of ergoline:

The tritiation of ergoline took place under the same conditions as that of benzoyl-MAG$_3$-ergoline.

The product obtained has a radioactivity of 1.91GBq and a radiochemical purity of 95%.

24. RHENIUM(V) GLUCONATE AS PRECURSOR FOR PREPARATION OF RHENIUM COMPLEXES

B. Noll, U. Kolbe, St. Noll, H. Spies

Preparation of oxotechnetium(V) complexes is conveniently based on ligand exchange reaction on reactive Tc(V) precursors. Among them, Tc gluconate is particularly well qualified for both the synthesis of solid Tc complexes and for "carrier-added" preparations used for biological studies, because all reactions are carried out in a neutral aqueous medium, the exchange reaction proceeds rapidly with a variety of ligands, and the resulting Tc complexes are, as a rule, of a high radiochemical purity [1,2].
We were therefore interested in making available the corresponding rhenium gluconate for synthesis of rhenium(V) complexes. Preparation of Re(V) gluconate is somewhat more complicated then preparation of Tc gluconate because perrhenate is less reducible than the pertechnetate ion. The preparation of Re(V) gluconate solution is described and subsequent exchange reactions with are carried out benzenethiol and mercaptoacetyldiglycine (MAG_2) as typical representatives of sulphur donor ligands are carried out.

Experimental

UV/vis spectra were recorded on the spectrophotometer Specord M40, IR spectra on the Specord M80. The chromatographical behaviour was determined by HPLC on an RP 18 column with 85%(v/v) phosphate buffer pH 7.4 / 15% methanol as an eluent. The capillary electrophoresis experiments were carried out with a P/ACE instrument from Beckman using untreated fused silica capillaries of 20 and 40 cm length, 0.01M phosphate buffer pH 7 as an electrolyte, and working with a voltage of 15 kV.

Spectrophotometric control of the reduction of perrhenate by stannous chloride
2.75ml 0.5M solution of sodium gluconate and 0.58ml 0.15M ($8.7*10^{-5}$mol) ammonium perrhenate are degassed with argon in a closed cuvette (1cm). Then 175µl 0.5M ($8.7*10^{-5}$mol) stannous chloride in 0.1M HCl is introduced into the cuvette while stirring and the time function of reduction is recorded.

Rhenium gluconate
25ml 0.1M sodium gluconate ($2.5*10^{-2}$mol) and 5.6ml 0.3M ammonium perrhenate ($1,7*10^{-3}$mol) are put into a reaction bottle with a gas bubble counter and the solution is degassed with nitrogen for 10 minutes. Then 1.7ml 1M stannous chloride ($1.7x10^{-3}$mol) in 1M HCl is added. The reduction is completed within 60 minutes.

Ammonium tetrakis(benzenethiolato)oxorhenate(V) $NH_4[ReO(SPh)_4]$

30µl thiophenol (about 0.2mmol) was added to 2ml Re gluconate (0.05mmol). The resulting complex, which formed within one minute precipitated as black crystals, which were separated by filtration and washed with water and ethanol.

Yield: 16mg (50%)

Anal. Calc. for $C_{24}H_{24}NOS_4Re$: C 43.88; H 3.68; N 2.13; S 19.52%

Found: C 43.76, H 3.40; N 1.96; S 18.87%

IR spectrum: $\nu_{ReO} = 950cm^{-1}$

Tetraphenylarsonium(2-mercaptoacetyldiglycinato-S,N,N,O)oxorhenate(V) $AsPh_4[ReO(MAG_2)]$

10mg MAG_2 (0.05mmol) dissolved in 1ml 0.1N NaOH was added to 2ml (0.05mmol) aqueous Re(V) gluconate solution while stirring. After standing for 15minutes, 19mg (0.05mmol) tetraphenylarsonium chloride, dissolved in 0.5ml water, was added. The reaction mixture was extracted with methylene chloride (3 x 2ml), the combined extracts were dried over sodium sulphate and evaporated to dryness. Recrystallization of the residue from acetone produced 31mg (0.04mmol) dark brown crystals. M.p.: 203-205°C

Anal. Calc. for $C_{30}H_{26}N_2O_5SAsRe$: C, 45.74; H, 3.33; N, 3.56; S, 4.07%

Found: C, 45.80; H, 3.31; N, 3.55; S, 3.86%

^1H NMR (DMSO-d_6): 7.80ppm (m, 20H) phenyl, 4.83/4.16ppm(AB, 2H) and 4.01ppm (s, 2H) 2x N-CH_2, 3.89/3.62ppm (AB, 2H) S-CH_2.

IR (KBr): 976 cm^{-1} $\nu_{Re=O}$

UV/vis (ethanol) (λ_{max} (lg ε)): 412nm (2.15)

Results and discussion

While the reduction of the pertechnetate ion by stannous ions in an excess of sodium gluconate takes place fast and in quantitaty [1], reduction of perrhenate did not immediately proceed. The reaction rate depends on the concentration of perrhenate. At concentrations of perrhenate lower than $<6x10^{-4}M$ the reduction is incomplete if not impossible. At higher concentrations the reaction is complete, with clean conversion to the oxidation state +V.

In UV/vis spectroscopy the formation of Re gluconate is shown by a decrease in the absorption of the perrhenate ion (UV spectrum of NH_4ReO_4, Fig. 1) and the occurrence of a band at about 620nm indicating Re(V) gluconate. The increase of the absorption maximum at 625nm as a function of time is depicted in Fig. 2.

The blue coloured, clear solution of rhenium gluconate obtained in the concentration range of $5\text{-}7*10^{-2}$M is ready for use. As a frozen mixture under nitrogen, the solution can be stored for several weeks without any signs of decomposition.

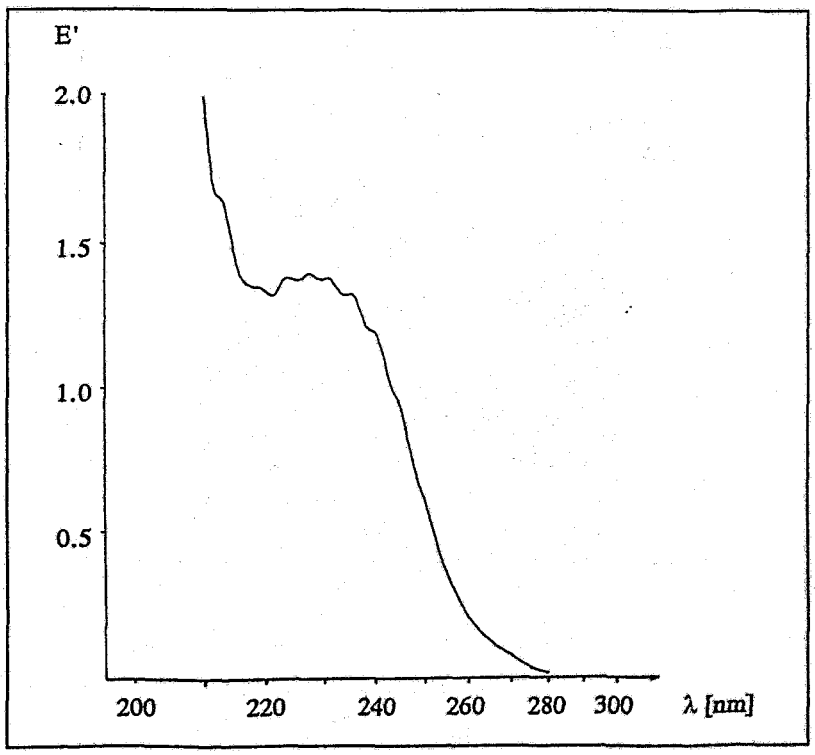

Fig. 1: UV spectrum of a $3.8*10^{-4}$M aqueous solution of ammonium perrhenate

The Re gluconate complex was separated from perrhenate by HPLC on an RP 18 column with 85% phosphate buffer pH 7.4 / 15% methanol as an eluent (r_{tReO4^-} = 2.0min, $r_{tRe\text{-}gluc.}$ = 2.5min). The anionic behaviour was determined by capillary electrophoresis.
As known from Tc(V) gluconate, an excess of ligand is required for stabilization of the rhenium complex in aqueous solution. Attempts to isolate the compounds failed. The preparation is nevertheless suitable for exchange reactions. The following experiments carried out with S and S/N donor ligands indirectly confirm the oxidation state +V for Re gluconate.

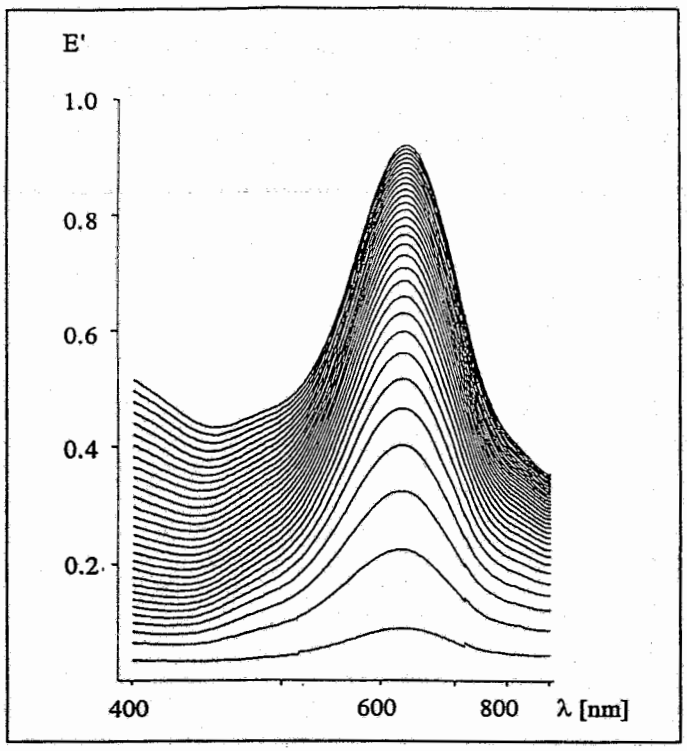

Fig. 2: Reduction of ammonium perrhenate (c = $2.5*10^{-2}$M) in a 0.5M sodium gluconate solution by 1mol stannous chloride/mol ammonium perrhenate, increase of the 620nm band within 60min

The reaction of Re gluconate with benzenethiol (molar ratio Re/benzenethiol 1:4) is completed within one minute. The complex precipitated was isolated as the ammonium salt and the anion was found to be identical (elemental analysis, UV/vis-spectrum, infrared band with the characteristic absorption at $949cm^{-1}$ for Re=O) with that prepared from $[ReOCl_4]^-$ [3].
In a similar manner $AsPh_4[ReO(MAG_2)]$ was obtained in good yields. The compound corresponds to the analogous Tc complex described in [4].

The facility of preparation and ability of Re(V) gluconate to react with S(N) donor ligands under mild reaction conditions demonstrate the usefulness of Re(V) gluconate as a precursor of Re(V) complexes.

References:

[1] Johannsen, B. et al., Radiochem. Radioanal. Letters **36** (1978) 107
[2] Spies, H. et al., Inorg. Chim. Acta **48** (1981) 255
[3] McDonell, A. C. et al., Austr. J. Chem. **36** (1983) 253
[4] Noll, B. et al., to be published in Inorg. Chim. Acta

25. SYNTHESIS OF A DADT PRECURSOR

T. Brankoff, H. Spies

Baidoo et al. [1,2,3] recently reported a new route to bifunctional Tc diaminodithiol chelates involving reaction of a reactive thiolactone precursor (1) with an appropriate amine. As this method seems to be a promising approach to Tc coupled biomolecules, which we are very keen to achieve, we worked on the synthesesis of the thiolactone precursor following Baidoo's procedure.

Following the procedure [2], the eight-step synthetic sequence was accomplished with a 5% overall yield. The reaction scheme is seen in Fig. 1.

The yield of 2,2'-dithio-bis(2-methylpropanal) (2) from synthesis with isobutyraldehyde (1mol) according to [4] in two batches was 70%. (2) was converted into 3,3,10,10-tetramethyl-1,2-dithia-5,8-diazacyclo-4,8-diene (3) analogue [4,5]; the yield of crude substance was 70%. The product of sodium borohydride reduction of the Schiff base in ethanol at 25°C is hexahydro-6,6,9,9-tetramethyl-1H-imidazo[2,1-d][1,2,5]dithiazepine (4) [2,3,6] with a yield of 80%. N-alkylation of (4) with methyl iodide in the presence of 50% KF on celite [2,3] produced hexahydro-1,6,6,9,9-pentamethyl-1H-imidazo[2,1-d][1,2,5]dithiazepine (5) in a yield of 82%. (5) was obtained as a colourless oil, which solidified after lyophilization in vacuum and cooling at 5°C.

Cleavage of both rings of (5) into 2,2,4,9,9-pentamethyl-4,7-diaza-1,10-decanedithiol (6) was accomplished with $LiAlH_4$ in dry tetrahydrofuran under argon [2,3]. The free base was immediately converted into the dihydrochloride. Nevertheless no more than a 35% yield was obtained. For protection of the SH groups in (6) p-methoxybenzyl chloride [2,3] was used. The product (7) results in a 70% yield in the form of the dihydrochloride. Alkylation of the second nitrogen in (7) was carried out with ethyl bromoacetate [2,3] yielding (8) in about 50%. Compound (8) serves as the stock from which 4-[2-[(2-mercapto-2-methylpropyl)-methyl-amino]ethyl]-6,6-dimethyl-2-thiomorpholinone (1) will be obtained in anhydrous HF in a teflon apparatus [7], if necessary.

The compounds synthesized (Tab. 1) were characterized by IR (Specord 80, KBr), ^1H NMR spectrometry (Bruker, 250 MHz) and elemental analysis. The calculated values of the elemental analysis were confirmed. For TLC, silica gel 60 F-254 (Merck), $CHCl_3/CH_3OH = 94/6$ and iodine vapour were used .

Tab. 1: Analytical data of compounds 2 - 8

Comp.	m.p./b.p. /°C/	TLC Rf	IR /cm^{-1}/	^1H NMR /ppm/
2	b.p. 80 - 90 (10^{-1}Torr)	0.70	1730 HC=O	
3	m.p. 164 - 166 (ethyl acetate)	0.50	1660 C=N	1.29 - 1.37 (12H) 3.15 - 4.09 (4H) 6.78 HC=N (2H) ($CDCl_3$)
4	m.p. 57 - 60 (pentan)	0.35	3290 NH	1.15 - 1.22 (12H) 2.51 - 3.41 (8H) (CD_3SOCD_3)
5	m.p. ~20 [3]: b.p. 122 ($2.4 \cdot 10^{-3}$ Torr)	0.60	2800 NCH_3	1.17 - 1.25 (12H) 2.51 - 3.1 (10H) (CD_3SOCD_3)
6 *2HCl	m.p. 175 - 180	0.35	2500 SH	1.46 - 1.52 (12H) 2.9 - 4.1 (12H) (CD_3SOCD_3)
7 *2HCl	m.p. 163 - 167	0.20	1180, 1245 CH_3O Aryl	1.32 $C(CH_3)_2$ (12H) 2.35 NCH_3 (3H) 2.5 - 3.72 CH_2 (12H) 3.76 OCH_3 (6H) 6.78 - 7.25 Aryl (8H) (free base, $CDCl_3$)
8	oil	0.55	1735 C=O	

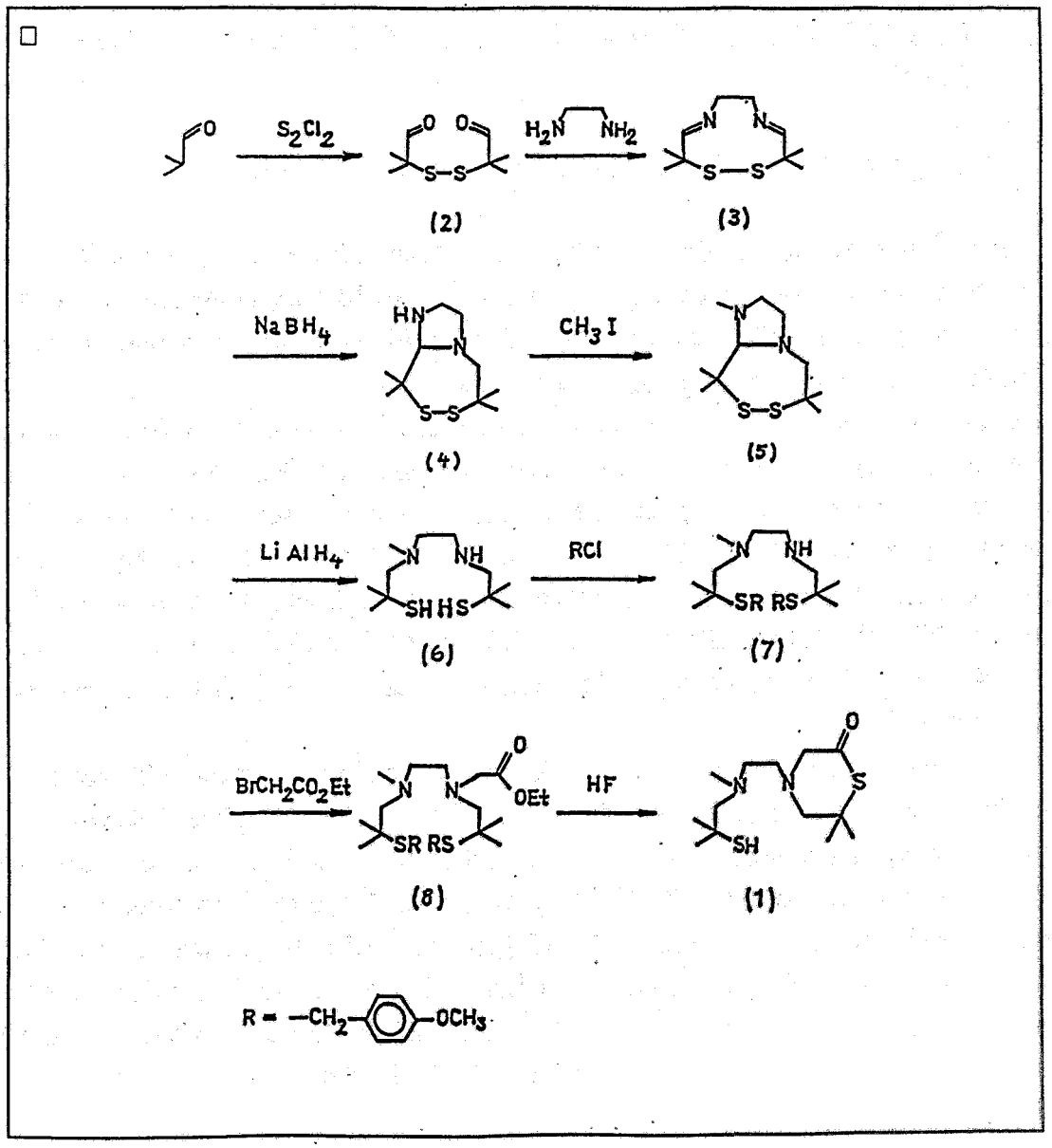

Fig. 1: Synthesis route

References:

[1] Lever, S. Z. , et al., Tetrahedron Lett. **29** (1988) 3219

[2] Baidoo, K. E. :Technetium-99m labeling of proteins. Ph. D. Thesis, Baltimore, Maryland, USA: The Johns Hopkins University, 1988; CA **110** (1989) 208525

[3] Baidoo, K. E. et al., Bioconjugate Chem. **1** (1990) 132

[4] Kung, H. F. et al., J. Nucl. Med. **25** (1984) 326

[5] Merz., K. W. et al., Arch. Pharm. (Weinheim) **296** (1963) 427

[6] Joshua, A. V. et al., J. Org. Chem. **52** (1987) 2447

[7] Sakakibara, S., et al. Bull. Chem. Soc. Japan **37** (1967) 2164

26. SEARCH FOR REDOX-ACTIVE MARKERS IN RADIOTRACER-DESIGN

R. Bergmann, St. Noll, B. Grosse, H. Spies, B. Johannsen, W. Brandau

^{18}F and ^{123}I-labelled nitroimidazole derivatives have become known as hypoxic cell markers [1-4]. It seems desirable to develop appropriate ^{99m}Tc labelled candidates, as well as exploring the potentials of other redox-active substrates of biochemical reactions, which may prove to be an enrichment of diagnostic nuclear medicine [9].

Bodor et al. [5] have demonstrated that drugs can be selectively delivered to the brain using a dihydropyridine/pyridinium salt redox delivery system. This type of dihydropyridine/pyridinium salt redox delivery system may potentially be useful for trapping tracers in the brain. If any lipophilic Tc tracers equipped with the dihydropyridine moiety are available, they should be able to cross the blood-brain barrier (BBB) due to their lipophilicity. In the brain, the labile dihydropyridine should be oxidized into the pyridinium salt. The BBB prevents rediffusion of the polar pyridinium compound, which results in an increased and sustained brain concentration.

In view of this, we are engaged in investigations regarding the preparation of Tc complexes containing the pyridinium/dihydropyridine moiety, their electrochemical behaviour and characterization in biological systems in vitro and in vivo, and have chosen 1-methyl-3-carbamoyl-1,4-dihydropyridine (MCD) as the pilot compound for preliminary studies.

Nicotinic acid derivatives and vitamins of the B group react with dehydrogenases. Initial rate and inhibition studies of the enzyme reaction of lactate dehydrogenase (LDH) (lactate:NAD^+ oxidoreductase, EC 1.1.1.2) were carried out in the absence and presence of MCD^+ to obtain information about the type of inhibition of MCD^+, the kinetic constants and the possible reduction of MCD^+.

The inhibition of the LDH by N-methyl-nicotineamide-iodide (MCD^+) was measured by the reactions (1) lactate + NAD^+ + MCD^+ $\Leftrightarrow$ pyruvate + NADH + H^+, with trapping of the pyruvate by the reaction (2) pyruvate + L-glutamate $\Leftrightarrow$ L-alanine + 2-oxoglutarate.

I. Synthesis of 1-Methyl-3-carbamoyl-1,4,-dihydropyridine

A two step synthesis of 1-methyl-3-carbamoyl-1,4-dihydropyridine was carried out according to [6] in a modified procedure: quaternisation of nicotinamide (1) to form 1-methyl-3-carbamoyl-pyridinium iodide (2) followed by reduction of the quaternary salt, produced 1-methyl-3-carbamoyl-1,4-dihydropyridine ($MCDH_2$) (4). Reduction with sodium dithionite in a slightly alkaline medium occurs via sulphinate adduct (3) [7].

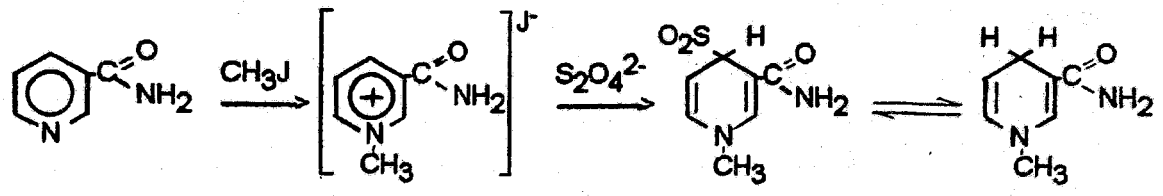

(1) (2) (3) (4)

The reaction was monitored by thin layer chromatography and UV spectroscopy at intervals of 5 min. For the chromatographic system and the R_F values see below. Fig. 1 shows the UV spectrum of (4) in diethylether (a) and in buffer pH 7 (b) after 30 min.

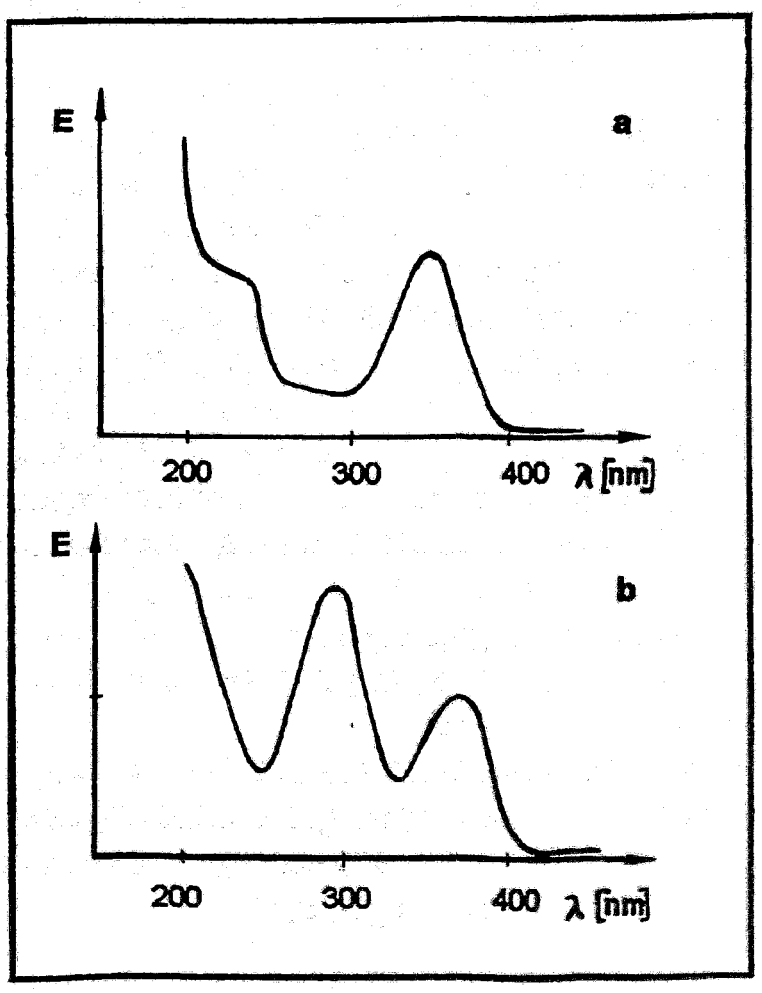

Fig.1. The UV spectrum of 1-methyl-3-carbamoyl-1,4-dihydropyridine

Experiments

1. 1-methyl-3-carbamoyl-pyridinium iodide (2)

3g (0,024mol) nicotinamide was dissolved in 15ml of warm methanol. To this solution 3ml (0,46mol) of methyl iodide was added and the mixture was refluxed for 30min. After cooling the yellow residue was separated and crystallised from a mixture of 50ml of methanol and 5ml of water.

Yield: 3,5g (54%); mp 206°C (Ref. 203-204°C [8])

Thin layer chromatography: chromatographic system:

Silufol//n-butanol/acetic acid/water 2:1:1 R_F 0,25 (UV, 254nm)

UV_{max} (water)	265nm; 270nm, sh	
IR (KBr):	ν_{CH3} 2980,	$\nu_{C=O}$ 1695cm^{-1}
^{1}H-NMR (DMSO)TMS	δ 4.41 (N-CH_3,3H);	δ 8.23-8.28 (C_5-H,1H)
	δ 8.89-8,93 (C_4-H,1H);	δ 9.11-9.13 (C_6-H,1H)
	δ 9.41 (C_2-H,1H)	

2. 1-methyl-3-carbamoyl-1,4-dihydropyridine (4)

To a solution of 2.66g (0.01mol) of (2) in 200ml of bidistilled water 5g (0.06mol) of sodium bicarbonate was added. The mixture was stirred in an ice bath under nitrogen and 7.1g (0.04 mol) sodium dithionite was added. Stirring and cooling under nitrogen was continued for 30 min and then the mixture was extracted with 200ml diethylether. The ether layer was separated, dried with sodium sulphate and the yellow oily residue was isolated by freeze-drying.

During the reaction time samples of 3ml were taken, extracted with 3ml diethylether and the ether layer was investigated by UV spectroscopy and thin layer chromatography.

Yield: 0.99g (72%). The product was found to be relatively unstable as regards-oxidation by air.

Thin layer chromatography: chromatographic system:

Silufol//n-butanol/acetic acid/water 2:1:1 R_F 0.2 (UV, 366nm)

UV_{max} (diethylether)	350nm;	
UV_{max} (buffer pH 7)	290nm, 360nm	
^{1}H NMR (MeOD)TMS	δ 3.13 (N-CH_3,3H);	δ 3.25 (Ch_2,2H)
	δ 4.91-4.97 (C_5-H,1H);	δ 5.94-5.99 (C_6-H,1H)
	δ 7.13 (C_2-H,1H)	

II. Inhibition of Lactate Dehydrogenase by N-Methyl-Nicotine amide

Materials and Methods

NAD^+, L-glutamate and carbonate were purchased from Boehringer Mannheim. L-lactate was obtained from SERVA. The LDH/GPT enzyme solution was obtained from Boehringer Mannheim (Test-combination L-lactic acid). Proteins were determined by the biuret or Lowry method.

Kinetic measurements

Kinetic measurements were carried out at 20°C in 25 mM carbonate buffer, pH 10, 23mM L-glutamate. The solution of the coenzymes, the MCD^+ and L-lactate were prepared daily. In these solutions the concentrations of NAD^+ and NADH were directly determined by the absorbance at 260 and 340nm, respectively, and those of the substrates by optical enzymatic methods.

The initial rates were measured in a total volume of 1 ml. The enzyme concentration was held constant throughout all experiments: an enzyme activity of 15U was added per test. The changes of absorbance at 340nm were recorded by a SECOMAM S1000 photometer (optical path: 1cm, scale expansion 0.1A). The reaction was started by addition of L-lactate.

Data processing

A preliminary graphical analysis showed that the kinetic data follow the general equation v=VS/(K+S) [10]. Hence, the least-squares method was applied and the EXCEL 3.0 and/or SPSS program was used to fit the kinetic data to an equation of the form $y = \alpha + \beta x$. The weights were taken as $w_i = 1/\sigma^2_i$., where σ^2_i is the sample variance of the ith observation.

For the primary plots, the observed reciprocal velocities (y_i) were ploted versus reciprocal substrate concentrations (x_i). In this case the calculation provides the apparent values of $1/V$, K/V, K and V, with their estimated variances. In order to obtain significant fits, the data were obtained at least in triplicate for each substrate concentration over a range of four to five concentrations.

For the secondary plots, the observed values of $1/V^{app}$ and/or K/V (slopes) were ploted versus the reciprocal concentrations of the substrates.

Results

Initial rate studies

Initial rate studies were carried out on the enzyme in one direction of the reaction by varying each substrate concentration for at least four fixed concentrations of the other (Fig. 1a, 2a). From these data two primary linear Lineweaver-Burk plots were obtained: all the plots intersected at one point. The values from these plots were used to construct secondary plots

(1b, 1c, 2b, 2c). These replots were also linear and provided the best estimates of the two Michaelis constants ($K_{lactate}$, K_{NAD^+}), the dissociation constant of the NAD^+ ($K_{S\ (NAD)}$) and of the maximum rate (V^{app}_{max}). In the Table 1 the values of the Michaelis constants are given in Tab. 1.

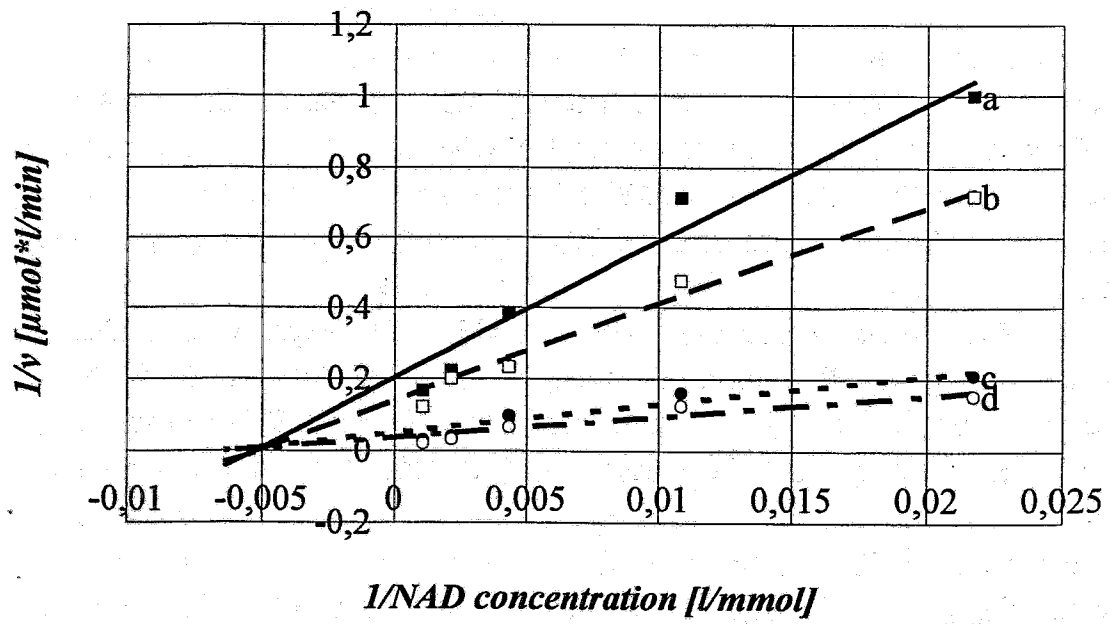

Fig. 1a: Lineweaver & Burk diagram of the LDH kinetic at different lactate concentrations (a: 1mmol/l, b: 2mmol/l, c: 5mmol/l, d: 10mmol/l).

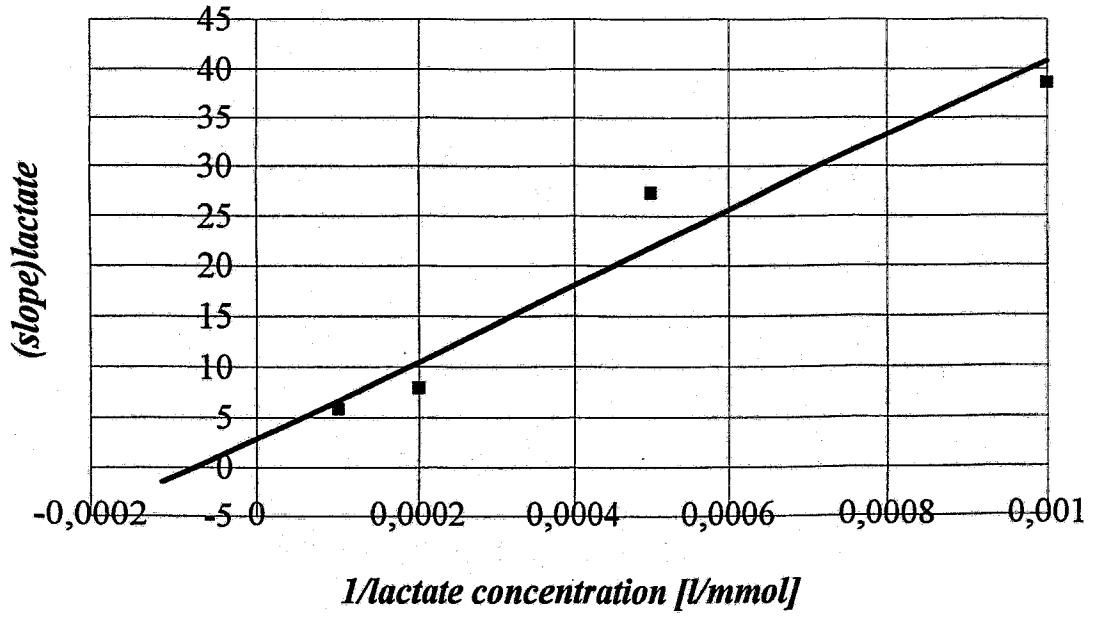

Fig 1b: Determination of the dissociation constants by the slope method. The slope of the graphs of Fig. 1a are plotted versus there reciprocal lactate concentrations.

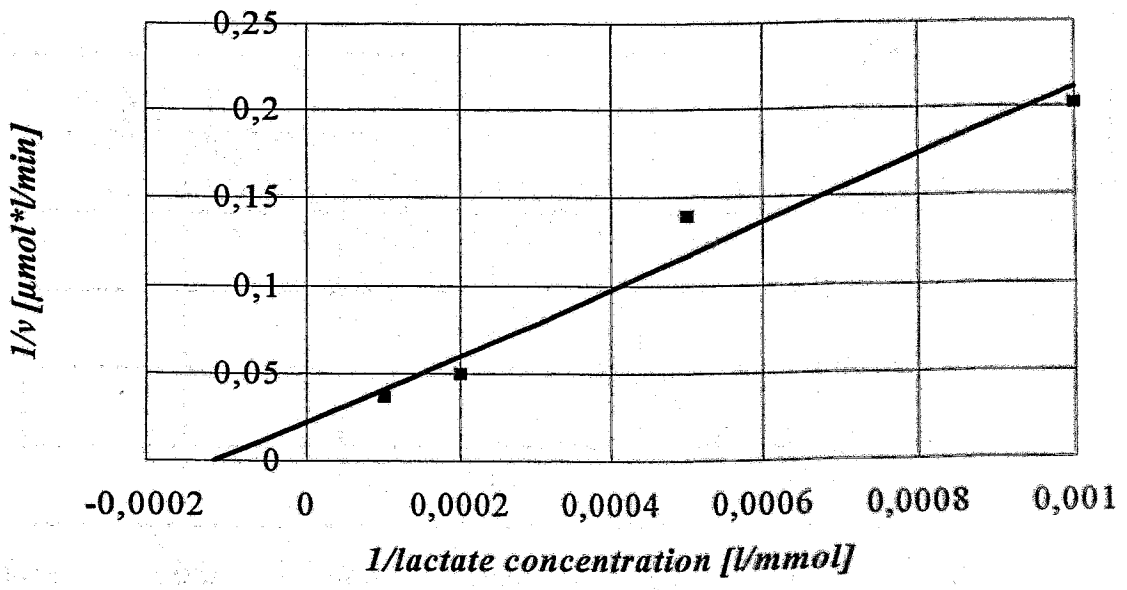

Fig 1c: Determination of the dissociations constants. The relative maximum reaction rates found as intercepts in the Fig 1a are plotted as a function of the reciprocal lactate concentration

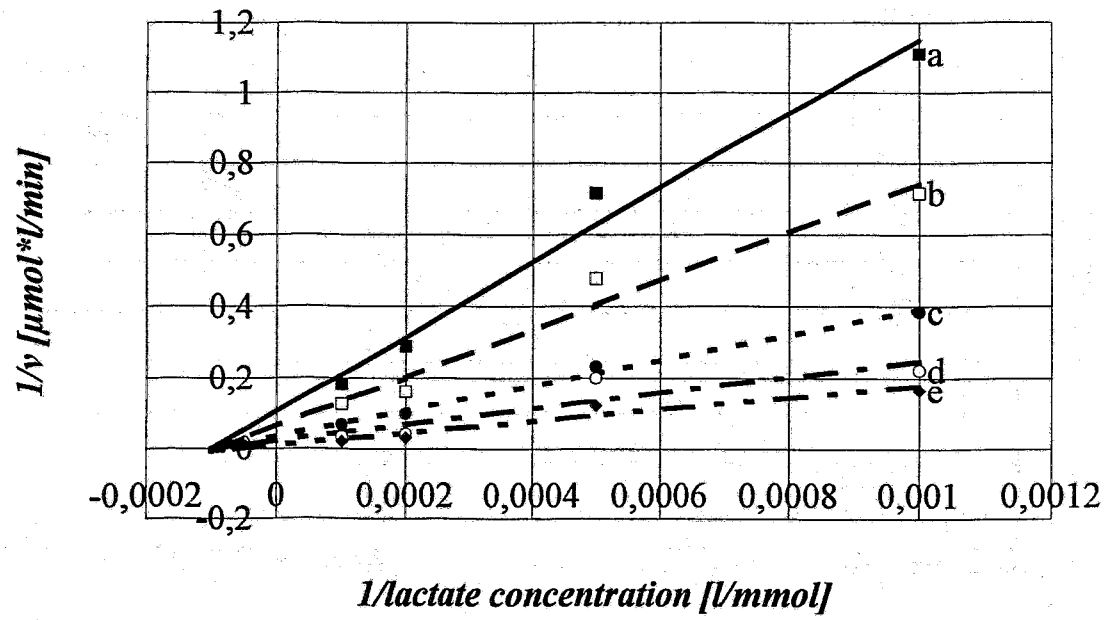

Fig. 2a: Lineweaver & Burk diagram of the LDH kinetic at different NAD^+ (a: 46µmol/l, b: 92µmol/l, c: 230µmol/l, d: 460µmol/l, e: 920µmol/l).

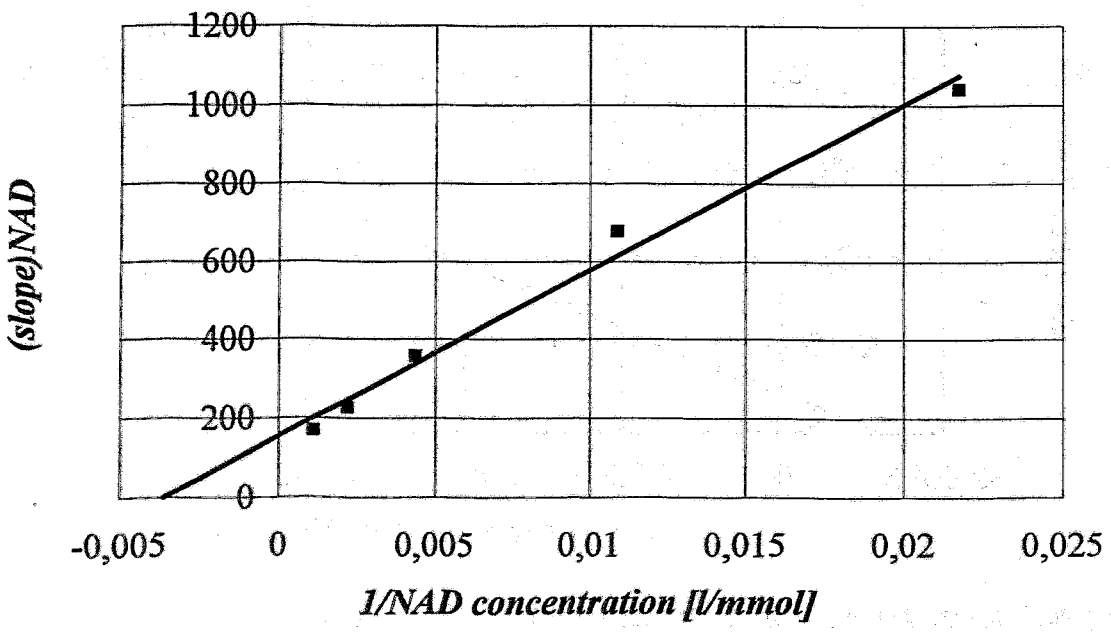

Fig 2b: Determination of the dissociation constants by the slope method. The slope of the graphs of Fig. 2a are plotted versus there reciprocal lactate concentrations.

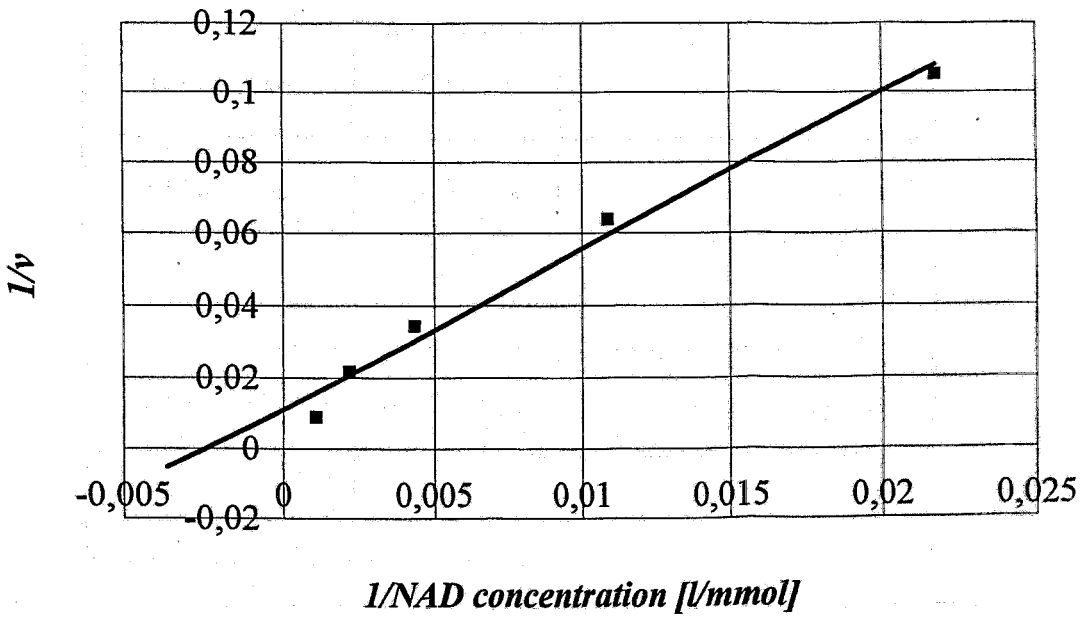

Fig 2c: Determination of the dissociations constants. The relative maximum reaction rates found as intercepts in the Fig 1a are plotted as a function of the reciprocal lactate concentration.

Inhibition studies

Experiments were carried out to study the mechanism of MCD inhibition. When the inhibitor is MCD^+ and the variable substrate is NAD^+, the inhibition type appears to be a competitive one (Fig 3). But there is no significant distinction from the non-competitive type. Further investigations are necessary to clarify the inhibition type.

Tab. 1: Kinetic parameters of lactate dehydrogenase

$K_{lactate}$	11.4 ± 3.9	mmol ± SD
K_{NAD^+}	0.27 ± 0.2	mmol ± SD
$K_{s(NAD)}$	0.24 ± 0.05	mmol ± SD
V^{app}_{max}	0.085 ± 0.036	mmol/l/min ± SD
K_{MCD^+}	93 ± 5	mmol± SD

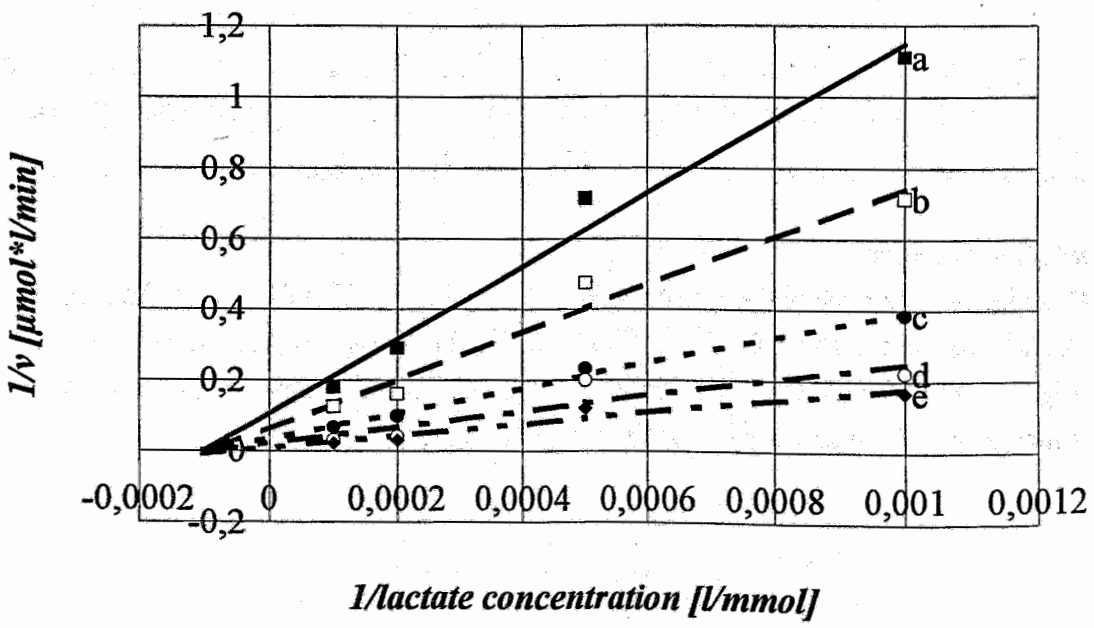

Fig 3: Determination of the dissociation constant of the MCD enzyme complex by the Dixon plot of the LDH reaction. The reciprocal reaction rates are plotted as functions of the MCD concentration at different NAD^+ concentrations (a 46 µmol/l, b 92 µmol/l, c 230 µmol/l, d 460 µmol/l, e 920 µmol/l).

The reaction is stoichiometric with the amount of L-lactic acid. Initial rate measurements and analysis of inhibition patterns show the competitive MCD^+ inhibition of the NAD^+ binding. The dissociation constant (K_{MCD^+}) is 350 times higher than the K_{NAD^+}. $MCDH_2$ does not

inhibit the LDH reaction. MCD^+ is not reduced by LDH. The kinetic pattern of the enzyme is consistent with a mechanism of the Theorell-Chance type, with a kinetically irrelevant ternary complex.

References:

[1] Jerabek, P. A., et al., Int. J. Rad. Appl. Instrum. 8A **37** (1986) 599.

[2] Freauff, S. J., et al., J. Nucl. Med. **28** (1987) 68-75

[3] Rasey, J. S., et al. J., Nucl. Med. **31** (1990) 756

[4] Mathias, C. J., et al. Life Sci. **41** (1988) 199-206

[5] Bodor, N., et al., J. Pharm. Soc., **74** (1985) 241

[6] Bodor, N., et al., Med. Chem., **26** (1983), 313

[7] Blankenhorn, G., et al., J. Am. Chem. Soc. **102** (1980) 1092

[8] Holmann, W.E., et al., 39th Annual Meeting of the Society of Nuclear Medicine, Abstr. No. 400, J Nucl. Med. **33** (1992)

[10] Bergmeyer, H. U., (ed.) Methods of Enzymatic Analysis Vol.I, Verlag Chemie, Weinheim, Deerfield Beach, Basel (1983)

27. ELECTROCHEMICAL REDUCTION OF 1-METHYL-3-CARBAMOYL-PYRIDINIUM IODIDE

I. Hoffmann, H. Spies, B. Johannsen

The dihydropyridine/pyridinium system may be potentially useful for trapping Tc tracers in the brain. We are therefore interested in the electrochemical behaviour of the dihydro-pyridine/pyridinium system and investigated the reduction of 1-methyl-3-carbamoylpyridinium iodide in various aqueous solutions at different pH using polarographic, voltammetric, coulometric and spectrophotometric methods.

Chemicals

1-methyl-3-carbamoylpyridinium iodide [mp = 207-209°C; UV $_{max}$ (H_2O) 265nm]
supporting electrolytes: 0.1M KCl pH = 5.3; phosphate buffer (Sörensen) pH = 7.0;
Britton-Robinson buffer pH = 9.1; 0.1M Me_4NOH/0.1M Me_4NCl
All solutions were deoxygenated by argon (99.998%).

Apparatus

DC/AC polarograph (GWP 673, ZWG Berlin); Cyclic voltammograph (CV-27, BAS);
UV-VIS spectrophotometer (Specord M40, Carl Zeiss Jena)

Electrodes

working electrodes: static mercury drop electrode (GQE 100, ZWG Berlin),
glassy carbon electrode;
reference electrode: saturated calomel electrode; counter electrode: Pt or Hg-pool

Results and discussion

DC polarograms of 1-methyl-3-carbamoylpyridinium iodide were recorded in various solutions (Fig.1). All curves show two cathodic reduction waves. The changes in height of the waves are caused by different concentrations. The half wave potentials of the first wave are identical, but those of the second wave differ from each other. It can be assumed that these differences result from adsorption of reaction products which increase the resistance to charge transfer at the electrode surface, combined with an overvoltage. In phosphate solution a maximum is superimposed on the second wave. In 0.1M Me_4NOH/0.1M Me_4NCl supporting electrolyte, a low additional wave can be observed near the first wave.

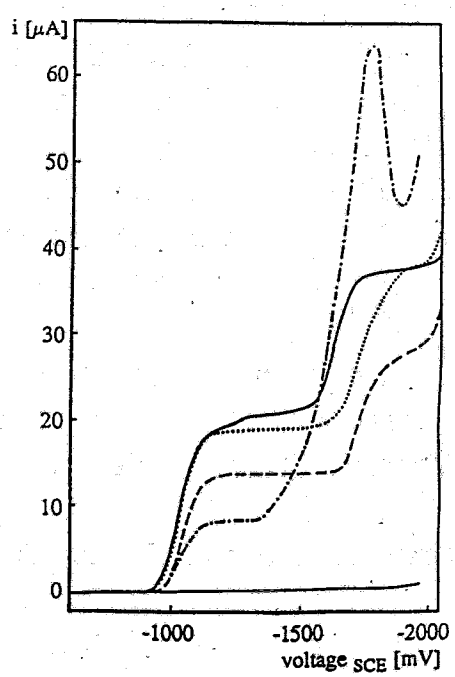

Cyclic voltammograms were recorded at the hanging mercury drop electrode and the glassy carbon electrode. In all tested solutions a reduction peak is found in the potential range of the first wave of the dc polarogram at about -1000 mV (Figs. 2, 3). In the potential range of the second wave (-1700 mV) a low reduction peak was only observed in the Me_4NOH/ Me_4NCl solution. In this supporting electrolyte an additional peak exists in the potential range of the first wave (-1250mV). All reduction steps are irreversible. The anodic oxidation peak (Figs. 2, 3) may be due to the formation of dimeric products [1].

Fig. 1:
DC polarograms of 1-methyl-3-carbamoylpyridinium iodide (c) in --- 0.1M KCl (c = 3.5mM); ----- phosphate buffer (c = 2mM); ···· Britton-Robinson-buffer (c = 4.7mM); ——Me_4NOH/Me_4NCl (c = 5.1 mM)

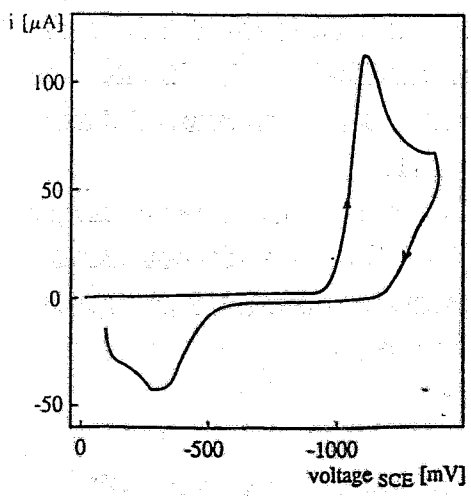

Fig. 2:
Cyclic voltammogram of
1-methyl-3-carbamoylpyridinium iodide
(phosphate buffer, scan rate = 0.25V/s)

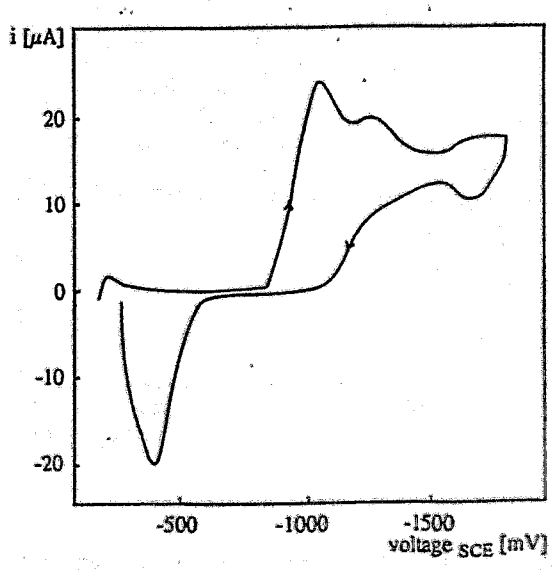

Fig. 3:
Cyclic voltammogram of
1-methyl-3-carbamoylpyridinium iodide
(Me_4NOH/Me_4NCl, scan rate = 0.25V/s)

Electrolyses of 1-methyl-3-carbamoylpyridinium iodide in the potential region of the second wave were performed in Britton-Robinson buffer and in the Me_4NOH/Me_4NCl system. Reduction was carried out at the stirred mercury pool. During reaction the yellow colour of the solution in the cathodic compartment became more intensive.

In Britton-Robinson buffer two maxima are observed in the UV spectrum at 278 and 300nm after reduction. A dark precipitate is formed in the anodic compartment. The solution of this precipitate in ether shows a maximum in UV at 350nm, which is characteristic of dihydropyridine [1].

In the Me_4NOH/Me_4NCl solution no insoluble products were observed during coulometry at -1900mV/SCE. The polarograms of pyridinium (1) and after partial (2, 3, 4) and nearly complete reduction (5) are depicted in Fig. 4. Fig. 5 shows the UV spectra of diluted solutions

corresponding to the polarograms in Fig. 4. The UV maxima at 270nm and 357nm indicate the formation of a dihydro-pyridinium compound [1].

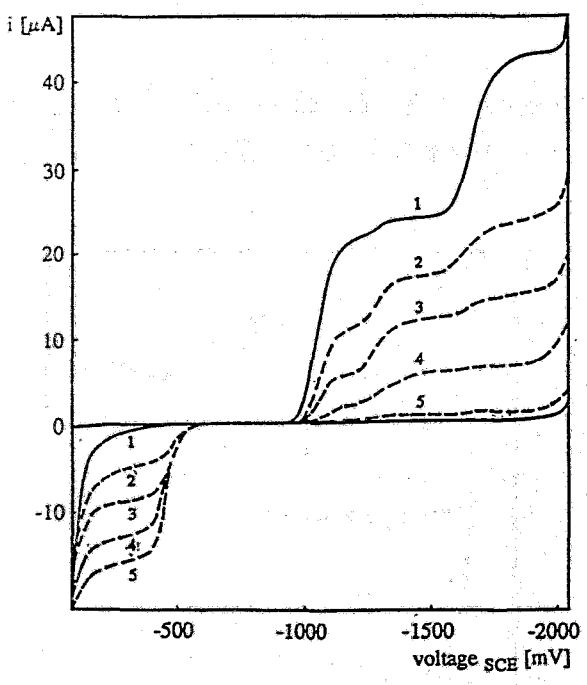

In the dc polarogram (Fig. 4) the first reduction wave consists of two parts whose relation changes during reduction. This behaviour could be explained by formation of isomeric reduction products. An anodic wave increases on nearly the same scale, corresponding to the anodic peak of the cyclic voltammogram in Fig. 3. The anodic step is described in the literature in connection with the existence of dimeric products [1].

From these coulometric measurements at -1900mV/SCE the electron transference number of two is determined for the second wave.

Fig. 4: Coulometric reduction of 1-methyl-3-carbamoylpyridinium iodide in Me_4NOH/Me_4NCl; (c = 5.5mM; Hg-pool; voltage = -1900mVSCE)

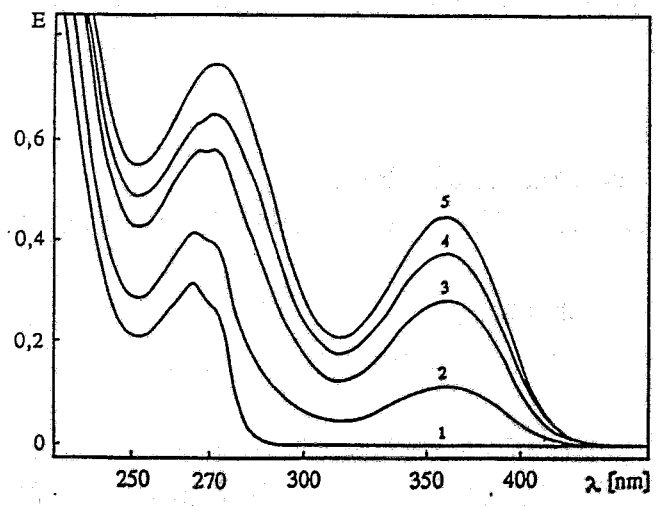

Fig. 5: Changing of UV-spectra caused by reduction of 1-methyl-3-carbamoylpyridinium iodide in Me_4NOH/ Me_4NCl (c = 0.25mM)

Reference:

[1] Carelli, I.,et al., J. Electroanal. Chem. **107** (1980) 391

IV.
PUBLICATIONS, LECTURES AND POSTERS

PUBLICATIONS

Bandoli, G., U. Mazzi, H.-J. Pietzsch. H. Spies:
Structure of (N-(2-sulfidophenyl)salicylideneiminatoS,N,O)(benzenethiolato)-oxotechnetium(V)
Acta Crystallogr., **C 48** (1992) 1422

Johannsen, B.
Prinzipien der immunologischen Tumormarkerbestimmung
in: D. Elling und V.Pink (Hrg.): Tumormarker in der gynäkologischen Onkologie Springer-Verlag Heidelberg, 1992

Noll, B., B. Johannsen, K. May, H. Spies
Preparation of the Renal Function and Imaging Agent ^{99m}Tc-MAG$_3$ Starting from S-unprotected Mercaptoacetyltriglycine"
Appl.Radiat.Isot. **43** (1992) 899

Pietzsch, H.-J., H. Spies, P. Leibnitz, G. Reck, J. Beger, R. Jacobi
Technetium Complexes with Thioether Ligands. 1. Cationic Technetium(III) Complexes Containing Tetradentate Thioether/Monothiole Ligands; X-Ray Structure Analysis of Bis(Benzenethiolato)(5,8,11,14-Tetrathiaoctadecane)Technetium(III)Hexafluorophosphate "
Polyhedron **11** (1962) 1623

Pietzsch, H.-J., H. Spies, P. Leibnitz, G. Reck, J. Beger, R. Jacobi
Technetium Complexes with Thioether Ligands. 2. Synthesis and Characterization of Neutral Oxotechnetium(V) Complexes with Bi- and Tetradentate Thioethers. X-Ray Structure Analysis of m-Oxo-bis(5,8dithiadodecane)dichlorooxotechnetium(V) and (1,8-dihydroxy-3,6-dithia-octane)oxotechnetium(V)
Polyhedron **12** (1993) 187

Seifert, S.. R. Münze, P. Leibnitz, G. Reck, J. Stach:
Preparation, characterization and crystal structure of a mixed ligand complex of technetium with DPPE and oxalic acid: Oxalato-bis(1,2-bis(diphenylphosphino)ethane)technetium(III)
Inorg.Chim.Acta **193** (1992) 167

Uhlemann, E., H. Spies, H.-J. Pietzsch, R. Herzschuh
TcN- und ReN-Komplexe mit Thio-ß-diketonen
Z.Naturforsch. **476b** (1992) 1441

LECTURES

Johannsen, B.
Bedeutung der Technetium-Chemie für die Nuklearmedizin
Gastvorträge "Nuklearmedizinische Grenzgebiete", Basel, Schweiz, 12.2.1992

Johannsen, B., B. Noll, St. Noll, H. Spies
Characterization of technetium-99 complexes with S-unprotected mercaptoacetylpeptides (MAG_3, MAG_2, MAG_1 and derivatives)
IXth Intern. Symp. on Radiopharmaceutical Chemistry, Paris, 6.-10.4.1992

Johannsen, B.
Möglichkeiten und Grenzen von Technetium in der Medizin
FZR Rossendorf, 26.6.1992

Johannsen, B., B. Noll, St. Noll, H. Spies, P. Leibnitz, G. Reck
Characterization of technetium-99 complexes with mercaptoacetyltriglycine (MAG_3, MAG_2, MAG_1 and derivatives)
29th Intern. Conference on Coordination Chemistry, Lausanne, Schweiz, 19.-24.7.1992

Johannsen, B
Chemie von Technetium im Schwefel-Ligand-System
Nuklearmedizinische Gespräche, Dresden, 11.11.1992

Pietzsch, H.J., H. Spies, P. Leibnitz, G. Reck, S. Seifert, R. Syhre, B. Johannsen
Technetium(III) complexes with tetradentate thioether ligands: Synthesis, characterization and biological evaluation.
Symp. Eurobic I. Metal ions in biological systems,
Newcastle upon Tyne, England, 8.-12.7.1992

Pietzsch, H.J., H. Spies, P. Leibnitz, G. Reck, J. Beger, R. Jacobi, S. Seifert, R.Syhre, B.Johannsen:
Synthesis, characterization and molecular structures of technetium with tetradentate thioether ligands
29th Intern. Conference on Coordination Chemistry, Lausanne, Schweiz, 19.-24.7.1992

Pietzsch, H.J., H. Spies, S. Seifert, R. Syhre, B. Johannsen
Technetium thioether/thiolato complexes: A new class of cationic compounds
European Association of Nuclear Medicine Congress 1992,
Lissabon, Portugal, 22.-26.8.1992

POSTERS

Johannsen, B., B. Noll, St. Noll, H. Spies
Characterization of Technetium-99 Complexes with S-unprotected Mercaptoacetylpeptides (MAG_3, MAG_2, MAG_1 and Derivatives)
IX International Conference on Radiopharmacological Chemistry, Paris,6.-10.April 1992

Johannsen, B., B. Noll, St. Noll, H. Spies, P. Leibnitz, G. Reck
Characterization of technetium-99 complexes with mercaptoacetylpeptides (MAG_3, MAG_2, MAG_1 and derivatives
29th International Conference on Coordination Chemistry (ICCC), Lausanne, 19.-24.Juli 1992

Pietzsch, H.-J., H. Spies, P. Leibnitz, G. Reck, S. Seifert, R. Syhre, B. Johannsen
Technetium(III) complexes with tetradentate thioether ligands: Synthesis, Characterization and biological evaluation
EUROBIC I: Metal ions in biological systems., Newcastle, 8.-12.Juli 1992

Pietzsch, H.-J., H. Spies, P. Leibnitz, G. Reck, J. Beger, R. Jacobi, S. Seifert, R. Syhre, B. Johannsen, F. Tisato, F. Refosco, U. Mazzi
Synthesis, characterization and molecular structure of technetium complexes with bi-, tri- and tetradentate thioether ligands
29th International Conference on Coordination Chemistry (ICCC), Lausanne, 19.-24.Juli 1992

Pietzsch, H.-J., H. Spies, P. Leibnitz, G. Reck
Synthesis, characterization and molecular structure of nitridotechnetium(V) complexes with thiacrown ethers
29th International Conference on Coordination Chemistry (ICCC), Lausanne, 19.-24.Juli 1992

Pietzsch, H.-J., F. E. Hahn, A. Dittler-Klingemann, H. Spies
Synthesis, characterization and molecular structure of Tc(III) complexes with the tripodal ligand tris-(2-mercaptoethyl)amin
29th International Conference on Coordination Chemistry (ICCC), Lausanne, 19.-24.Juli 1992

Pietzsch, H.-J., H. Spies, S. Seifert, R. Syhre, B. Johannsen
Technetium thioether/thiolato complexes: A new class of cationic compounds
European Association of Nuclear Medicine Congress 1992,
Lissabon, Portugal, 22.-26.8.1992

Pietzsch, H.-J., H. Spies, P. Leibnitz, G. Reck
Synthesis, characterization and molecular structure of nitridotechnetium(V) complexes with thiacrown ethers
Tagung der Deutschen Kristallographischen Gesellschaft, Bochum, November 1993

V.
SCIENTIFIC COOPERATION

In multidisciplinary research such as carried out by this Institute, collaboration, the sharing of advanced equipment and, above all, exchanges of ideas and information obviously play an important role. Effective collaboration has been established with colleagues at universities, in research centres and hospitals.

Cooperative relations and joint projects

The ***Technische Universität Dresden*** (Dr. Scheller, Inst. of Analytical Chemistry) plays an essential part in SPECT tracer research by performing analytical characterization of new tracers and providing support with the synthesis of organic compounds (Dr. Habicher, Inst. of Organic Chemistry).

Very effective cooperation also exists with the ***Bundesanstalt für Materialforschung Berlin*** (Dr. Reck, Mr. Leibnitz) who have carried out X-ray crystal structure analysis of new technetium and rhenium complexes.

Our long-standing cooperation with the University of Padua (Prof. Mazzi) and the "Demokritos" National Research Centre for Physical Sciences in Athens (Dr. Chiotellis) has now been instrumental in advancing the chemistry of thioether complexes.

Joint work on technetium complexes with tripodal ligands has been carried with the ***Freie Universität Berlin*** (Prof. Hahn, Inst. of Inorganic and Analytical Chemistry).

Cooperation on a special research topic concerning technetium tracers is in progress with the ***Forschungszentrum Jülich*** (Prof. Stöcklin) .

Common objects of radiopharmacological and medical research link the Institute with the ***Medizinische Akademie "Carl Gustav Carus" Dresden***, above all with its Departments of Nuclear Medicine (Prof. Franke), Psychiatry (Prof. Felber), Neurology (Prof. Kunadt) and Clinical Chemistry (Prof. Jaroß, Dr. Bergmann). A joint team of staff members from both the Institute and the Academy's Clinic of Nuclear Medicine are currently working at the Rossendorf PET centre.

Identification of common objectives in technetium radiopharmacy has led to collaborative research with the ***Humboldt-Universität Berlin*** (Dr. Michael of the "Charité" Hospital's Clinic of Nuclear Medicine) and with the ***Bundesgesundheitsamt Berlin*** (Dr. Schüttler).

Close cooperation exists with the Montreal Neurological Institute (Prof. Gjedde, Prof. Thompson), Canada, in the field of PET image data reconstruction and pharmacological studies.

In helpful discussions, visiting scientists have contributed to shaping projects and defining areas of cooperation in respect of PET tracers (Prof. Firnau, Hamilton, Canada, and Prof.

Wiebe, Edmonton, Canada; Prof. Meyer, Hannover) and technetium tracers (Dr. Brandau, Münster; Prof. Mäcke, Basel, and Prof. Wenzel, FU Berlin). The time and effort given by Prof. Thompson, Canada, to setting up the "Positome IIIp" positron camera is highly appreciated.

Fruitful collaboration with the ***Institut für Diagnostikforschung***, Berlin, is focused on technetium complexes with selected ligands.

IAEA Fellowship Training

Mr. M.Rahman and Mr. A.Haque from the Bangladesh Atomic Energy Commission, Dhaka, completed a fellowship training in Rossendorf from 31 March to 16 August 1992.
The programme included Tc-99m kit production and quality control, ligand synthesis as well as manufacturing Tc-99m generators based on both (n,γ)- and fission Mo-99 molybdenum.
The training programme was arranged and supervised by the VKTA`s Radiopharmaceutical Laboratory in conjunction with our Institute.

DAAD Scholarship

Mr. I. Suparman from the Indonesian National Atomic Energy Agency , Radioisotope Production Centre, Jakarta, stayed in Rossendorf from 31 May to 29 November 1992. He performed studies on gammmaspectrometric determination of U-235 uranium in solutions of fission products. He also investigated the adsorption of molydenum on various absorbent materials and prepared a special documentation on Tc-99m generator parameters.
The research assignment was arranged by the VKTA`s Radiopharmaceutical Laboratory and Waste Department in conjunction with our Institute.

VI.
SEMINARS

Dr.W.Brandau, Universität Münster
Neue N_xS_y-Liganden für ^{99m}Tc und neue iodmarkierte Fettsäuren
22. Januar 1992

Prof. M. Wenzel, FU Berlin
Radioaktive Metallocenderivate als potentielle Radiopharmaka
31. März 1992

Dr. Rozyan Yazid, Indonesien
Radioproduction Center in Jakarta - production program and facilities
5. Mai 1992

Dr. P. Brust, Universität Leipzig
Untersuchungen von ausgewählten Hirnfuktionen mit PET
12. Mai 1992

Prof.G.-J. Meyer, Hannover
Die Herstellung von PET-Radiopharmaka: Probleme der Zulassung und Anwendung
22. Juni 1992

Dr.Pigeot/Dr.Kübler, Universität Dortmund
Einbeziehung biometrischer Methoden in die Planung biologischer Experimente
3. Juli 1992

Prof. G. Firnau, Hamilton, Kanada
Wie man mit der Positronen-Emissions-Tomographie dopaminerge Areale im Gehirn untersuchen kann
20. August 1992

Prof.J.Beger, Bergakademie Freiberg
Organische Komplexbildner für die Metallextraktion
15.September 1992

Prof. L.I. Wiebe, Edmonton, Kanada
Hypoxic Cell Sensitizers for Diagnostic Scintigraphy of Tissue Hypoxia
2. Oktober 1992

Dr. D. Scharnweber, Rossendorf
Anwendung der Impedanzspektroskopie in biologischen Systemen
9. Oktober 1992

Prof. H. Mäcke, Univ.-Klinik, Kantonsspital Basel
Chemische Aspekte der Markierung von Biomolekülen mit metallischen Radionukliden
23. Oktober 1992

Prof.. C. Gloe, Inst. f. Festkörper- u. Werkstofforschung Dresden/TU Dresden
Extraktion von Metallionen mit cyclischen und offenkettigen Schwefelverbindungen
30. Oktober 1992

Dr. M. Findeisen, Institut für Oberflächenmodifizierung Leipzig
NMR-Spektroskopie an Technetiumkomplexen
3. November 1992

Dr. Ostertag, Deutsches Krebsforschungszentrum Heidelberg
Physikalische Voraussetzungen quantitativer PET-Messungen
12. November 1992

OA Dr. M. Cordes, Univ.-Klinikum Berlin-Charlottenburg
PET in der Neurologie, Onkologie und Kardiologie
20. November 1992

VII.
ACKNOWLEDGEMENTS FOR FINANCIAL AND MATERIAL SUPPORT

The Institute is part of the Research Center Rossendorf Inc, which is financed by the Federal Republic of Germany and the Free State of Saxony on a fifty-fifty basis.
In addition, the Free State of Saxony provided support for three projects (FZR/3, FZR/9 and FZR/17) covering the installation of positron emission tomography (PET), improved analytical equipment and measures required to meet legal standards for radiochemical laboratories.

The research projects concerning technetium compounds and transport systems were supported by the ***Deutsche Forschungsgemeinschaft*** and the ***Fonds der Chemischen Industrie.***

A one-year project on characterization of radiotracers preparatory to, and for the purpose of, reducing the number of animal studies was facilitated by financial and material support provided within a scientific job-creating programme (ABM).

The work on technetium chemistry was supported in part by a contract with the ***Institut für Diagnostikforschung,*** Berlin.

Prof. Stöcklin, Jülich, has continued to assist us in the process of setting up the Institute.

A major step forward to the establishment of a PET centre was possible thanks to a special offer by Professors Gjedde and Thompson, Canada, concerning the "POSITOME IIIp" camera, and financial support provided for this by the ***Kulturstiftung Dresden der Dresdner Bank.***

The ***Kernforschungszentrum Karlsruhe*** (Dr. Schweickert, Dr. Bechtold of the Cyclotron Department) assigned a technology tranfer project on ^{123}I-radiopharmceuticals to a group associated with the Institute.

Pending the award of a licence for radioactive work at Rossendorf, laboratories outside our Institute generously helped to overcome the critical situation. We are particularly indebted to the Clinics of Nuclear Medicine of the ***Humboldt Universität*** and the ***Medizinische Akademie "Carl Gustav Carus" Dresden.***